理學博士學位論文

분열성 효모에서 수명과 감수분열을 조절하는 Homeobox 전사인자 Phx1의 역할

The Role of Homeobox Protein Phx1 in Long-Term Survival and Meiosis of *Schizosaccharomyces pombe*

2012年 8月

서울大學校 大學院

生命科學部

金 知 潤

The Role of Homeobox Protein Phx1 in Long-Term Survival and Meiosis of *Schizosaccharomyces pombe*

by

Ji-Yoon Kim

under the supervision of

Professor Jung-Hye Roe, Ph.D.

A Thesis Submitted in Partial Fulfillment
of the Requirements for the Degree of
Doctor of Philosophy

August, 2012

School of Biological Sciences
Graduate School
Seoul National University

ABSTRACT

In the fission yeast *Schizosaccharomyces pombe*, the *phx1*$^+$ (pombe homeobox) gene was initially isolated as a multi-copy suppressor of lysine auxotrophy caused by depletion of copper/zinc-containing superoxide dismutase (CuZn-SOD). Overproduction of Phx1 increased the synthesis of homocitrate synthase, the first enzyme in lysine biosynthetic pathway, which is labile to oxidative stress. Phx1 has a well conserved DNA-binding domain called homeodomain at the N-terminal region and is predicted to be a transcription factor in *S. pombe*. However, its role has not been revealed in further detail.

To investigate the functions of Phx1, its expression pattern and the phenotype of its null mutant were examined. The amount of *phx1*$^+$ transcripts sharply increased as cells entered the stationary phase and was maintained at high level throughout the stationary phase. Nutrient shift down to low nitrogen or carbon sources caused *phx1*$^+$ induction during the exponential phase, suggesting that cells need Phx1 for the maintenance function during starvation. Fluorescence from the chromosomally encoded Phx1-GFP demonstrated that it is localized primarily in the nucleus, and is distinctly visible during the stationary phase and under nutrient starvation. The *phx1* null mutant showed decreased viability in long-term culture, whereas overproduction of Phx1 increased the viability. In addition, the Δ*phx1* mutant was sensitive to various oxidants, heat shock, and ethanol treatment. It was found that the Δ*phx1* mutant accumulated more reactive oxygen species (ROS) than the wild type at the stationary phase. When we examined sporulation of the Δ*phx1* / Δ*phx1* diploid strain, significant decrease in the formation of meiotic spores was observed.

In order to identify target genes regulated by Phx1, microarray analysis

was performed. Genome-wide transcriptional profiling of wild-type and Δ*phx1* cells grown to the stationary phase revealed that Δ*phx1* mutant increased and decreased the expressions of 97 and 99 genes, respectively. These genes were involved in various biological process including carbohydrate metabolism, sexual reproduction, thiamine synthesis, response to stress, and transport. Phx1 particularly increased the expression of genes for pyruvate decarboxylases (PDC) (*pdc1*$^+$, *pdc4*$^+$) and thiamine biosynthesis (*nmt1*$^+$, *nmt2*$^+$, and *bsu1*$^+$). In accordance with transcriptional regulation, the enzyme activity of pyruvate decarboxylase and the amount of thiamine were lower in Δ*phx1* mutant than in the wild type. Furthermore, both Δ*pdc1* and Δ*pdc4* mutants showed defects in long-term survival, suggesting that PDC, being under the control of Phx1, is the primary factor that allow long-term survival.

In order to find signals that activate Phx1, we examined the effect of Sck2 and cAMP/Pka1 pathways that are known to have pro-aging effects in *S. pombe*. It has been noted that Phx1 has motifs that can be phosphorylated by Sck2 or Pka1. Estimation of long-term survival for Δ*sck2* Δ*phx1* and Δ*pka1* Δ*phx1* mutants indicated that Δ*phx1* counteracted the lifespan extension phenotypes of Δ*sck2* and Δ*pka1*. It suggests that Sck2 and Pka1 negatively regulate Phx1 as upstream regulatory factors. Effect of Sty1 MAPK pathway that regulates cellular stress responses has also been examined. Interestingly, *phx1*$^+$ expression did not increase at the stationary phase in Δ*sty1* mutant, being independent of Atf1 which is a major target of Sty1. Bimolecular fluorescence complementation (BiFC) analysis indicated that Phx1 interacts with Sty1. These results indicate that Phx1 could be a phosphorylation target of Sty1 as well.

In summary, this work revealed that Phx1 is a transcriptional regulator whose synthesis is elevated during stationary phase and by nutrient

starvation in *S. pombe*. It functions in long-term survival and stress tolerance against oxidation, heat and ethanol treatment, and plays a key role in the formation of meiotic spores from diploid zygotes. In addition, the activity of Phx1 is modulated by Pka1, Sck2 and Sty1 kinases as upstream regulatory factors. Its contribution to long-term survival is exerted primarily through enhancing the expression and activity of at least two pyruvate decarboxylases in the cell. How PDC can serve such a function requires further study.

Key Words

: *Schizosaccharomyces pombe,* Phx1, homeobox, transcriptional regulator, stationary phase, nutrient starvation, long-term survival, stress tolerance, oxidative stress, heat shock, ROS accumulation, meiosis, sporulation, DNA microarray, pyruvate decarboxylases, thiamine biosynthesis, Sck2 pathway, cAMP/Pka1 pathway, Sty1 MAPK pathway, Bimolecular Fluorescence Complementation.

CONTENTS

LIST OF FIGURES

LIST OF TABLES

ABBREVIATIONS

2OXO	2-oxoisovalerate
a.a.	amino acid
ADH	alcohol dehydrogenase
BiFC	bimolecular fluorescence complementation
bp	base pair
CLS	chronological lifespan
CR	calorie restriction
CuZnSOD	Cu, Zn-containing superoxide dismutase
DCFH-DA	2´,7´-dichlorofluorescin diacetate
DEPC	diethylpyrocarbonate
EDTA	ethylenediamine tetraacetate
EMM	Edinburgh minimal medium
EX	exponential phase
GFP	green fluorescence protein
GO	Gene ontology
H_2O_2	hydrogen peroxide
HACL	2-hydroxyacyl-CoA lyase
HD	homeodomain
HET-P	5-(2-hydroxyethyl)-4-methylthiazole phosphate
HMP-PP	4-amino-5-hydroxymethyl-2-methylpyrimidine diphosphate
ILV	acetolactate synthase
IR	Interaction Region
kDa	kilo dalton
Kpi	potassium phosphate
LiAc	lithium acetate
MAP	mitogen-activated protein
Mb	mega base pair
MI	meiotic division I
MII	meiotic division I
NJ	neighbor joining

nmt	no message on thiamine
OD	optical density
ORF	open reading frame
PCR	polymerase chain reaction
PDC	pyruvate decarboxylase
PEG	polyethylene glycol
PFRD	pyruvate feredoxin reductase
PKA	protein kinase A
PMSF	phenylmethylsulphonyl fluoride
PP	pyrophosphate
PPDC	phosphopyruvate decarboxylase
Pyr	pyrimidine
qRT-PCR	quantitative real-time PCR
ROS	reactive oxygen species
rRNA	ribosomal RNA
SPDC	sulfopyruvate decarboxylase
ST	stationary phase
TCA cycle	tricarboxylic acid cycle
TH3	transhydrogenase dIII
TK	transketolase
TKC	transketolase C-terminal
TMP	thiamine monophosphate
TOR	target of rapamycin
TPP	thiamine pyrophosphate
VC	Venus N-terminal fragment
VN	Venus C-terminal fragment
w/v	weight per volume
WT	wild type
YES	Yeast Extract with supplements (complex media)
YGK4	oxalyl-CoA decarboxylase

CHAPTER I.

INTRODUCTION

I.1. Homeodomain Proteins

Homeobox genes, first identified to control development in *Drosophila* species, encode highly conserved domains of about 60 amino acids, which comprise helix-turn-helix DNA-binding motif (Gehring 1987). Homeobox genes are found in various organisms from yeasts to vertebrates, and most homeodomain-containing proteins are believed to act as transcriptional factors (Banerjee-Basu and Baxevanis 2001). In vertebrates, Hox proteins participate in various differentiation programs such as limb development and also in regulating cell cycle, apoptosis and cancer (Zakany and Duboule 2007; Miotto and Graba 2010; Shah and Sukumar 2010). In fungi, homeodomain proteins are best known to determine mating-types in *Saccharomyces cerevisiae, Schizosaccharomyces pombe*, as well as in other fungi (Kelly *et al.* 1988; Kronstad and Staben 1997; Mukai *et al.* 1997). Controls of phosphate starvation response, hyphal formation, or cell cycle by homeodomain proteins have also been reported (Burglin 1988; Torres-Guzman and Dominguez 1997; Aligianni *et al.* 2009).

In *S. pombe*, there are three homeobox family genes; the mating-type control gene *matPi*, *yox1*$^+$ whose product is a regulator of G1/S transition of the cell cycle, and *phx1*$^+$ that was initially isolated as a high-copy suppressor of the growth defect caused by mutation in Cu, Zn-containing superoxide dismutase (CuZnSOD) production (Kwon *et al.* 2006).

I.2. Discovery of Phx1

The *phx1*$^+$ (pombe homeobox) gene was initially isolated as a multi-copy suppressor of lysine auxotrophy caused by depletion of copper/zinc-containing superoxide dismutase (CuZn-SOD) (Kwon *et al.* 2006). Phx1-overproducing cells overcame this auxotrophy by increasing the synthesis of

homocitrate synthase, the first enzyme in lysine biosynthetic pathway. Since homocitrate synthase is labile to oxidative stress, it has been postulated that Phx1 may serve as a regulator that increases the fitness of *S. pombe* cells against oxidative stress. However, no further information about the role of Phx1 has been available.

The *phx1*$^{+}$ gene encodes a protein of 942 amino acids (103.9 kDa), with a conserved homeobox domain (a.a. 167-227) near the N-terminus. The homeobox domain consists of a flexible stretch of nine residues (N-terminal arm) followed by three α-helices (Arnaise *et al.* 2001). Multiple alignments of Phx1 and other related proteins from *Yarrowia lipolytica* (Hoy1), *Podospora anserina* (Pah1), *Aspergillus nidulans* (RfeB), and *Saccharomyces cerevisiae* (Pho2) indicated that the homeodomains were highly conserved, especially in the third helix (Fig. I-1A). Besides the homeodomain region, a small stretch of residues (from a.a. 520 to 566) was found to be conserved, sharing about 40% identical residues with the corresponding region of Pho2. Interestingly, this region was reported to be involved in interaction with binding partners of Pho2 such as Pho4, Bas1, and Swi5 in *S. cerevisiae* (Bhoite *et al.* 2002; Hannum *et al.* 2002). It implies that Phx1 may have binding partners and similar regulatory mechanisms as revealed in the action of transcription factor Pho2p in *S. cerevisiae* (Fig. I-1A).

A class of atypical homeodomain proteins has three extra residues between helix I and II. Phylogenetic analysis of Phx1 and other homeodomain proteins in fungi, plants and animals indicated that Phx1 is a typical homeodomain protein. Furthermore, Phx1 showed relatively closer phylogenetic relationships with Pho2 of *S. cerevisiae* and Hoy1 of *Y. lipolytica* than other homeodomain proteins of *S. pombe* (Fig. I-1B).

Fig. I-1. Multiple sequence alignments and phylogenetic relationships of homeodomain proteins.

(A) Multiple sequence alignments of the homeodomain (HD; 167-227) and the short conserved region (putative Interaction Region) of Phx1 with those of other fungi; Hoy1p of *Yarrowia lipolytica* (*Yl*), Pah1p of *Podospora anserina* (*Pa*), RfeB of *Aspergillus nidulans* (*An*), and Pho2p of *Saccharomyces cerevisiae* (*Sc*). The sequences were aligned using Vector NTI AlignX program (Invitrogen Co.). The three α-helices of homeodomains were indicated above and the consensus was shown at the bottom. The particularly conserved motifs in putative IR were lined above. The sequences were retrieved from the GenBank database. [CAA93700, CAA84415, CAC16792, CBF86004.1, CAA64906 for Phx1, Hoy1p, Pah1p, RfeBp, Pho2p, respectively].

(B) Phylogenetic tree of some homeodomain proteins of representative species in fungi, animals, and plants. Homeodomain sequences of each protein were retrieved from Swissprot database. Yox1 and MatPi of *Schizosaccharomyces pombe* (S.p.), Pho2, Yox1, Yhp1, and Mata1 of *Sacharomyces cerevisiae* (S.c.), Hoy1 and Mata1 of *Yarrowia lipolytica* (Y.l.), Otp of *Mus musculus* (M.m.), Pah1p of *Podospora anserina* (P.a.), Antp and Abd-A of *Drosophila melanogaster* (D.m.), Ceh-31 of *Caenorhabditis elegans* (C.a.), Hat1 and Stm of *Arabidopsis thaliana* (A.t.), Aβ1-1 of *Coprinus cinereus* (C.c.), and Kn1 of *Zea mays* (Z.m.) were used as queries. The tree was generated by MEGA 5 program.

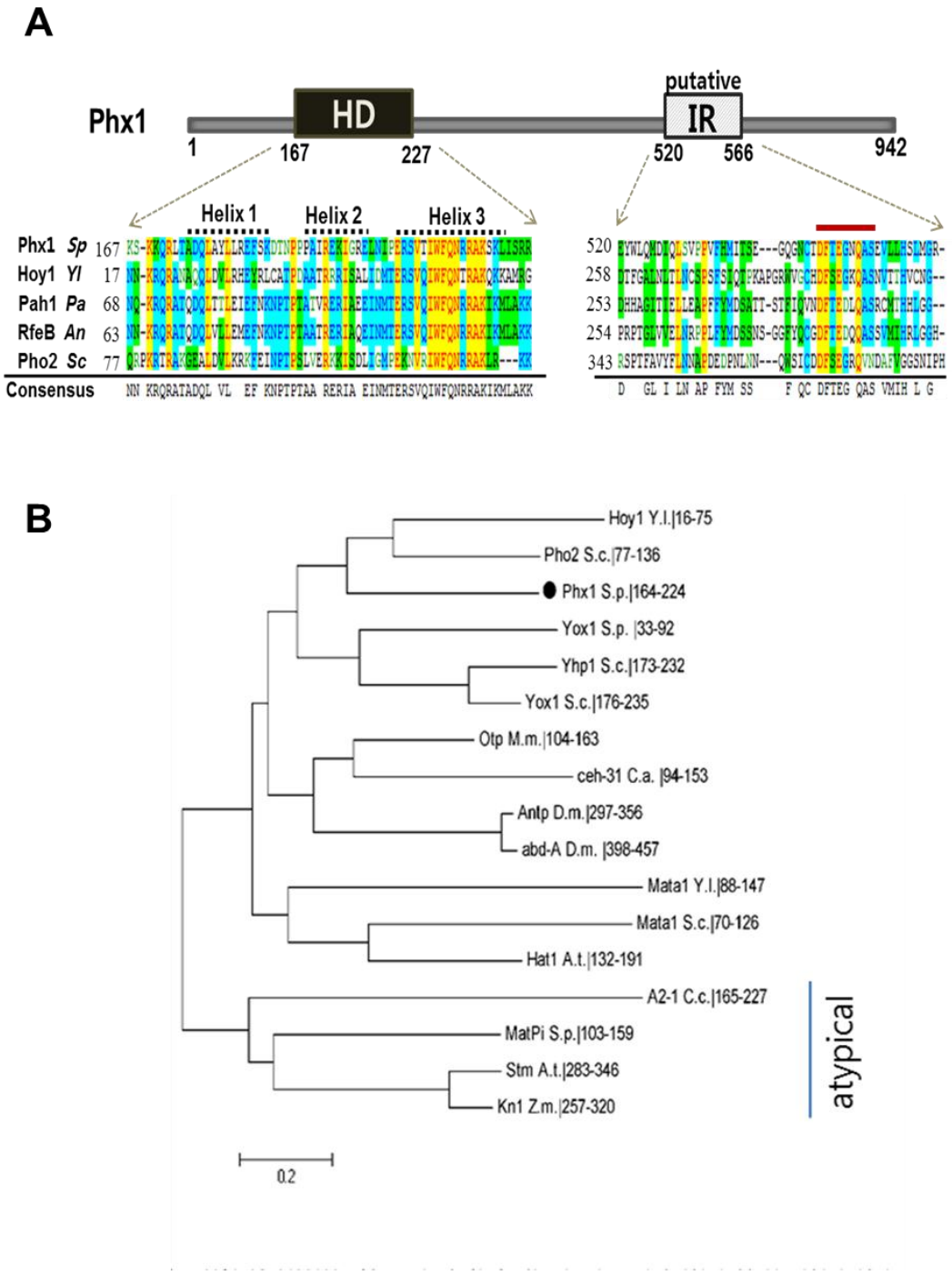
A
Phx1
HD
putative
IR
1
167
227
520
566
942
Helix 1
Helix 2
Helix 3
Phx1 Sp 167
Hoy1 Yl 17
Pah1 Pa 68
RfeB An 63
Pho2 Sc 77
Consensus
520
258
253
254
343
B
Hoy1 Y.l.|16-75
Pho2 S.c.|77-136
Phx1 S.p.|164-224
Yox1 S.p. |33-92
Yhp1 S.c.|173-232
Yox1 S.c.|176-235
Otp M.m.|104-163
ceh-31 C.a. |94-153
Antp D.m.|297-356
abd-A D.m. |398-457
Mata1 Y.l.|88-147
Mata1 S.c.|70-126
Hat1 A.t.|132-191
A2-1 C.c.|165-227
MatPi S.p.|103-159
Stm A.t.|283-346
Kn1 Z.m.|257-320
atypical
0.2

I.3. Aging in Yeast

The molecular mechanisms that regulate cellular aging have been partially conserved throughout evolution. Aging research with yeast has progressed rapidly and made it possible to identify signaling pathways and media conditions, which regulate longevity (Kaeberlein *et al.* 2007).

I.3.1. Chronological aging

Chronological aging in yeast has been defined as the viability of non-dividing cells after transition to stationary phase, mimicking the aging process of non-proliferating cells in multicellular organisms. It has been proposed that cell death in long-term culture is mainly due to ethanol production, toxicity by reactive oxygen species (ROS), and loss of mitochondrial function (Longo and Fabrizio 2002; Fabrizio *et al.* 2005).

I.3.2. Replicative aging

Replicative aging is measured by the number of daughter cells which single mother cell can generate before death. It is linked to exponential growth and has associated with the accumulation of rDNA circles in the nucleolus of old cells in *S. cerevisiae*. NAD^+-dependent deacetylases Sir2 and Hst2 contribute to the extension of replicative lifespan by reducing the accumulation of rDNA circles (Lamming *et al.* 2005; Ha and Huh 2011). In *S. pombe*, replicative aging has been studied by Barker and Walmsley (Barker and Walmsley 1999), but no long-lived mutant of this aging has been identified yet.

Although the processes of chronological and replicative aging may differ, some signaling pathways are involved in both replicative and chronological aging, suggesting a common link between them. For example, the deletion of

the gene encoding protein kinase SCH9 extends both chronological and replicative lifespan in budding yeast (Kaeberlein *et al.* 2005).

I.3.3. Signaling pathways of aging

In *S. cerevisiae*, two nutrient-responsive pathways are known to be involved in aging. They are TOR/SCH9 pathway and cAMP/PKA pathway which seem to sense glucose and nitrogen levels and coordinate the cellular response. Chemical or genetic inhibition of either of these two pathways brings about chronological life span extension (Wei *et al.* 2008). Recently, similar results have been reported in *S. pombe* (Roux *et al.* 2006). However, the downstream targets and mechanisms of these pathways have not been fully revealed yet. Recently another signaling pathway linked to life span extension has been found in *S. pombe*. That is stress-activated MAP kinase pathway, Sty1 pathway (Zuin *et al.* 2010). Aging cells experience some kinds of stress such as oxidative stress. Oxidative stress is supposed to be the main cause of the molecular damage associated to aging (Muller *et al.* 2007). However, recently reactive oxygen species (ROS) have been considered as triggering molecules for fitness of lifespan (hormesis of ROS) by enhancing stress defenses. Therefore, the studies of stress-responsive pathway associated with aging are important.

I.3.3.1. Sck2 pathway

In *S. cerevisiae*, deletion of the *SCH9* gene enhances chronological lifespan (Fabrizio and Longo 2003). *SCH9* encodes a serine/threonine protein kinase that was isolated as a high-copy suppressor of the growth defect of PKA-defective cells. *S. cerevisiae* SCH9 is a homologue to Akt/PKB which is implicated in insulin signaling in mammals and functions in a pathway that regulates longevity and stress resistance in *C. elegans*. In *S. pombe*, there are

two homologues of the *S. cerevisiae SCH9* gene: *sck1*$^+$ and *sck2*$^+$. They also encode serine/threonine protein kinases. Disruption of *sck2*$^+$ caused no obvious phenotype, but when combined with the disruption of *sck1*$^+$, it showed low spore germination efficiency. When *sck2*$^+$ was overexpressed, it suppressed the defects of Δ*pka1* mutants, including ectopic mating, slow growth and short cell morphology (Fujita and Yamamoto 1998). Between *sck1*$^+$ and *sck2*$^+$, only the *sck2*$^+$ gene is known to regulate aging (Roux *et al.* 2006). When the *sck2*$^+$ gene is deleted, cells live longer than wild-type cells in long-term culture. However, the downstream mechanisms or targets of aging-related Sck2 pathway have been little known.

I.3.3.2. cAMP / PKA pathway

Previous studies have found that the deletions of the genes *CYR1* encoding an adenylate cyclase and *RAS2* encoding a small GTPase enhance chronological lifespan of *S. cerevisiae* (Fabrizio and Longo 2003; Fabrizio *et al.* 2005). Both CYR1 and RAS2 are the components of glucose signaling PKA pathway. cAMP/PKA pathway stimulates cell proliferation and glycolysis, but decreases stress resistance. In *S. pombe*, the losses of the components of cAMP/Pka1 pathway also extend long-term viability (Roux *et al.* 2006; Roux *et al.* 2009). The cAMP/Pka1 pathway is essential for entry and maintenance of stationary phase in *S. pombe* (Wang *et al.* 2005). Pka1 phosphorylates and inactivates the transcription factor Rst2 by switching localization of Rst2 in the presence of glucose (Higuchi *et al.* 2002). In nutrient starvation conditions, the level of cAMP decrease and make Cgs1, the regulatory subunit of protein kinase A (PKA), interact with the catalytic subunit Pka1. And then, Rst2 accumulates in the nucleus and activate the transcriptions of target genes required for stationary-phase activity such as gluconeogenesis (*fbp1*$^+$ encoding fructose-1,6-bisphosphatase) or sexual development (*ste11*$^+$

encoding transcription factor for meiosis).

I.3.3.3. Sty1 pathway

The mitogen-activated protein (MAP) kinase Sty1 (also known as Spc1 and Phh1) pathway copes with the various environmental stresses through regulating stress-responsive gene expressions in *S. pombe*. Furthermore, Sty1 pathway is involved in the maintenance of viability of nutrient starved cells (Zuin *et al.* 2010). Sty1 can be activated by different kinds of stresses, including hydrogen peroxide (H_2O_2) and glucose or nitrogen starvation (Vivancos *et al.* 2006). Upon stress conditions, Sty1 is phosphorylated by Wis1 and translocated into the nucleus, followed by regulating target factors (ex. Atf1) by phosphorylation (Wilkinson *et al.* 1996). Atf1 is a Sty1-dependent transcription factor required for the inductions of stress-responsive genes. Although the stress response triggered by Sty1 allows cells to survive on stress conditions, the role of Sty1 in nutrient starvation and aging remains little known. Several reports just indicate that Sty1 pathway has some interconnections with cAMP/Pka1 pathway (Neely and Hoffman 2000) and participates in lifespan extension by calorie restriction (Zuin *et al.* 2010).

In *S. cerevisiae*, *SCH9* has been found as a high-copy suppressor of the phenotypes caused by defects of PKA signaling pathway, suggesting it controls a redundant or parallel signaling pathway to PKA. Actually, SCH9 pathway participated in the longevity regulation in parallel with PKA pathway and these two pathways converged to Rim15-dependent mechanisms (Wei *et al.* 2008) (Fig. I-2A). In *S. pombe*, *sck2*$^+$, the homologue of *S. cerevisiae SCH9*, also suppressed the defects of Δ*pka1* mutant. Therefore, Sck2 and Pka1 pathways have possibility to cooperate with each other for longevity regulation. In addition, Sck2 and Pka1 pathways have antagonistic

Fig. I-2. Longevity regulatory pathways of budding and fission yeasts.

(A) In *S. cerevisiae*, Sch9, Tor, and Ras/cAMP/PKA sense nutrient conditions and control signaling pathways mediated via Rim15. In turn, transcription factor Gis1 and Msn2/4 activate stress response genes for cellular protection, followed by enhance of longevity. Although major portion of calorie restriction (CR) effect seems to be mediated by the regulation of Tor/Sch9 and Ras/cAMP/PKA, another pathways involved in CR-inducing lifespan extension may be exist, independently of Sch9 and PKA pathway.

(B) In *S. pombe*, glucose-sensing regulator Pka1 inhibits Sty1 activation. Calorie restriction induces low PKA activity, and then enhances longevity through Sty1-Atf1 regulation. Low PKA activity also activates Rst2, a transcription factor for gluconeogenesis and sexual development. Sck2 may be upstream signal transduction pathway of Sty1, but detail mechanism remains unknown. Furthermore, it is still veiled whether Tor pathway regulates Sck2 or not.

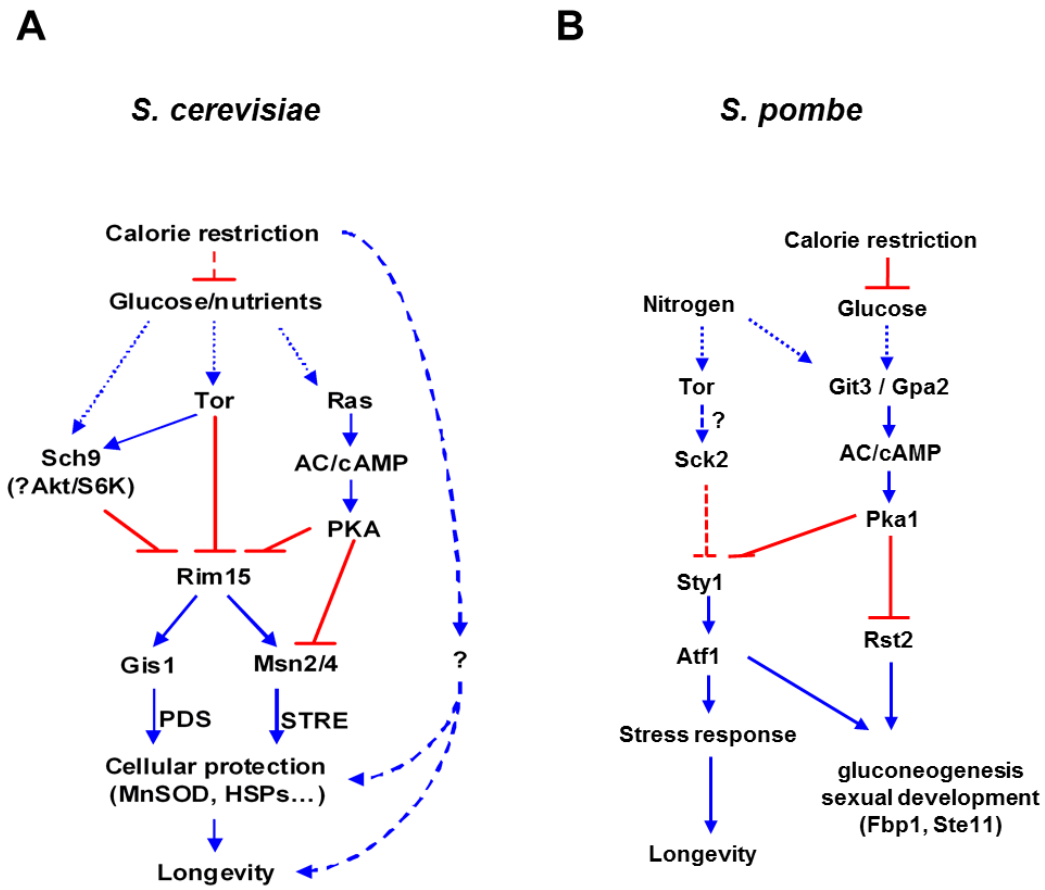

(Wei M et al, 2008)

relation with Sty1 pathway on aging (Zuin *et al.* 2010) (Fig. I-2B). But, how they interconnect or what the mediators of them are have not been fully understood.

I.4. Meiotic Gene Expression in *S. pombe*

When cells meet nutrient starvation condition such as nitrogen or carbon starvation, haploid yeast cells try to find out mating partner and mate with each other. After conjugation, cells subsequently undergo meiotic division and sporulation. All of these sexual developmental processes are controlled by an extensive gene expression program and several transcriptional regulators (Mata *et al.* 2002; Mata *et al.* 2007). Mata *et al*. found that about hundreds of genes were upregulated during this developmental process, and they defined four classes according to expression time; response to nutritional changes (transient, continuous, delayed), premeiotic S phase and recombination (early), meiotic division I and II (middle), and spore formation (late) (Fig. I-3A). Transcriptional regulation occurs in successive waves, each under the control of different transcription factors (Fig. I-3B). A subset of the genes induced in response to nutritional changes is controlled by the transcription factor Ste11. Rep1 activates a subset of the early genes, while the forkhead-family protein Mei4 controls the expression of middle genes. The basic leucine zipper transcription factor Atf21 and Atf31 control a subset of late genes. Two zinc-finger transcription factors Rsv1 and Rsv2 also participate in regulating the induction of late genes.

Besides triggering simultaneous expression of gene waves, these transcription factors also repress genes in the previous wave and induce other factors that in turn regulate a subsequent wave.

Fig. I-3. Sexual developmental process in *S. pombe*.

(A) In *pat1*-driven meiosis, premeiotic S phase starts at about 2 hour after inactivation of Pat1p (data not shown) and is accompanied by chromosome pairing and recombination. The first meiotic division (MI) takes place at 5 hour, and the second division (MII) at about 5.5 hour. The forespore membrane is formed between 5.5 and 6.5 hour. Mature spores (spo) appear at 10-12 hour.

(B) Model for transcriptional regulatory network controlling meiosis and sporulation. Arrows indicate activation and cross bars indicate repression.

A

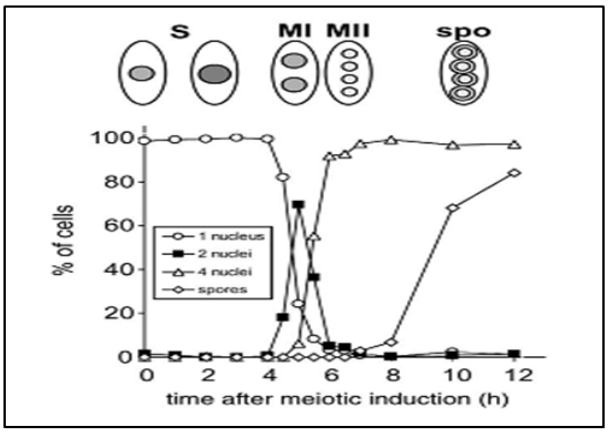

(Mata et al. 2002)

B

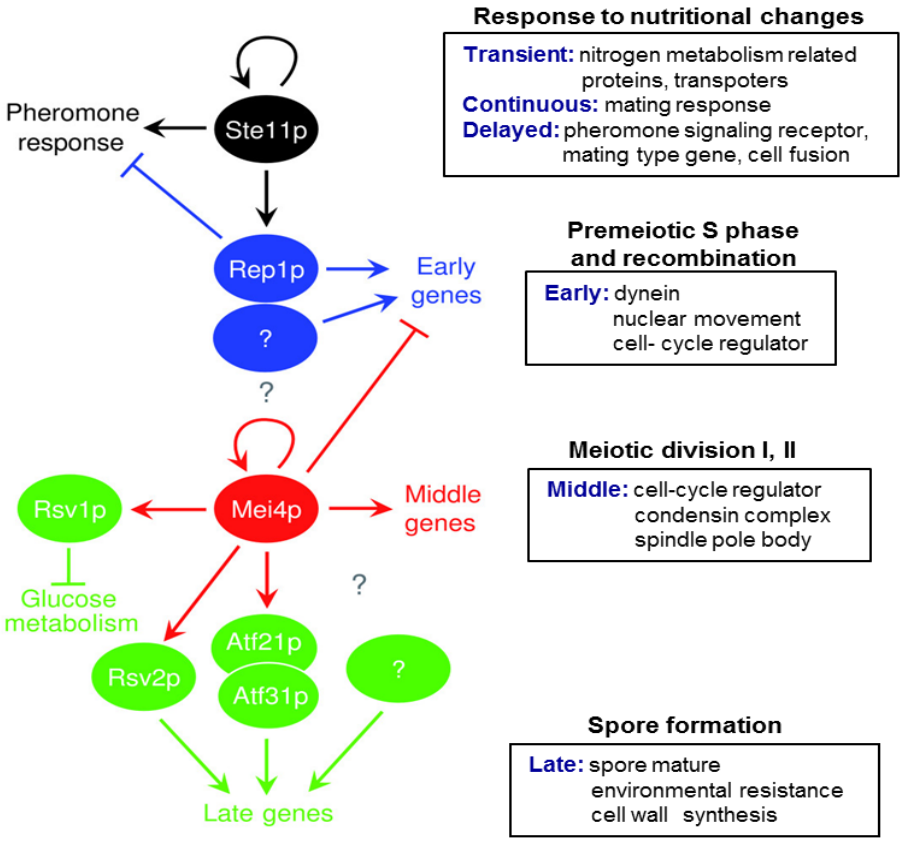

(Mata *et al*. 2007)

I.5. Pyruvate Decarboxylase (PDC) in Yeast

I.5.1. TPP-dependent enzyme family

Thiamine pyrophosphate (TPP) cofactor-dependent enzymes have diverse functions, including nonoxidative decarboxylation of α-keto acids, oxidative decarboxylation of α-keto acids, carboligation, and cleavage of C-C bonds. The common feature of all TPP-dependent enzymes is the binding of TPP at the interface of a conserved pyrophosphate (PP)- and pyrimidine (Pyr)-domain (Costelloe *et al.* 2008).

TPP-dependent enzymes are classified into six groups depending on the domains which are alternatively arranged in the primary structure, or appear on different subunits (Fig. I-4). Enzymes of the transketolase (TK)-like group (TK, D-xylulose-5-phosphate synthase (DXPS), dihydroxyacetone synthase (DHAS), and phosphoketolase (PKL)) contain the PP-, Pyr- and TKC (transketolase C-terminal)-domains on the same subunit and are homodimeric, except for PKL, which is a homohexamer. Pyruvate feredoxin reductase (PFRD) enzymes contain the PP-, Pyr-, TKC-, and four additional domains, designated by D3, D4, D5, and D7, in various arrangements. In case of the 2-oxoisovalerate dehydrogenase (2OXO)-like enzymes, the PP-domain is found on a different subunit, unlike the Pyr- and TKC-domains are in same subunit. Pyruvate decarboxylase (PDC)-like group (PDC, indolepyruvate decarboxylase (IPDC), phenylpyruvate decarboxylase (PhPDC), pyruvate oxidase (PO), acetolactate synthase (ALS), glyoxylate carboligase (GXC), benzaldehyde lyase (BAL), oxalyl CoA decarboxylase (OCADC), and benzoylformate decarboxylase (BFDC)) are homotetrameric and contain a transhydrogenase dIII (TH3)-domain between the Pyr- and PP- domains. In addition to TPP, PO, ALS, and GXC, each requires FAD, which binds to the

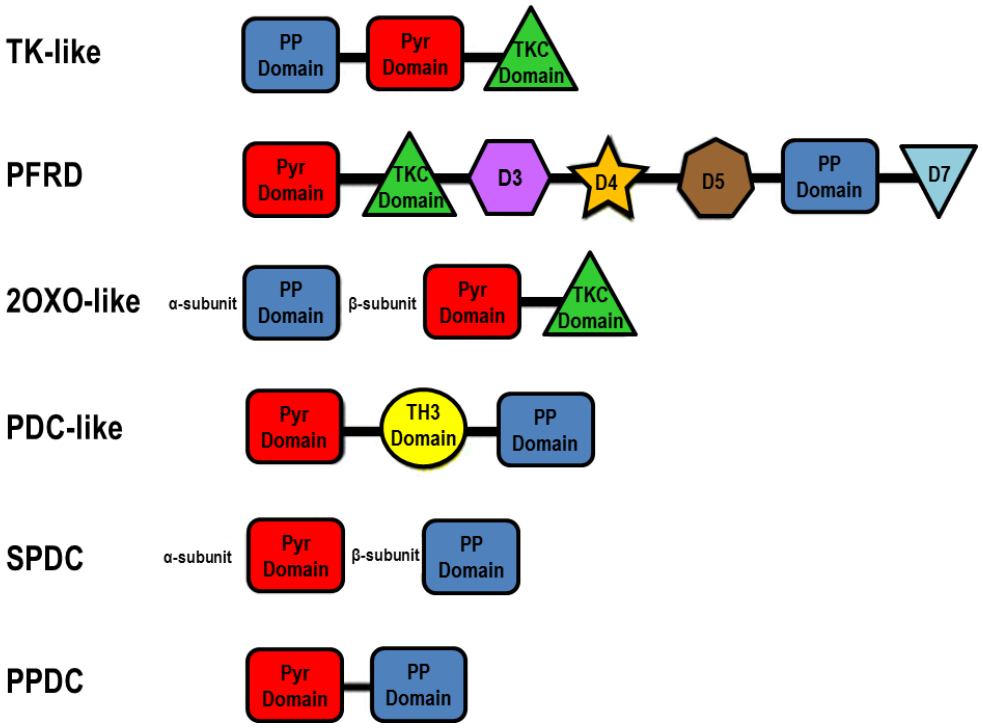

(Costelloe, S. J. *et al.*, 2008)

Fig. I-4. Domain arrangements of TPP-dependent enzyme family.

Members of the TPP-dependent enzyme family can be classified by their domain architecture. All members contain the catalytic PP- and Pyr-domains which bind TPP. α and β subunits denote cases where the PP- and Pyr-domains are found on different subunits. TPP is bound at the interface of two subunits, except in PFRD and DXPS, where TPP is bound by PP- and Pyr-domains on the same chain.

TH3-domain. Finally, both sulfopyruvate decarboxylase (SPDC) and phosphopyruvate decarboxylase (PPDC) consist only of PP- and Pyr-domains. In SPDC, the PP- and Pyr-domains form the separate subunits (α and β) of an $\alpha_2\beta_2$-heterotetramer. In PPDC, the PP- and Pyr- domains are fused and form a homotrimer.

I.5.2. Pyruvate decarboxylase in yeast

Pyruvate decarboxylase (PDC) is a key enzyme in alcohol fermentation. This enzyme was isolated from yeast, some bacteria, and a number of plants. To date about 40 nucleotide sequences of PDC genes are determined. The catalytic mechanism of *S. cerevisiae* has been investigated. PDC catalyses the non-oxidative conversion of pyruvate (or other 2-oxo acids) to acetaldehyde and CO_2. The reaction sequence proceeds at the C2 atom of the thiazolium ring of the coenzyme thiamine pyrophosphate (TPP) (Konig 1998).

In *S. cerevisiae*, pyruvate decarboxylase occurs in three isoforms. Pdc1, the main enzyme produced during growth on rich medium, Pdc5, which is produced under thiamine limitation, and Pdc6, which is part of a sulphur-sparing expression program activated under heavy metal stress. Expression of *PDC1* and *PDC5* is strongly stimulated in the presence of glucose as carbon source. In addition, expression of *PDC5* is strongly stimulated when *PDC1* is deleted.

The Pdc2 has been known to be a regulator of *PDC* gene expressions as well as *THI* gene expressions. In the absence of Pdc2, expression of *PDC1* is diminished and *PDC5* expression completely abolished even under stimulating conditions (Mojzita and Hohmann 2006).

I.6. Thiamine Biosynthesis in Yeast

Thiamine (vitamin B1) is an essential molecule for all living organism. De novo thiamine biosynthesis may occur in bacteria, some protozoa, plants, and fungi, while animals must uptake it from the environment (Kowalska and Kozik 2008; Bettendorff and Wins 2009). Like other thiamine-synthesizing organisms, yeasts first separately synthesize two precursors, 5-(2-hydroxyethyl)-4-methylthiazole phosphate (HET-P) and 4-amino-5-hydroxymethyl-2-methylpyrimidine diphosphate (HMP-PP), which are then assembled into TMP (thiamine monophosphate) by thiamin-phosphate synthase (Fig. I-5). The substrates for yeast thiazole synthesis are cysteine as a sulfur donor, glycine and D-pentulose-5-phosphate. The substrates for pyrimidine moiety are histidine and pyridoxal-5-phosphate. Yeast can salvage HET-P and HMP-P by an uptake of HET and HMP from the environment followed by its phosphorylation. In *E. coli*, TMP may be phosphorylated to the TPP by a thiamin phosphate kinase. Unlike many bacteria, yeast cannot directly phosphorylate TMP to obtain TPP. Instead, TMP is hydrolyzed to thiamine by thiamine monophosphatase, and then thiamine may be pyrophosphorylated to TPP by thiamine pyrophosphokinase. TPP also can be produced from free thiamin taken up by yeast cells from the environment. The external thiamine phosphate derivatives are first dephosphorylated in the periplasm and then transported across the cell membrane as a form of free thiamine by thiamine transporter. TPP serves as an intracellular negative signal and controls the transcriptional level of genes which are involved in thiamine metabolism. The several genes which control thiamine and TPP biosynthesis were identified currently in yeast. There are at least 15 genes coding for the enzyme catalyzing each steps of thiamine biosynthetic pathway, at least 3 genes whose products are involved in the transport of thiamine, and 3 genes involved in the genetic

Fig. I-5. The pathway of thiamine biosynthesis in yeasts.

THI4 is only one gene which is assigned to the de novo HET-P synthesis. The encoded THI6 protein is a bifunctional enzyme, TMP diphosphorylase/HET kinase. THI6 protein is involved in the salvage phosphorylation of HET. Four genes, *SNO2/SNO3* and *SNZ2/SNZ3*, are involved in the synthesis of pyridoxal phosphate, the precursor of HMP-P. Later steps of HMP-P synthesis are controlled by genes of the *THI5/11/12/13* family and *THI20/21* family. *THI20/21* encode HMP-P kinase, which is trifunctional proteins, as they can phosphorylate HMP by salvage pathway, and contain an additional C-terminal domain with a thiaminase II (thiamine degrading) activity. The condensation of HET-P and HMP-PP into TMP is catalyzed by the encoded THI6 protein. After dephosphorylation of TMP by various non-specific phosphatases, the free thiamine is converted to TPP by thiamine pyrophosphotase, a product of the *THI80* gene. *THI10 (THI7)* gene encodes thiamine transporter located in the plasma membrane and PHO3 is a periplasmic acid phosphatase. THI2, THI3, and PDC2 are DNA-binding proteins which can form ternary complex and regulate the transcription of *THI* genes. TPP can bind to THI3 protein, intracellular thiamine sensor (Kowalska and Kozik 2008). The genes in parentheses are *S. pombe* orthologs to the corresponding genes of *S. cerevisiae*.

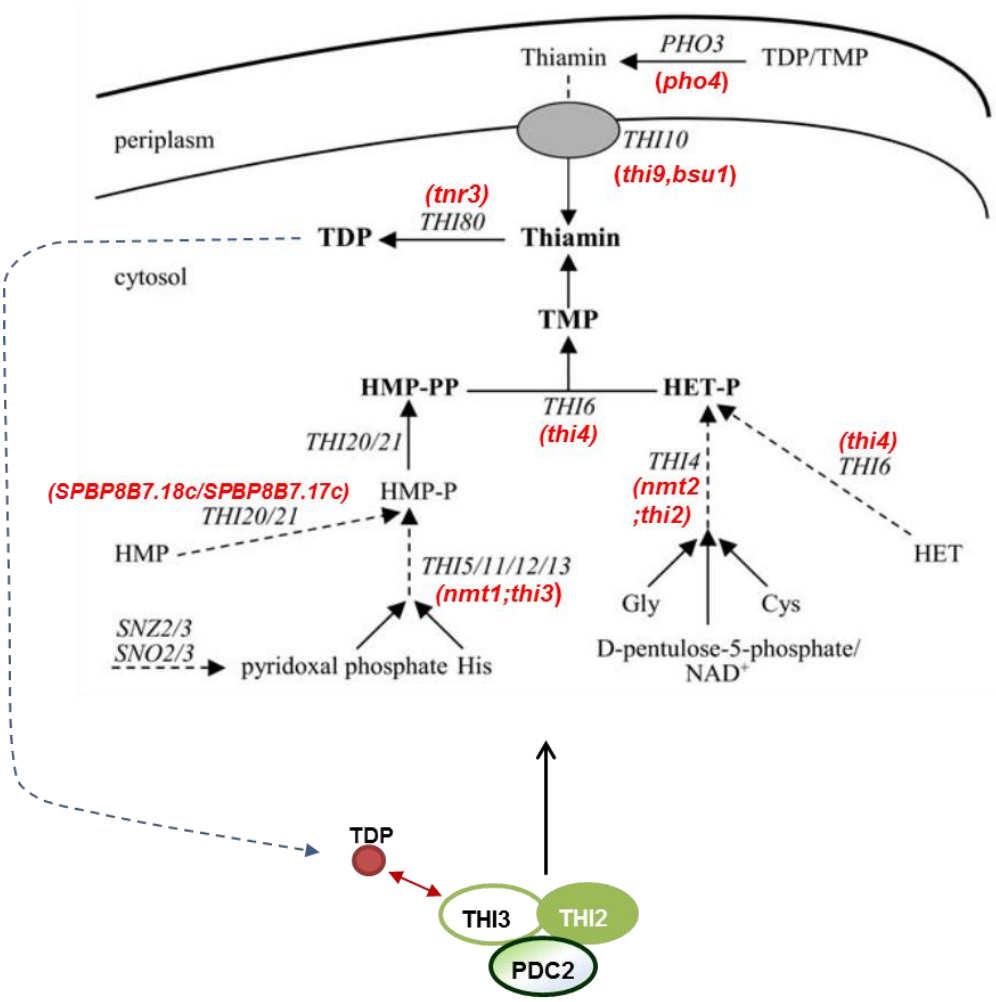

(Thi1, Thi5 and unknown factors in *S. pombe*)

regulation of thiamine biosynthesis in *S. cerevisiae*. Three positive-acting transcriptional regulators of thiamine biosynthesis and transport are THI2, THI3, and PDC2 in *S. cerevisiae*. The THI2 protein is a typical DNA-binding protein, THI3 is a TPP-binding protein, and PDC2 is an isoform of TPP-dependent pyruvate decarboxylase, also containing a DNA-binding N-terminal region. Recently, the model for regulation of thiamine biosynthesis has been suggested (Nosaka 2006). It is that THI2, THI3, and PDC2 form a ternary complex and bind to upstream regulatory sequences of *THI* genes in the absence of TPP, and induce their transcription. In the sufficient TPP condition, TPP binds to THI3 which can act as an intracellular thiamine sensor, preventing the ternary protein complex assembly, and represses *THI* gene transcription.

In *S. pombe*, many genes involved in thiamine metabolism are highly conserved as like in other eukaryotes and also thiamine biosynthetic pathway is very similar with that in *S. cerevisiae*. Thiamine represses mRNA synthesis of many genes, including *thi2*$^+$ (*nmt2*$^+$), *thi3*$^+$ (*nmt1*$^+$), *thi4*$^+$, *pho4*$^+$, *thi9*$^+$, and *bsu1*$^+$ (The function of each gene was described in Fig. I-5). All known thiamine-repressible genes are under the control of the positive regulator Thi1, Thi5 (McQuire and Young 2006). The gene *thi1*$^+$ and *thi5*$^+$ encodes for a Cys6 zinc finger motif-containing protein which might act as a transcription factor necessary for the expression of thiamine-regulated genes. However, details of the regulation of thiamine biosynthesis in *S. pombe* have not been clarified yet, and there might be another unknown factor which could regulate the thiamine biosynthesis.

I.7. Biology of Fission Yeast *Schizosaccharomyces pombe*

The fission yeast *S. pombe* is becoming increasingly attractive model organism as an experimental system for investigating problems of eukaryotic

cells and molecular biology. This small, relatively simple eukaryote shares many cellular properties with larger, multicellular organisms (Zhao and Lieberman 1995). The single genus *Schizosaccharomyces* embraces a small group of possibly quite divergent ascomycete yeasts that share the common feature of division by medial fission. *S. pombe* is classified as a fungus, namely an ascomycete fungus characterized by the formation of an ascus. Recently, DNA and RNA sequence analyses have been used to determine sequence divergence among ascomycete fungi, thus, to quantitate genetic differences between species. These molecular techniques demonstrate that fission yeast *S. pombe* is phylogenetically as distant from budding yeasts as it is from humans. The *Schizosaccharomyces* lineage separated about 1 billion years ago to form an ancestral branch of the ascomycetes, denoted archaeascomycetes. The conservation of gene activity between *S. pombe* and mammals was clearly demonstrated by the functional complementation of a number of *S. pombe* mutants by cognate genes from mammalian cells. *S. pombe* can therefore provide a novel host system to investigate the structure, function, and expression of eukaryotic genes, especially those of mammalian origin.

I.7.1. Life cycle of *S. pombe*

During its normal life cycle, fission yeast cells are haploid, meaning that they have only one copy of each chromosome. Haploid yeast cells are used for research because both recessive and dominant mutations will result in a mutant phenotype. Haploid cells multiply asexually through mitosis. Newly born daughter cells grow at the tips of their cylindrical rod shape. When they have grown to a mature length, cells stop growing and produce septa in the middle of the cells. The septum divides the mother cell into two equal-size daughter cells. In rich medium, the daughter cells will separate to start over the haploid cell cycle; each haploid cell cycle takes about 3 hours (In contrast,

the mammalian cell cycle takes about 24 hours.) (Fig. I-6A). In the wild, yeast cells often live under nutrient-deprived conditions. Because *S. pombe* is a dimorphic yeast, it can switch from a yeast-form morphology to a pseudo-hyphal morphology, in which the daughter cells remain attached. Pseudo-hyphal growth allows the cells to spread out more efficiently and forage for fresh nutrients (Fig. I-6B).

S. pombe has two opposite mating types, namely '+' and '-' mating types. When rich conditions are followed by starvation conditions, haploid yeast-form cells of the opposite mating type will conjugate pair-wise and fuse at their tips (Fig. I-6C). Subsequently, the nuclei will fuse to form diploid cells, called zygotes (Fig. I-6D). Usually, zygotes undergo meiosis immediately, followed by sporulation and formation of four-spore zygotic asci. The ascus wall will auto-lyse, liberating the haploid ascospores, which are able to survive long periods of stress (Fig. I-6E). When environmental conditions become favorable for growth, the spores will germinate and the haploid cell cycle will begin again (Fig. I-6F). If zygotes encounter rich conditions, they infrequently can undergo mitosis instead of meiosis and enter the diploid cell cycle (Fig. I-6G).

Diploid cells divide by medial fission, like haploid cells, but are longer and wider than haploid cells. Haploid cells measure 7-8 (newly born) to 12-15 µm (at division) in length and 3-4 µm in width, while diploid cells measure 11-14 (newly born) to 20-25 µm (at division) in length and 4-5 µm in width (Fig. I-6H). Diploid cells will continue mitotic growth until nutrients run out. Then, they undergo meiosis and form azygotic asci, containing four haploid ascospores (Fig. I-6I). After environmental conditions become favorable for growth, the spores will germinate and the normal haploid cell cycle will begin (Fig. I-6J).

Fig. I-6. Life cycle of fission yeast *S. pombe*.

('www information on *Schizosaccharomyces pombe* by Frans Hochstenbach at the University of Amsterdam' (*http://www.bio.uva.nl/pombe/cycle/lifetext.html*))

(A) Haploid cells multiply asexually through mitosis.
(B) Pseudo-hyphal morphology cells.
(C) Conjugation of two different mating type cells.
(D) Formation of zygotes, the diploid cells.
(E) Formation of four-spore zygotic asci.
(F) Spore germination.
(G) Diploid cells divided by medial fission.
(H) Diploid cells are longer and wider than haploid cells.
(I) Formation of azygotic asci.
(J) Life cycle of fission yeast. (top left) Haploid mitotic cell cycle; (center and lower left) haploid cells mating to form a diploid zygote, followed by meiosis and sporulation leading to zygotic ascus formation; (lower right) re-entry of diploid zygotes into mitotic cycle (copied from MacNeill and Nurse, 1997).

A.

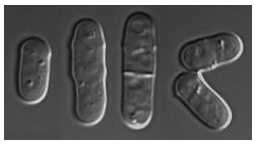

B.

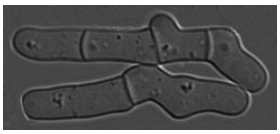

C.

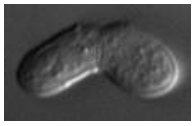

D.

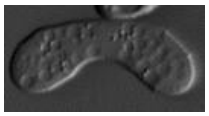

E.

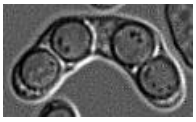

F.

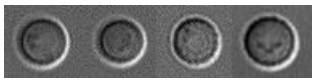

G.

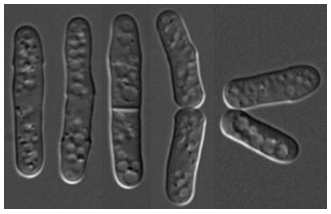

H.

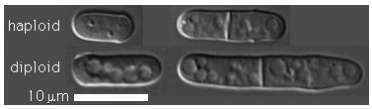
haploid
diploid
10 µm

I.

J.

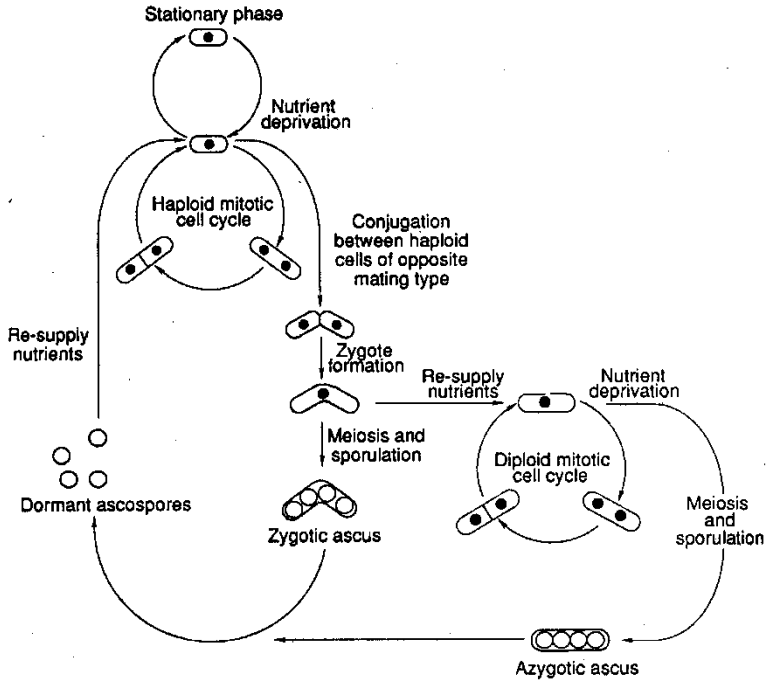
Stationary phase
Nutrient deprivation
Haploid mitotic cell cycle
Conjugation between haploid cells of opposite mating type
Re-supply nutrients
Zygote formation
Re-supply nutrients
Nutrient deprivation
Meiosis and sporulation
Diploid mitotic cell cycle
Meiosis and sporulation
Dormant ascospores
Zygotic ascus
Azygotic ascus

I.7.2. Cell cycle of *S. pombe*

S. pombe has been used for cell cycle investigations since 1950s. A major reason for choosing *S. pombe* in initial studies was its mode of growth by length extension, which continues until the onset of mitosis. The cell cycle of *S. pombe* is typically eukaryotic, consisting of distinct G1, S, G2, and mitotic (M) phases. The G2 phase occupied three quarters of the cycle of a cell growing under normal conditions, with the remainder being divided roughly equally among the M, G1, and S phases. At mitosis, chromosome condensation can be visualized, and a long mitotic spindle forms that separated the chromosomes into daughter nuclei. The nuclear envelope remains intact throughout, however, as in most fungi. Mitosis is followed by formation of the septum centrally across the cell, which brings about physiological division of the cytoplasm. Subsequently the septum is cleaved, resulting in separation of the two daughter cells. In general S and M phases are interdependent, so that arresting S phase prevents spindle formation and chromosome condensation and blocking cells in mitosis prevents DNA synthesis in the following cycle. A similar dependency relationship of "checkpoint" ensures that, in general, septum formation only takes place once mitosis is completed.

I.7.3. Genomic structure of *S. pombe*

The fully annotated genome sequence of *S. pombe* has just been completed (Wood *et al.* 2002). It becomes the sixth eukaryotic genome to be sequenced, following *Saccharomyces cerevisiae*, *Caenorhabditis elegans*, *Drosophila melanogaster*, *Arabidopsis thaliana*, and *Homo sapiens*. The 13.8 Mb genome of *S. pombe* is distributed between chromosomes I (5.7 Mb), II (4.6 Mb), and III (3.5 Mb), together with a 20 kb mitochondrial genome. It contains the smallest number of protein-coding genes yet recorded for a eukaryote: 4,824 genes

(including 11 mitochondrial genes), substantially less than the 5,570 ~ 5,651 genes predicted for *S. cerevisiae*, the 6,752 genes predicted for *Mesorhizobium loti*, the largest published prokaryote genome sequence to date, and the 7,825 genes estimated in the 8.67 Mb genome of the prokaryote *Streptomyces coelicolor* (Wood *et al.* 2002).

I.7.4. Deletion mutants library of *S. pombe*

Recently, the project 'Construction of genome-wide deletion mutant library in *S. pombe*' was started by Dr. Kwang-Lae Hoe at KRIBB (Korea Research Institute of Biotechnology and Bioscience, Korea) through collaboration with Sir Paul Nurse at CRC (Cancer Research Center, UK, currently at the Rockefeller University in USA) and Bioneer Coporation (Korea).

The 4,836 heterozygous diploid deletions covering 98.4% of the 4,914 protein coding open reading frames (ORFs) based on the annotated genome sequences were constructed (Kim et al. 2010a). Each deletion strain has a specific tag, so functional analysis can be performed both in a gene-specific manner and a genome-wide scale. Except some duplicated mutants, about 2,700 haploid deletion mutants were available for functional genomic study. All haploid deletion mutants were confirmed by sequencing, colony PCR, and tetrad analysis for "essentiality".

CHAPTER II.

MATERIALS AND METHODS

II.1. Strains and Culture Conditions

II.1.1. Bacterial and yeast strains, media and culture conditions

The bacterial and yeast strains used in this study are summarized in Table II-1. *E. coli* strain DH5α was used as the host for construction of all the recombinant DNAs. Except for TB medium (Terrific broth; 1.2% tryptone (Difco), 2.4% yeast extract (Difco), 0.4% (v/v) glycerol, 0.017 M KH_2PO_4 (Junsei), and 0.072 M K_2HPO_4 (Junsei)) for the large-scale preparation of plasmids, all the *E. coli* strains were grown in LB medium (1% tryptone, 1% NaCl, and 0.5% yeast extract) supplemented with appropriate antibiotics at 37 °C.

Growth and maintenance of *S. pombe* strains were generally done as described by Moreno *et al.* (Moreno *et al.* 1991) and Alfa *et al.* (Alfa and Cold Spring Harbor Laboratory. 1993). EMM (3 g/L potassium hydrogen phthallate (Sigma), 5.6 g/L $Na_2HPO_4 \cdot 12H_2O$ (Junsei), 5 g/L NH_4Cl (DSP), 2% (w/v) dextrose, 20 ml/L salts stock (50 x), 1 ml/L vitamins stock (1,000 x), 0.1 ml/L minerals stock (10,000 x), and 225 mg/L supplements as required) was used for both prototrophic and auxotrophic strains. Nitrogen-free medium was prepared by eliminating ammonium chloride (NH_4Cl) from EMM whereas the low glucose medium contained only 0.5% of glucose, instead of 2% of glucose in EMM. YES medium (0.5% yeast extract, 3% dextrose, and 225 mg/L adenine, leucine and/or uracil, if necessary) was used for wild type strains and mutants from the library stock (Bioneer Co.) containing auxotrophic marker(s). For conjugation and sporulation, ME medium (3% malt extract (Difco)) was used.

II.1.2. Stress treatments

For oxidative stress treatment, hydrogen peroxide (Fluka), superoxide

Table II-1. Bacterial and yeast strains used in this study

Strain	Genotype	Reference or source
E. coli		
DH5α	*F⁻DΔlacU169 (ϕ80lacZDΔM15) endA1 recA1 hsdR17 deoR supE44 thi-1 λ⁻ gyrA96 relA1*	Lab stock
S. pombe		
972	*h⁻ wild type*	Lab stock
ED665	*h⁻ ade6-M210 leu1-32 ura4-D18*	Lab stock
ED666	*h⁺ ade6-M210 leu1-32 ura4-D18*	Lab stock
ED667	*h⁻ ade6-M216 leu1-32 ura4-D18*	Lab stock
ED668	*h⁺ ade6-M216 leu1-32 ura4-D18*	Lab stock
JH43	*h⁻ ade6-M210 leu1-32*	Jeong, J.H.
ESX5	*h⁻ ade6-M210 leu1-32 ura4-D18 phx1:: ura4⁺*	Kwon, E.S.
ESX8	*h⁺ade6-M210 leu1-32 ura4-D18 phx1:: ura4⁺*	Kwon, E.S.
ESXF1	*phx1⁺-EGFP/ΔNTphx1::ura4⁺ in ED665*	Kwon, E.S.
URA4-D18	*h- ura4-D18*	Lab stock (Arndt et al. 1996)
JY01	*h- ura4-D18 Δphx1::ura4⁺*	This study
BG_4180 (Δ*thi5*)	*h⁺ ade6-M216 leu1-32 ura4-D18 thi5::kanMX4*	Bioneer Co.
BG_1625 (Δ*pdc1*; SPAC13A11.06)	*h⁺ ade6-M210 leu1-32 ura4-D18 pdc1::kanMX4*	Bioneer Co.
BG_0617 (Δ*pdc3*; SPAC186.09)	*h⁺ ade6-M216 leu1-32 ura4-D18 pdc3::kanMX4*	Bioneer Co.
BG_1593 (Δ*pdc4*; SPAC3G9.11c)	*h⁺ ade6-M216 leu1-32 ura4-D18 pdc4::kanMX4*	Bioneer Co.
BG_0925 (Δ*sck2*)	*h⁺ ade6-M216 leu1-32 ura4-D18 sck2::kanMX4*	Bioneer Co.
BG_2342 (Δ*pka1*)	*h⁺ ade6-M210 leu1-32 ura4-D18 pka1::kanMX4*	Bioneer Co.
BG_4138 (Δ*rsv1*)	*h⁺ ade6-M216 leu1-32 ura4-D18 rsv1::kanMX4*	Bioneer Co.
BG_1112 (Δ*sty1*)	*h⁺ ade6-M216 leu1-32 ura4-D18 sty1::kanMX4*	Bioneer Co.
BG_3309 (Δ*atf1*)	*h⁺ ade6-M216 leu1-32 ura4-D18 atf1::kanMX4*	Bioneer Co.
JY02	*h⁻ ade6-M210 leu1-32 ura4-D18pdc1::kanMX4*	This study
JY03	*h⁻ ade6-M210 leu1-32 ura4-D18pdc3::kanMX4*	This study
JY04	*h⁻ ade6-M210 leu1-32 ura4-D18pdc4::kanMX4*	This study
JY05	*h⁻ ade6-M210 leu1-32 ura4-D18sck2::kanMX4*	This study
JY06	*h⁻ ade6-M210 leu1-32 ura4-D18sck2::kanMX4 phx1:: ura4⁺*	This study
JY07	*h⁺ ade6-M210 leu1-32 ura4-D18 pka1::kanMX4 phx1:: ura4⁺*	This study

generators paraquat (methyl viologen; sigma) and menadione (vitamin K3, non-salt form from ICN), and a thiol-specific oxidant diamide (sigma) were used. Heat was treated at 42°C (for cell viability) or 50°C (for transcriptional induction). For chronic stress, exponentially (OD_{600} 0.5-1) or stationary (OD_{600} 8-9) grown cells in liquid EMM were spotted on EMM solid media containing indicated oxidants after appropriate dilution and incubated for 3~4 days. Cells would be continuously exposed to the treatment from single cell to a colony. All the acute stresses were applied to exponentially (OD_{600} 0.5-1) or stationary (OD_{600} 8-9) grown cells in liquid EMM for 40 or 20 min (heat shock). The stress-treated cells were spotted on EMM solid media for sensitivity analysis, or harvested for RNA preparation to examine *phx1*$^+$ induction.

For the ethanol tolerance assay, exponential- or stationary-phase cells were transferred to the fresh liquid medium containing 0, 10 or 20% ethanol and incubated at room temperature for 30 minutes. The cell suspension was then quickly diluted with distilled water to attenuate the action of the ethanol, followed by being plated on YE and EMM after appropriate dilution and incubated at 30°C for 2~3 days.

II.2. Recombinant DNA Techniques

II.2.1. Plasmids and construction

The plasmids and libraries used in this study are summarized in Table II-2. pUC18R and pTZ18R, the multifunctional plasmids, were used as general gene cloning vectors in *E. coli*. Gene disruption constructs were prepared with those plasmids using the insertion of appropriate genetic markers such as *ura4*$^+$ or *LEU2*$^+$.

pREP2, pREP42, and pWH5, the *E. coli* and *S. pombe* shuttle vectors, were used for expression vectors in *S. pombe*, and pRIP series vectors were used for

Table II-2. Plasmids used in this study

Plasmid	Description	Reference or source
pTZ18R	general cloning vector (2.87 kb)	Lab stock
pWH5	general cloning shuttle vector, *LEU2*+ marker (10.5 kb)	Wright et al. (1986)
pREP2	constitutively-expressed nmt promoter, *ura4*$^{+}$ marker, *bla* gene(8.9 kb)	Lab stock
pREP42	pREP2 variation, containing medium strength nmt promoter.	Lab stock
pREP41-VC	C-terminal VC tagging, *LEU2*+ marker	Lab stock (Kim et al., 2010b)
pREP42-VN	C-terminal VN tagging	Lab stock (Kim et al., 2010b)

chromosomal integration.

To employ bimolecular fluorescence complementation (BiFC) assay in *S. pombe,* pREP42-VN or pREP41-VC were used for C-terminal tagging of proteins. VN or VC is the N- or C-terminal fragment of Venus, variant of yellow fluorescent protein (Nagai *et al.* 2002).

II.2.2. DNA manipulation

The chromosomal DNA of *S. pombe* was prepared as described by Alfa *et al*. (Alfa and Cold Spring Harbor Laboratory. 1993) with some modifications. Plasmid DNA from *E. coli* was prepared by alkaline lysis method. A variety of restriction and modifying enzymes were used according to the manufacturer's recommendations (KOSCOCHEM, NEB, Takara, Boeringer-Manheim, Gene Craft, BIOTOOLS, etc.). DNA fragments were purified from agarose gels using GeneClean Kit II (BIO101) and UltracleanTM15 (MOBIO).

II.3. Transformation of *Escherichia coli* and Yeast

For the purpose of general cloning, *E. coli* DH5α competent cells were used for transformation by heat shock method (42°C for 1 min 30 sec.).

The *S. pombe* transformation was routinely done using lithium acetate (LiAc)/ Polyethylene glycol (PEG) method according to Moreno *et al*. ((Moreno *et al.* 1991).

II.4. Cell Extract Preparation and Analytical Methods

II.4.1. Protein extraction and measurement

Harvested cells were washed in 10 mM potassium phosphate (KPi) buffer, pH 7.0 and were resuspended in 0.5 ml of 10 mM potassium phosphate buffer containing 1 mM phenylmethylsulphonyl fluoride (PMSF) and disrupted by

abrasion with 0.5 mm glass beads (0.5 mm, Biospec) in Eppendorf tubes for 2 min X 5 times using a vortex mixer. Cell debris was removed by two consecutive centrifugations and the amount of protein in the supernatant was determined by Bradford assay (Bradford 1976).

II.4.2. Pyruvate decarboxylase activity assay

Cell extracts were prepared from cells grown in EMM to exponential phase (OD_{600} of 0.5~1) or stationary phase (OD_{600} of 8~9). For PDC assay, 20 μg of proteins were used and the activity of PDC was determined with a reaction mixture containing 50 mM sodium pyruvate, 0.1 mM NADH, 1 mM $MgCl_2$, and 50 mM Tris-HCl buffer (pH 7.6) with the addition of alcohol dehydrogenase (Sigma). The activity of PDC was established in the presence or absence of 0.1 mM thiamine pyrophosphate to affirm the contents of the enzyme apoform (Tylicki *et al.* 2008). Enzymatic analysis was determined from changes in the optical density at 340 nm. Analysis was performed on Simadzu UV-1650pc spectrophotometer.

II.5. RNA Preparation and Analytical Methods

II.5.1. RNA isolation and purification

For Northern analysis, cells were grown up to OD_{600} of 0.2 (early exponential phase), 0.5~1.0 (mid-exponential phase), 7.0 (late exponential phase), or 8~9 (early stationary and late stationary). Cells were harvested and washed with 0.1% DEPC-treated distilled water. After resuspending the pellet in AE buffer (50 mM sodium acetate, pH 5.3, 10 mM EDTA, pH 8.0), 1/10 vol. of 10% SDS and equal vol. of AE-saturated phenol/chloroform were added. Cells were lysed by agitating vigorously with vortex mixer for 1 min, incubated at 65°C for 10 min and then chilled rapidly on ice for 5 min. After

centrifugation at 4°C, the aqueous phase was recovered for precipitation with 2 vol. of absolute ethanol.

For quantitative real-time PCR, cells were resuspended with 500 µl of TES (10 mM Tris pH 7.5, 10 mM EDTA pH 8, 0.5% SDS), immediately added 500 µl acidic phenol-chloroform (Sigma P-1944), vortexed, and incubated in 65°C heat block for 1 hour. And then chilled rapidly on ice for 1 min. After centrifugation at 4°C, the aqueous phase was recovered, and acidic phenol-chloroform extraction was repeated one more. Next, 500 µl of chloroform:isoamyl alcohol (24:1) (Sigma C-0549) was added and centrifuged for 5 min at 4°C. The aqueous phase was taken for precipitation with 2 vol. of absolute ethanol.

RNA pellets from ethanol precipitation were dissolved in RNase-free water and quantified by spectrophotometer UV-1650PC (Shimadzu).

II.5.2. Northern hybridization

RNA samples prepared from grown cells at different conditions were separated on agarose gels containing formaldehyde, and transferred onto a Hybond-N^+ membrane (Amersham) for hybridization. Gene-specific probes for *phx1*$^+$, *ctt1*$^+$, *trr1*$^+$, and *gpx1*$^+$ genes were generated by PCR and radio-actively labeled method as recommended by the manufacturer. After hybridization, signals were visualized and quantified by PhosphorImager (BAS-5000) with Multi Gauge (Fuji) program.

II.5.3. cDNA preparation

For cDNA preparation, 1 µg of total RNA was used as a template for reverse transcription. RNA was mixed with 0.2 µg of random hexamer (promega) and then reverse transcription was performed with RevertAid M-MuLV Reverse Transcriptase (Fermentas) for 1 hour.

II.5.4. Quantitative RT-PCR

Each RNA sample (1 g/µl) was reverse-transcribed into cDNA using RevertAid™ Reverse Transcriptase kit (Fermentas). PCR was performed with SYBR Green/ROX qPCR master mix (Fermentas) using gene-specific primers for corresponding genes and the *act1*$^{+}$ which serves as an internal control. Triplicate PCRs with gene-specific primer pairs for each gene were carried out as recommended by the manufacturer, using a quantitative real-time PCR machine (ABI PRISM®Sequence Detection System, Applied Biosystems) with analysis software SDS2.2 (Applied Biosystems). Primer pairs used in this study are listed in table II-3.

II.6. Gene Disruption and Phenotype Detection

II.6.1. Construction of the prototrophic Δ*phx1* mutants

We also generated the prototrophic Δ*phx1* mutant without auxotrophic markers. For this purpose, ESX8 and an uracil auxotroph (*h*$^{-}$ *ura4-D18*) (Arndt and Atkins 1996) were mated, and a prototrophic Δ*phx1* strain (JY01; *h*$^{-}$ *ura4-D18 phx1::ura4*$^{+}$) was obtained through spore selection and confirmation by PCR.

II.6.2. Construction of multiple disruptants

For double mutant construction, fresh grown single mutant cells are mixed with another single mutant having opposite mating-type on ME plate. Mixed cells were incubated at 25°C for 3 days and sporulated cells were monitored by microscope. Spores were germinated in YES and plated on selective solid media. Colonies were selected and confirmed by marker and PCR. Mating type of strain was verified by mating-type PCR (MT1: 5′-AGAAGAGAGAGT AGTTGAAG-3′, MP: 5′-ACGGTAGTCATCGGTCTTCC-3′, and MM: 5′-

Table II-3. Primers used for qRT-PCR

Name	Sequence
Act1 RT- F	TGAGGAGCACCCTTGCTTGT
Act1 RT-R	TCTTCTCACGGTTGGATTTGG
Phx1 RT-F	TCCAAATGCCGTTCCTGTCT
Phx1 RT-R	TGGGATTGCGGAATAAGAAGA
Nmt1 RT- F	GAAATCGATGGCGGCATT
Nmt1 RT- R	ACGCACCAGCGCTCAAG
Nmt2 RT- F	CGGCGCTTTCTGTGTCAAG
Nmt2 RT- R	GACGCATGTCGTGAAGGTTAGA
Bsu1 RT- F	TGCTATTTGGCCCGTGTTTT
Bsu1 RT- R	ACGTACAACTAGCACCCATTTCC
Thi4 RT- F	CGTTACTCTTGCAGCATATGGTTCT
Thi4 RT- R	GCAAAATCAGCAACTTCATCGT
Pho4 RT- F	TGAAAATGCCGACCAGTTGTC
Pho4 RT- R	CGGCCCAAGTCAAAAAGTTC
Thi9 RT- F	TTTGTCGCATCGATCACTCAA
Thi9 RT- R	TTAAACGTGCTAACTTCAGCAAAGA
Tnr3 RT- F	CAGCGGCCTTGAGTGGAA
Tnr3 RT-R	GCTGACGAGTCCTCCAAATTG
Thi1 RT- F	GGAAGATGTCAGCAAGTCGAATT
Thi1 RT- R	GCGCAGCTGAAAATAATCTGTTAC
Thi5 RT- F	GAAAATTCGATGCAGTGGTTCTG
Thi5 RT-R	CATTGCGAAGGCGTAGCA
Pdc1 RT- F	GCCCCGAGATGTTTTGATCA
Pdc1 RT- R	TGCAATCAAGGACACCAAAGTT
Pdc2 RT- F	GAGGATGCTCCCGTTATGATTG
Pdc2 RT- R	AGACAGGCTTGTGTTGGAGGAT
Pdc3 RT- F	GCCATCGTCACCACTTTTGG
Pdc3 RT- R	CCGGCGAAACCGTTGA
Pdc4 RT- F	TGGCCGTTCGGTTAGCA
Pdc4 RT-R	CACCGGGAACCACAAAATG
Sck2 RT- F	TTCTCCCGCATACAACCGTAT
Sck2 RT- R	CTGAGAGGCTGGAAAACAGTATTG
Pka1 RT-F	TCCTGAAAGCGCGAGTAGAAG
Pka1 RT-R	GTCCCGCGAATGTCTTTGAT
Fbp1 RT- F	CCATGGCCTTCCTTGTTGA
Fbp1 RT- R	GCGATCTCCTTTGTCGTTTACC
Rsv1 RT- F	GGAGCAGACACTGGATGTCAAC
Rsv1 RT-R	TCACCTTCCGGTTTCGAATC
Sty1 RT- F	TTTGGAGTGCGGGTTGTATTT
Sty1 RT- R	GCCGGGAAACAAGGGTTTT
Atf1 RT- F	CCCTTCATTAACATTACGCCAAA
Atf1 RT- R	TGGATCCATTCTCGGCATTT

TACGTTCAGTAGACGTAGTG-3')

II.7. Measurement of Long-Term Survival

To measure chronological life span, cells were inoculated at initial OD_{600} of 0.02 in liquid EMM, and grown until OD_{600} reached the maximum value of about 8 to 9. From this time point (day 0), aliquots were taken daily and plated on complex (YES for auxotrophs and YE for prototrophs) solid medium, following appropriate dilutions to plate out similar number of cells. Cell colonies were counted after 3 to 4 days incubation at 30°C. The viable cell count at day 0 was regarded as 100% survival rate. For nutrient-specific starvation, cells grown to OD_{600} of 0.5 to 1 in liquid EMM were washed with sterile distilled water, and resuspended in EMM without NH_4Cl or EMM with 0.5% instead of 2% glucose. Following further incubation for 24 h at 30°C, cells were grown on solid YE medium to count colonies as described above.

II.8. Measurement of Oxygen Consumption

The respiration rate was measured polarographically at 25°C using YSI5300 Biological Oxygen Monitor Micro System (Yellow Spring Instrument). After collection of the cells by centrifugation at 3000 g, cells were suspeneded in 50 mM potassium phosphate (pH 6.5), 0.1 M glucose at 0.1 g (wet weight) cells/ml. 60 μl of cell suspension was introduced into the buffer-filled chamber and the amount of oxygen consumed was recorded.

II.9. Measurement of Intracellular H_2O_2 Level

Relative intracellular peroxide levels were determined using the redox-sensitive fluorescent probe 2′, 7′-dichlorofluorescin diacetate (DCFH-DA, sigma). This dye is membrane-permeable and is trapped intracellularly

following deacetylation. The resulting compound, DCFH, reacts with ROS (primarily H_2O_2 and hydroxyl radicals) to produce the oxidized fluorescent form 2,7-dichlorofluoroscein (DCF).

Strains were grown in EMM media up to each culture time indicated in the figures. DCFH-DA was added to 0.5 ml cell cultures at final concentrations of 50 µM, from stock solutions of 50 mM in DMSO. Incubation proceeded at 30°C in the dark for 1 hour. Peroxide production was analyzed by flow cytometry, using an FACS Canto (Becton Dickinson) at low flow. DCF was monitored in FITC-A channel (detecting green fluorescence). A total of 10,000 live cells for each sample were analyzed for DCF -dependent fluorescence (as an indicator of intracellular H_2O_2 levels).

II.10. DNA Microarray Analysis

DNA microarrays displaying probes for >99% of all known and predicted genes of *S. pombe* spotted in duplicate onto glass slides were used. RNA extraction, hybridization and initial data processing and normalization were performed as previously described (Lyne *et al.* 2003). Four independent biological experiments were performed, including two dye swaps. The data were visualized and analyzed using GeneSpring (Agilent). The significance of overlaps between different gene lists was calculated in GeneSpring using a standard Fisher's exact test, and P values were adjusted with a Bonferroni multiple testing correction. Cut-off values of 2-fold or 0.6-fold change of the average value from four biological repeats. Gene annotations were downloaded from *S. pombe* GeneDB.
(http://www.genedb.org/genedb/pombe/).

II.11. Detection of Mating and Sporulation Efficiency

II.11.1. Iodine staining

Conjugation and sporulation were induced by spotting each 3 μl of late-exponentially growing cells and its opposite mating-type cells onto agar plates containing EMM without NH_4Cl. Then, the plates were incubated at 25°C for 3 days. Subsequently, the cells were treated with iodine vapor for 5 min to monitor ascospore formation.

II.11.2. Assay for mating efficiency

For assay of mating efficiency, two mating-type *S. pombe* cells for mating were grown on EMM medium plate separately, and then mixed on ME plates. These were incubated for 3 days, and the cultures were examined under a microscope, in order to count the numbers of zygotes and spores. The mating efficiency (ME) was calculated with the formula ME = (2Z + 2A + 0.5S) ÷ (H + 2Z + 2A + 0.5S), where H is the number of haploid cells, Z is the number of zygotes, A is the number of asci, and S is the number of free spores.

II.11.3. Assay for sporulation efficiency of diploid

Pairs of ED665 (h^-) and ED668 (h^+), as well as ESX5 (Δ*phx1*, h^-) and ESX8 (Δ*phx1*, h^+), were mated with each other on ME plate and incubated at 25°C for 2 days. Diploid cells were selected for the complementing markers on EMM. Following growth to the stationary phase in liquid EMM, the formation of asci that contain tetrad spores was examined by microscopy, following nuclear staining by DAPI. Three independent experiments were carried out to quantify the efficiency of ascus formation. At least 500 cells in each culture were counted.

II.12. Quantification of Thiamine and Its Derivatives

II.12.1. Extraction of thiamine

Thiamine was extracted by HCl according to a modified protocol of White and Spencer (1979). Cells were grown in EMM liquid media at 30°C and harvested and washed with distilled water at each time point. They were resuspended in 0.5 ml 0.6 M HCl and extracted for 5 min at 25°C. Extracted cells were pelleted and the supernatant was filtered through a Millex GV filter (Millipore). If not immediately analyzed, extracts were stored at -20°C (Schweingruber *et al.* 1991).

II.12.2. Determination of thiamine and thiamine phosphates by HPLC

Thiamine and thiamine phosphates were derivatized to thiochromes and chromatographed by HPLC. 50 µl of thiamine extract and 50 µl of 0.02% $K_3Fe(CN)_6$ in 15% NaOH were mixed and 10 µl of this mixture was injected into an HPLC column (a PRP-1 main column, 10 µm, 250X4.1 mm, Hamilton no.79427). Elution was achieved with solvent A (8.5 mM sodium phosphate buffer pH 8.5 prepared with distilled water) and solvent B (methanol, HLPC-grade, Merck). Thiamine phosphates elute in the order triphosphate, diphosphate and monophosphate at 10% B; following a steep gradient, thiamine elutes at 50% B. Detection occurred in Varian Prostar HPLC fluorescence detector at an excitation of 365 nm and emission of 430 nm. The standards thiamine monophosphate (TMP) and thiamine pyrophosphate (TPP) were used in the form of their chlorides (Sigma).

II.13. Bimolecular Fluorescence Complementation (BiFC) Assay

For multi-copy BiFC analysis, *thi1*$^{+}$, *thi5*$^{+}$, *sck2*$^{+}$, *sty1*$^{+}$, *rsv1*$^{+}$, and *phx1*$^{+}$ gene including ORF was cloned into pREP42-VN or pREP41-VC using *NdeI* / *XhoI* site, respectively. Cloned vectors were co-transformed to ED665 cells and transformants were selected using auxotrophic marker. The cells containing both pREP41-*phx1*$^{+}$-VC and pREP42-*thi1*$^{+}$-VN/pREP42-*thi5*$^{+}$-VN/pREP42-*sck2*$^{+}$-VN/pREP42-*sty1*$^{+}$-VN/pREP42-*rsv1*$^{+}$-VN plasmids were inoculated in EMM and fluorescence signals were detected by Zeis Axiovert 200M.

CHAPTER III.

RESULTS AND DISCUSSION

III.1. Roles of Phx1 in Long-Term Survival

III.1.1. Expression of the *phx1*$^+$ gene increases at the stationary phase and by nutrient starvation

To monitor the expression profile of *phx1*$^+$ gene, we analyzed *phx1*$^+$ transcripts at different growth phases by Northern blotting. As demonstrated in Fig. III-1A, the level of *phx1*$^+$ transcripts was very low during early and mid-exponential phases (lanes 1 and 2). However, the level sharply increased during late exponential phase when cells approached the stationary phase (lane 3), and was maintained high during the stationary phase (lanes 4 and 5).

Since cells enter the stationary phase when starved for nutrients (Herman 2002), we examined the effect of nutrient shift-down during the exponential growth. For this purpose, prototrophic wild-type cells (972 strain) grown to mid-exponential phase in EMM were transferred to nitrogen-free EMM (EMM–N) or to low glucose EMM (EMM containing 0.5% glucose). The mRNA levels of *phx1*$^+$ were measured by quantitative real-time PCR (qRT-PCR) along with the control *act1*$^+$ mRNA. As demonstrated in Fig. III-1B, the relative level of *phx1*$^+$ mRNA increased dramatically at earlier growth time in N-source or C-source limited conditions compared with the non-starved condition. Auxotrophic strain (JH43) also have been checked and the patterns were similar with prototroph one (data not shown). These results indicate that the stationary phase induction of *phx1*$^+$ gene expression is due partly to nutrient starvation of N- or C-source.

III.1.2. Phx1 protein is localized primarily in nucleus at stationary phase and by nutrient starvation

In order to examine its expression and subcellular localization, we made a construct to encode Phx1 fused with GFP at C-terminus, by integrating the

Fig. III-1. Changes in *phx1*$^+$ mRNA level during vegetative cell growth and in nutrient starved conditions.

(A) Expression profile of *phx1*$^+$ gene during growth. After inoculation with freshly grown wild-type (JH43) cells in EMM to an initial OD_{600} of 0.02, RNA samples for different lengths of culture time were prepared and analyzed for *phx1*$^+$ mRNA by Northern blot. The sampling time corresponds to early exponential (EE, at around 12 h), mid-exponential (ME, at around 20 h), late exponential (LE, at around 28 h), early stationary (ES, at around 36 h), and late stationary (LS, at around 60 h) phases.

(B) Induction of *phx1*$^+$ mRNA by nutrient starvation. Prototrophic wild-type cells (972) were grown in EMM to OD_{600} of 0.5~1 and then transferred to modified EMM without NH_4Cl (EMM-N) or with low (0.5%) glucose, for further incubation. At 3, 6, 9 and 12 h after media transfer, cells were taken for RNA analysis by qRT-PCR. The amount of *phx1*$^+$ mRNA was measured by qRT-PCR, along with that of *act1*$^+$ mRNA as an internal control. Average induction folds from three independent experiments were presented with standard deviations.

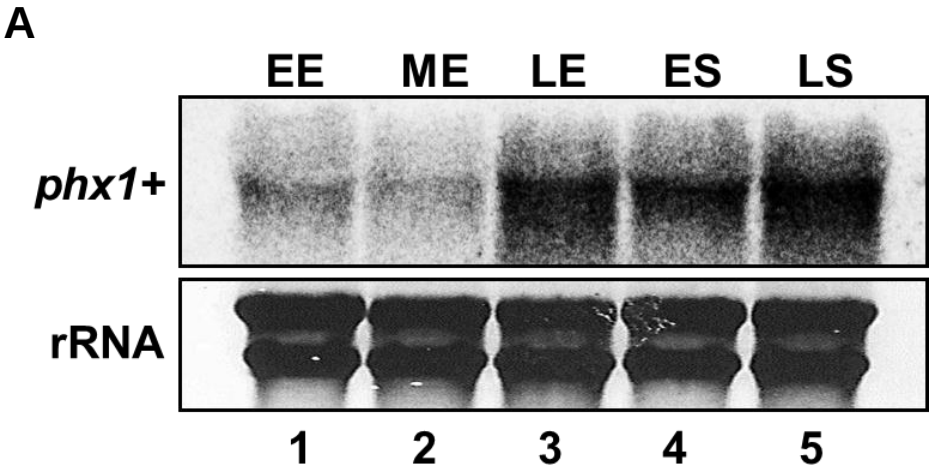
A
EE
ME
LE
ES
LS
phx1+
rRNA
1
2
3
4
5

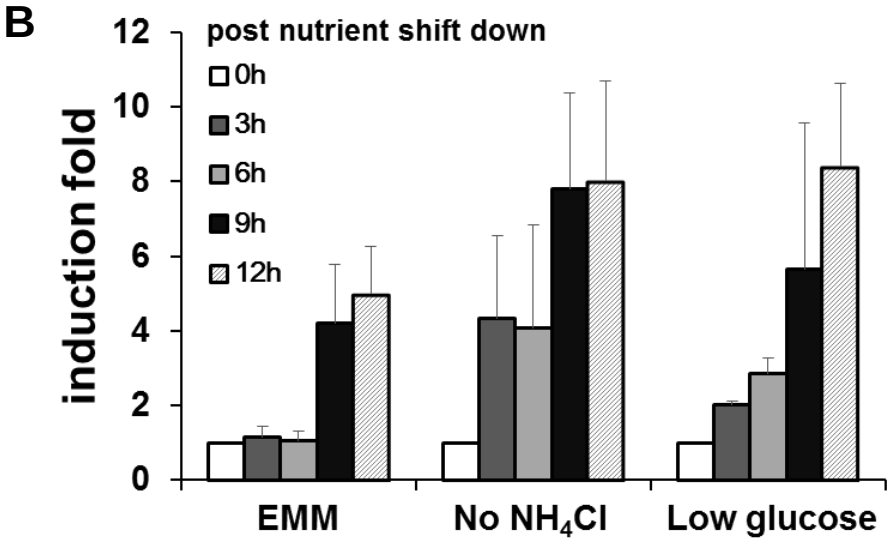
B
post nutrient shift down
0h
3h
6h
9h
12h
induction fold
0
2
4
6
8
10
12
EMM
No NH4Cl
Low glucose

fused gene into the chromosome. Cells were grown in Edinburgh minimal medium (EMM) and examined for fluorescence at different growth phases. The GFP fluorescence began visible at late exponential phase and became very evident in the nucleus during the stationary phase (Fig. III-2A). The nuclear localization of Phx1 is in agreement with the genome-scale analysis data of protein localization in *S. pombe* (Matsuyama *et al.* 2006). Furthermore, this coincides with the transcription level of *phx1*$^+$ (Fig. III-1A). Since mRNA level of *phx1*$^+$ increased in N-source or C-source limited conditions (Fig. III-1B), Phx1 protein level was also examined in these conditions. GFP-tagged Phx1 protein accumulated in the nucleus earlier in both N-starved and C-starved conditions than in non-starved condition (Fig. III-2B). Interestingly, the cells in EMM without glucose (0% C) showed accumulated Phx1-GFP protein in the nucleus at 30 min after media transfer and seemed to die rapidly. Anyway, all of these results indicated that the level of Phx1 protein is determined largely by its transcript level.

III.1.3. The *phx1*$^+$ gene is required for long-term survival during the stationary phase and under nutrient-starved conditions

As *phx1*$^+$ gene was induced during stationary phase and by nutrient starvation, we investigated its role in cell survival under those conditions. For this purpose, Δ*phx1* null mutant was constructed (ESX5, by Dr. Kwon) and examined for its growth phenotype. The mutant strain did not show any significant difference in morphology, growth rate, or viability during the vegetative growth phase. However, when grown to the stationary phase in liquid EMM, Δ*phx1* cells lost viability more quickly than the wild type when monitored by colony formation (Fig. III-3A). This defect in long-term viability of Δ*phx1* mutant was rescued by ectopic expression of *phx1*$^+$ (Fig. III-3B). In addition, overproduction of Phx1 in the wild-type strain

Fig. III-2. Intracellular localization of Phx1-GFP fusion protein during the growth and in nutrient-starved conditions.

(A) Localization of Phx1-GFP. Cells containing the chromosomally integrated fusion gene for Phx1-GFP were grown in liquid EMM at 30°C. Aliquots taken during the early exponential (OD_{600} of 0.2-0.3, EE), middle exponential (OD_{600} of 1, ME), late exponential (OD_{600} of 7-8, LE), early stationary (OD_{600} of 8-9, ES) and late stationary (OD_{600} of 8-9, LS) phases were examined for fluorescence and DIC images by fluorescence microscopy (Axiovert 200M, Carl Zeiss). Wild-type (JH43) cells that were not containing GFP protein were observed as a negative control.

(B) Localization of Phx1-GFP under nutrient starvation. Cells containing the chromosomally integrated fusion gene for Phx1-GFP were grown to middle exponential phase (OD_{600} of 1) in liquid EMM at 30°C. After then, cells were transferred to nutrient-starved media (N; EMM with no nitrogen source, 0.5% C; EMM containing 0.5% glucose, 0% C; EMM with no glucose). Aliquots taken from the culture after media transfer at indicated times were examined for fluorescence and DIC images by fluorescence microscopy (Axiovert 200M, Carl Zeiss).

(C) Growth curve of wild-type (JH43) and chromosomally integrated Phx1-GFP strains (ESXF) in condition (A) and (B). The times for microscopy are indicated in the graph.

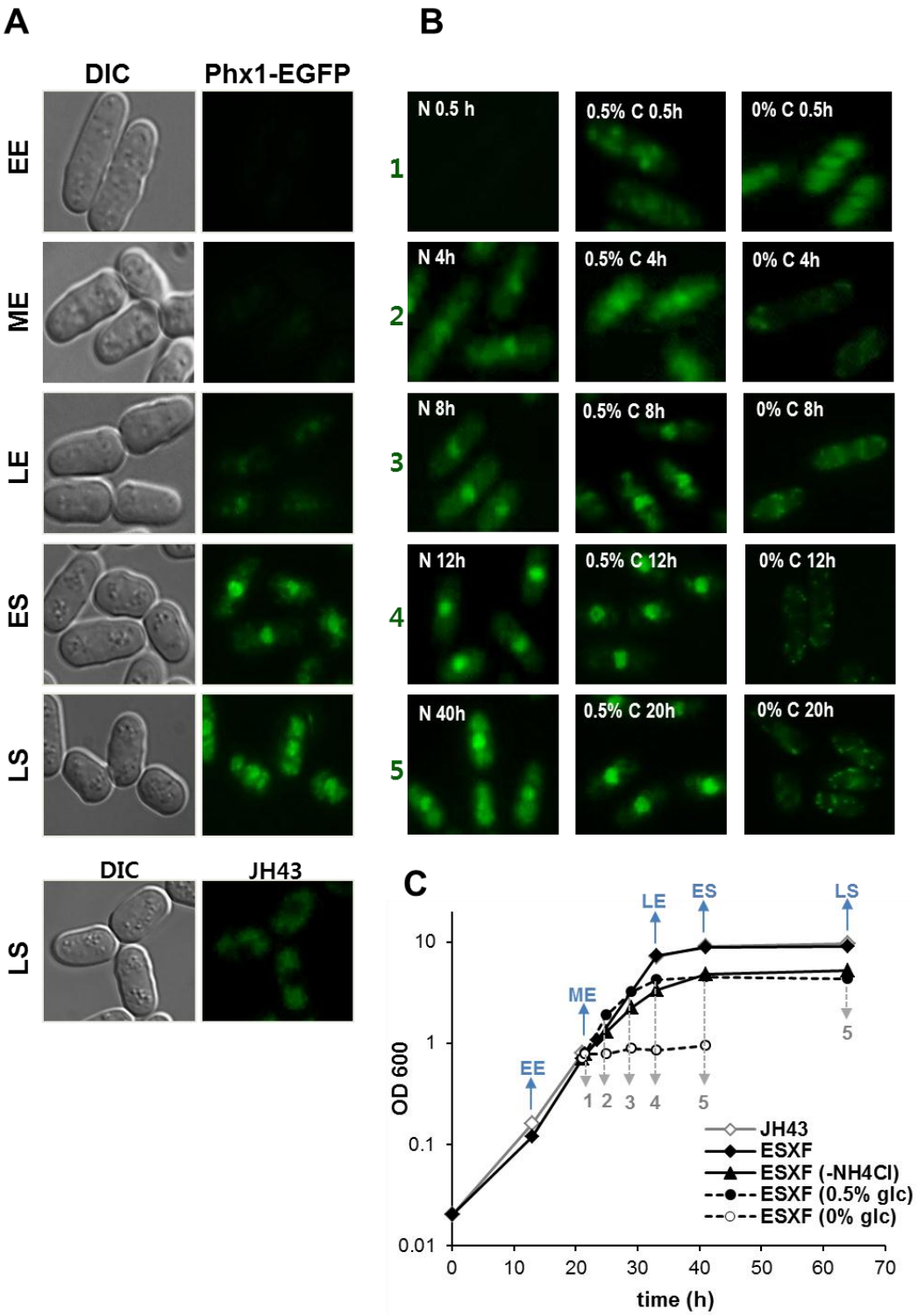
A
DIC
Phx1-EGFP
EE
ME
LE
ES
LS
DIC
JH43
LS
B
N 0.5 h
0.5% C 0.5h
0% C 0.5h
1
N 4h
0.5% C 4h
0% C 4h
2
N 8h
0.5% C 8h
0% C 8h
3
N 12h
0.5% C 12h
0% C 12h
4
N 40h
0.5% C 20h
0% C 20h
5
C
LE
ES
LS
ME
EE
1 2 3 4 5
5
OD 600
10
1
0.1
0.01
0 10 20 30 40 50 60 70
time (h)
JH43
ESXF
ESXF (-NH4Cl)
ESXF (0.5% glc)
ESXF (0% glc)

Fig. III-3. Viability of Δ*phx1* mutant cells in long-term culture.

Wild-type and Δ*phx1* mutant cells were grown in liquid EMM until they reached the stationary phase at OD_{600} of 8-9 (day 0). From this time point, aliquots were plated out on solid complex medium daily, and the surviving colonies were counted after 3~4 days of incubation at 30°C. At least three independent experiments were carried out to obtain survival curves for each strain. **(A)** The viability of wild type (JH43) and Δ*phx1* mutant (ESX5) in EMM. **(B)** The viability in EMM of wild type (JH43) and Δ*phx1* (ESX5) mutant cells containing pWH5 vector or pWH5-*phx1*$^{+}$ plasmid. **(C, D)** The viability of prototrophic wild type (972) and Δ*phx1* (JY01) in modified EMM without N-source **(C)** or with 0.5% glucose **(D).**

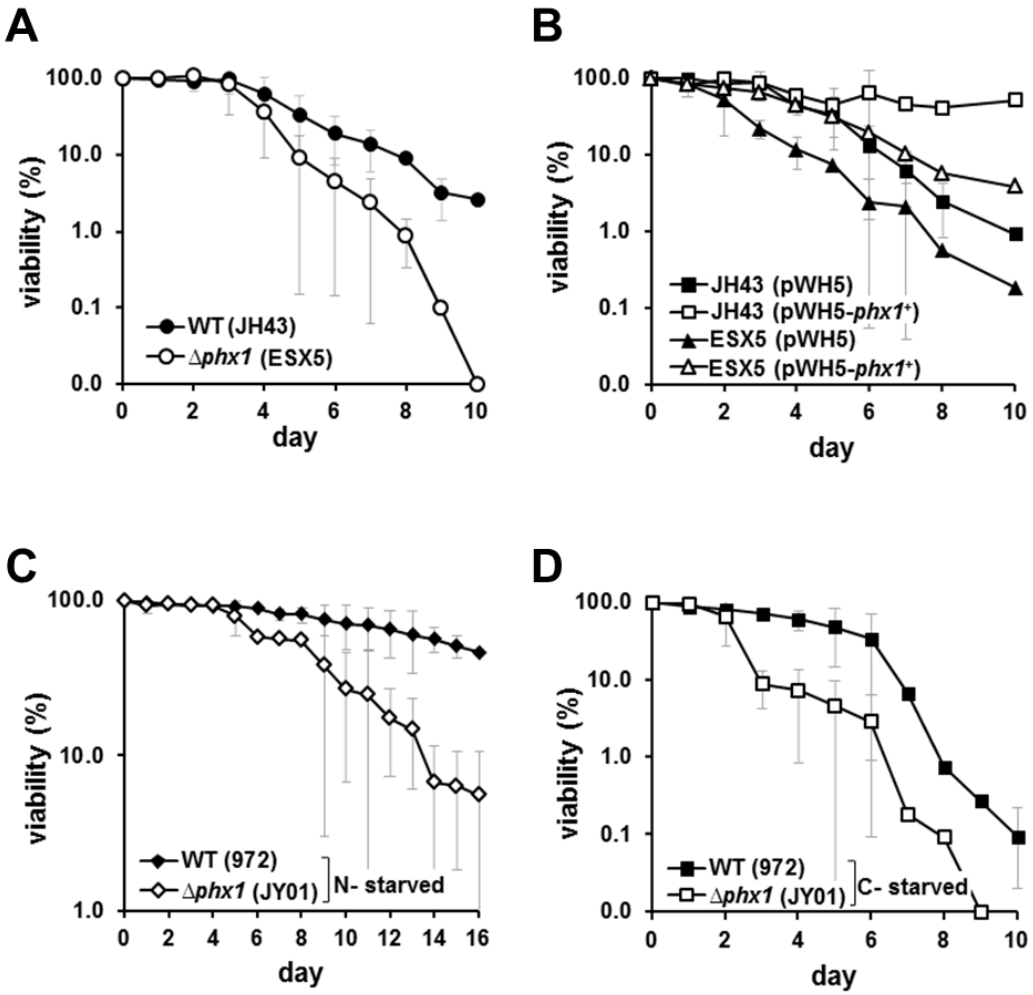
A
100.0
10.0
1.0
0.1
0.0
viability (%)
0
2
4
6
8
10
day
WT (JH43)
Δphx1 (ESX5)
B
100.0
10.0
1.0
0.1
0.0
viability (%)
0
2
4
6
8
10
day
JH43 (pWH5)
JH43 (pWH5-phx1+)
ESX5 (pWH5)
ESX5 (pWH5-phx1+)
C
100.0
10.0
1.0
viability (%)
0
2
4
6
8
10
12
14
16
day
WT (972)
Δphx1 (JY01)
N- starved
D
100.0
10.0
1.0
0.1
0.0
viability (%)
0
2
4
6
8
10
day
WT (972)
Δphx1 (JY01)
C- starved

greatly enhanced long-term viability (Fig. III-3B). Therefore, it is clear that Phx1 confers cells with fitness during long-term cultures, enhancing their survival rates. When long-term survival experiments of Fig. III-3A were repeated with the strains (wild type 972 and Δ*phx1* JY01) without auxotrophic markers, similar pattern was observed (data not shown).

We then examined the viability of Δ*phx1* under nutrient-starved conditions. The wild type (strain 972) maintained its viability for a longer period of time in N-starved medium. In comparison, Δ*phx1* (strain JY01) lost its viability at earlier time (Fig. III-3C). In C-starved condition as well, Δ*phx1* lost its viability much quicker than the wild type (Fig. III-3D). Therefore, it appears clear that Phx1 serves a critical role in conferring fitness to the stationary phase cells or cells under nutrient starvation, and thus enables them to maintain viability for longer period of time.

Genetic studies have identified some genes that function in extending lifespan. In *S. pombe*, as in *S. cerevisiae*, cAMP/Pka1 and Sck2 signaling pathways have been shown to regulate chronological aging (Fabrizio and Longo 2003; Roux *et al.* 2006; Zuin *et al.* 2010). It has also been reported that respiration-defective mitochondrial dysfunction shortens chronological life span through elevating oxidative stresses (Zuin *et al.* 2008). Whether Phx1 is related with these signaling pathways and/or mitochondrial functions, and how, if it is, will be an interesting question to solve in the near future.

III.2. Roles of Phx1 in Stress Response

III.2.1. Δ*phx1* mutant is sensitive to oxidative and heat stress

It is widely accepted that cells in the stationary phase experience not only nutrient starvation, but also other stresses such as oxidation of cell components that include proteins and nucleic acids (Jakubowski *et al.* 2000).

Therefore, stationary-phase cells activate various stress defense systems, and this defense is critical for long-term survival. To find out whether Phx1 is involved in tolerating various stresses other than nutrient starvation, we examined the sensitivity of Δ*phx1* mutant to various oxidants and heat. As exemplified in Fig. III-4A, Δ*phx1* mutant became sensitive to oxidants such as H_2O_2 (peroxidation agent), paraquat and menadione (superoxide-generating agent), diamide (thiol-specific oxidant) chronically and acutely, and also to acute heat-shock at 42°C. These results indicate clearly that Phx1 confers fitness to cells not only during nutrient starvation but also under oxidative and heat stress conditions. We analyzed whether these stress conditions induce the expression of the *phx1*$^+$ gene by qRT-PCR. The results in Fig. III-4B demonstrate that these acute stresses indeed elevated the level of *phx1*$^+$ mRNA.

III.2.2. Δ*phx1* mutant cells accumulate reactive oxygen species (ROS) at stationary phase

Since the cells lacking Phx1 were defective in gain of stress-resistance, we also measured the level of ROS production in Δ*phx1* mutant cells. Most ROS are generated as byproducts of the cellular respiration, therefore we first checked the respiratory rates. Oxygen consumption, as an indicator of respiratory rates, was higher in wild-type cells than in Δ*phx1* mutants during vegetative growth (Fig. III-5A). However, after the onset of stationary phase, the situation was reversed. Δ*phx1* mutant cells consumed oxygen more than wild-type cells during stationary phase. The lower rate in Δ*phx1* mutant cells after about 70 h was considered due to the cell death. For measurement of ROS production, we used the redox-sensitive fluorescent dye 2′,7′-Dichlorofluorescin diacetate (DCFH-DA). DCFH-DA is a cell-permeable non -

Fig. III-4. Stress-sensitivity of Δ*phx1* mutant cells and the inducibility of *phx1*$^+$ gene by various stresses.

(A) Stress-sensitivity of Δ*phx1* mutant cells. To examine sensitivity of the wild-type (JH43) and *Δphx1* mutant (ESX5) cells to chronic oxidative and heat stress, exponentially growing and stationary-phase cells in liquid EMM at 30°C were serially diluted, spotted onto EMM plates containing 0.2 mM of H_2O_2, 200 μM of paraquat, or 5 μM menadione. Spotted cells were incubated at 30°C for 4 to 5 days. To examine sensitivity of the wild-type (JH43) and *Δphx1* mutant (ESX5) cells to acute oxidative and heat stress, exponentially growing cells in liquid EMM at 30°C were treated with 10 mM of H_2O_2, 20 mM of paraquat, 20 mM of diamide, or 2 mM menadione for 40 min each, or transferred to 42°C incubator for 20 min. Following stress treatment, equal number of cells were serially diluted, spotted onto EMM plates, and incubated at 30°C for 4 to 5 days.

(B) Inducibility of *phx1*$^+$ gene by various stresses. The wild-type (JH43) cells were grown to mid-exponential phase (OD_{600} of 0.5-1) in liquid EMM at 30°C, and treated with 10 mM hydrogen peroxide, 20 mM paraquat (PQ), 20 mM diamide (DA), or 2 mM menadione (MD) for 40 min each, or heat-shocked at 50°C for 30 min. RNA samples were analyzed for the level of *phx1*$^+$ transcript in comparison with *act1*$^+$, an internal control, by qRT-PCR. The average induction folds with standard deviations (error bars) from three independent experiments were presented.

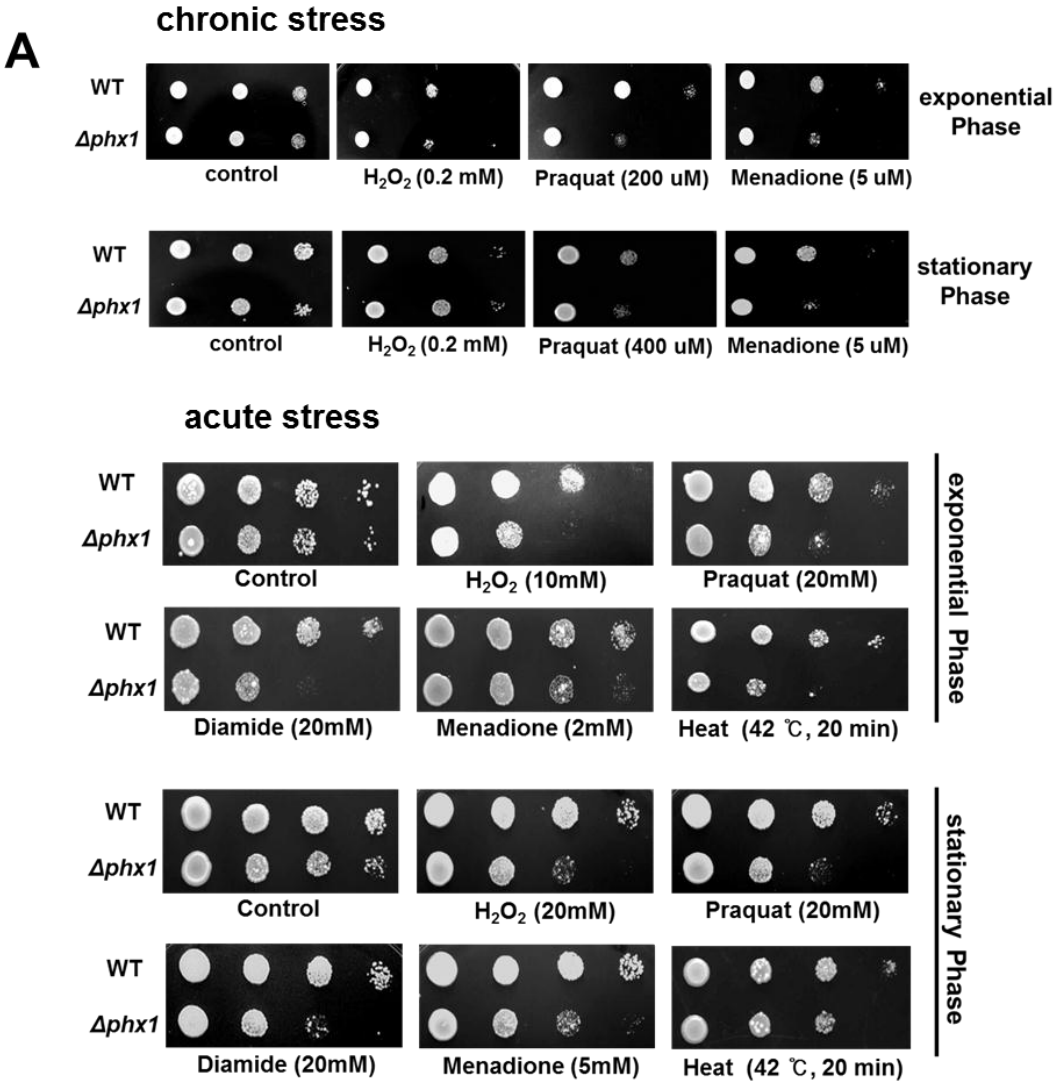
A
chronic stress
WT
Δphx1
control
H2O2 (0.2 mM)
Praquat (200 uM)
Menadione (5 uM)
exponential Phase
WT
Δphx1
control
H2O2 (0.2 mM)
Praquat (400 uM)
Menadione (5 uM)
stationary Phase
acute stress
WT
Δphx1
Control
H2O2 (10mM)
Praquat (20mM)
WT
Δphx1
Diamide (20mM)
Menadione (2mM)
Heat (42 ℃, 20 min)
exponential Phase
WT
Δphx1
Control
H2O2 (20mM)
Praquat (20mM)
WT
Δphx1
Diamide (20mM)
Menadione (5mM)
Heat (42 ℃, 20 min)
stationary Phase

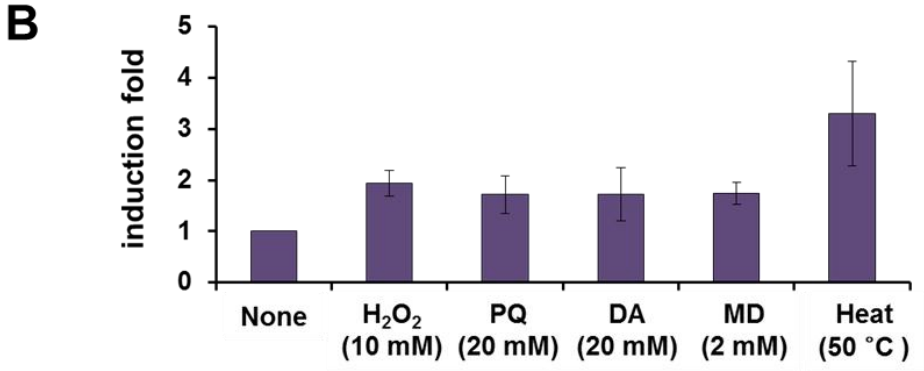
B
induction fold
0
1
2
3
4
5
None
H2O2 (10 mM)
PQ (20 mM)
DA (20 mM)
MD (2 mM)
Heat (50 °C)

Fig. III-5. Oxygen consumption and ROS production in Δ*phx1* mutant cells.

(A) Oxygen consumption along the growth. Wild-type strain (JH43) and Δ*phx1* (ESX5) mutant cells were grown in EMM media at 30°C. OD_{600} (diamonds) and oxygen consumption (circles) were recorded at different times during the growth curve.

(B) Relative intracellular H_2O_2 levels of cells grown in EMM media. Wild-type strain (JH43) and Δ*phx1* (ESX5) mutant cells were grown to stationary phase in EMM media at 30°C. At the indicated culture-time points, cells were incubated with the redox-sensitive fluorescent dye 2′,7′-Dichlorofluorescin diacetate (DCFH-DA), and the fluorescence of cells was analyzed by flow cytometry, as described in 'Materials and methods'. All the values are compared to that of wild-type strain cultures at 12 h, with an assigned value of 1. Cells grown from three independent cultures were examined to obtain average values.

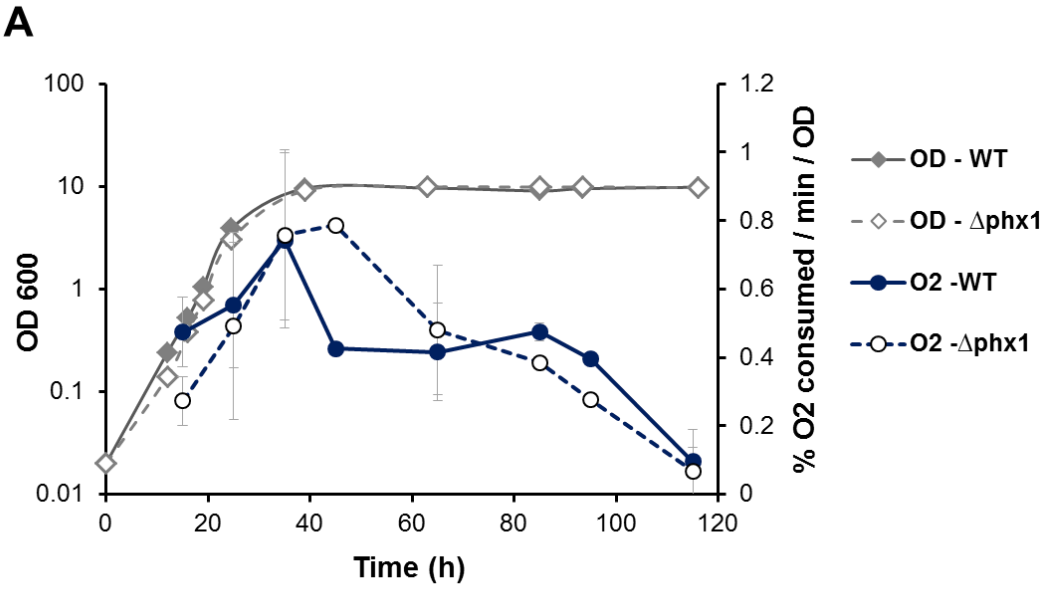
A
100
10
1
0.1
0.01
OD 600
0
20
40
60
80
100
120
Time (h)
1.2
1
0.8
0.6
0.4
0.2
0
% O2 consumed / min / OD
OD - WT
OD - Δphx1
O2 -WT
O2 -Δphx1

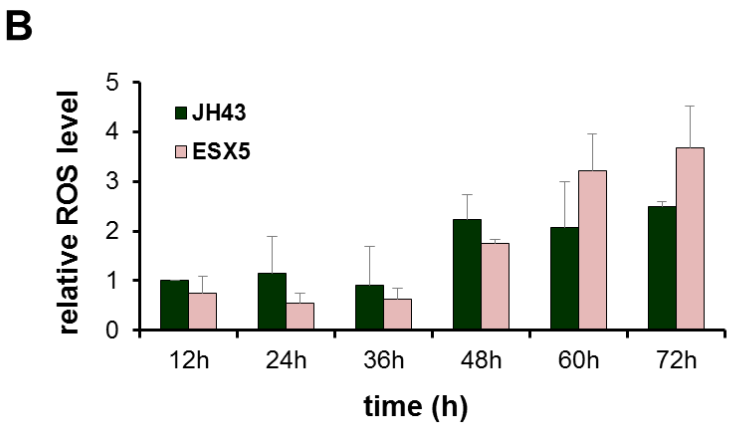
B
relative ROS level
5
4
3
2
1
0
JH43
ESX5
12h
24h
36h
48h
60h
72h
time (h)

fluorescent ROS indicator, which can passively diffuse across membranes and then can be de-esterified intracellularly and turns to highly fluorescent 2′,7′-dichlorofluorescein upon oxidation. Interestingly, ROS productions in the Δ*phx1* mutant and wild-type cells showed similar pattern with respiratory rates all along the growth phase (Fig. III-5B). ROS accumulation increased as cells growing in both wild-type and Δ*phx1* mutant cells. ROS level in Δ*phx1* mutant cells were lower than wild-type cells until 48 h, but the state was reversed after then, suggesting that decreased stationary-phase survival of Δ*phx1* mutants is partially due to ROS toxicity.

Unexpectedly, ROS level generated in Δ*phx1* mutant was lower than wild type at exponential phase. Recently, some reports proposed the hypothesis that long-lived yeast strains with reduced target of rapamycin (TOR) pathway have greater overall mitochondrial electron transport chain activity during exponential growth and this lead to increases ROS production, which an adaptive signal during growth that extends chronological lifespan (CLS) (Pan *et al*. 2011). This suggests that Δ*phx1* mutant cells may have defects of adaptation process during growth, causing short chronological lifespan.

III.2.3. Δ*phx1* mutant cells show low ethanol tolerance

As Phx1 was regarded as a regulator protein for stationary phase, we examined the Δ*phx1* mutant cells for ethanol tolerance as one of stationary-phase properties. Cells lacking Phx1 was sensitive to ethanol treatment at stationary phase in both complex (YES) and minimal (EMM) media (Fig. III-6). This result indicates that the increased sensitivity to ethanol of Δ*phx1* mutant cells was a reflection of incomplete maintenance in stationary phase along with oxidative and heat stress sensitivities.

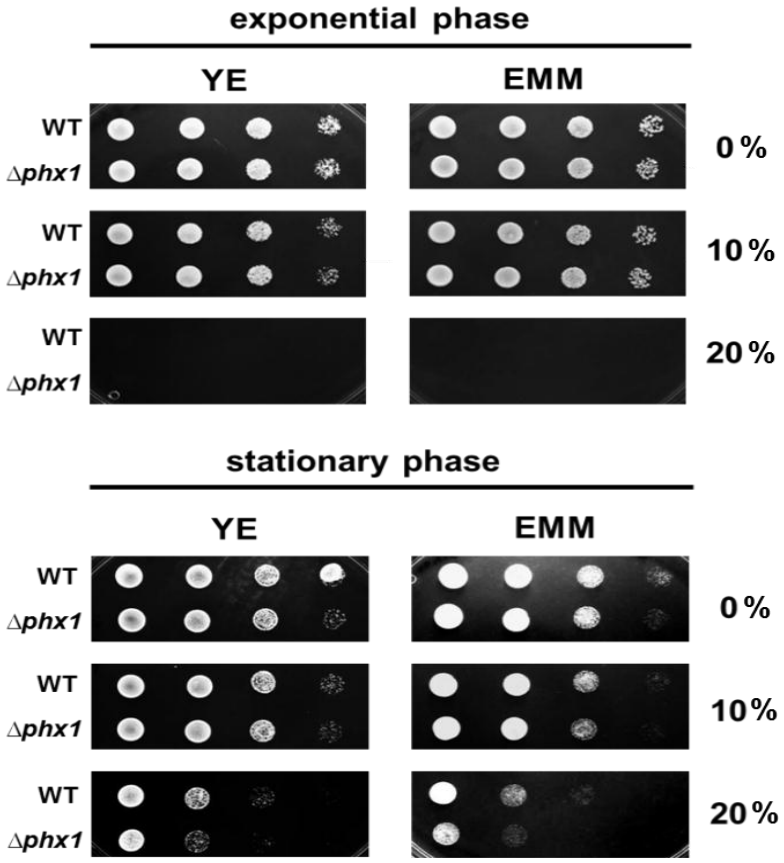

Fig. III-6. Ethanol tolerance of wild-type and Δ*phx1* mutant cells.

To examine sensitivity of the wild-type (972) and *Δphx1* (JY01) mutant to ethanol treatment, exponentially growing and stationary-phase cells in liquid EMM at 30°C were treated with 0, 10, and 20% of ethanol for 30 min. Following stress treatment, equal number of cells were serially diluted, spotted onto YE and EMM plates, and incubated at 30°C for 4 to 5 days.

III.3. Roles of Phx1 in Meiosis

III.3.1. The Δ*phx1* / Δ*phx1* diploids are defective in sporulation

When cells are starved of nutrients such as nitrogen or carbon sources, haploid yeast cells find other mating-type partners, conjugate to form diploids, which subsequently undergo meiotic division and sporulation. All of these sexual developmental processes are controlled by an extensive gene expression program (Mata *et al.* 2002; Mata *et al.* 2007). Genome-wide analysis of *S. pombe* transcriptome has revealed that *phx1*$^+$ (SPAC32A11.03C) is one of the genes that are highly induced during meiotic spore formation (Mata *et al.* 2002). This led us to examine whether Phx1 plays any role in meiosis. We first examined the mating efficiency of Δ*phx1* mutant cells. Using the iodine staining, we observed that crossing *h*$^-$ and *h*$^+$ haploid Δ*phx1* strains showed no difference in the mating efficiency with that of wild type (Fig. III-7A). Mating efficiency by counting the number of zygote and asci was confirmed this tendency again (Fig. III-7B). Crossing *h*$^-$ and *h*$^+$ haploid Δ*phx1* strains showed similar mating efficiency (54.2±0.5%) to that of the wild type (56.7±0.9%) (Fig. III-7B). Crossing the wild type and Δ*phx1* was similarly effective (53.1± 2.9%). This suggests that Δ*phx1* mutation does not significantly impair conjugation and diploid formation. Therefore we obtained homozygous diploid strain Δ*phx1* / Δ*phx1* and examined the formation of tetrad meiotic spores by incubating in EMM. In comparison to the wild type, the mutant cells were very low in forming tetrad-containing asci, and mostly remained as cells with single large nucleus as monitored by DAPI staining (Fig. III-7C). Therefore, it appears that Δ*phx1* / Δ*phx1* diploid cells are defective in completing the first meiotic division (Mata *et al.* 2002). The sporulation efficiency was determined by counting the number of asci among at least 500 cells counted. Compared with the wild-type cells which demonstrated up to about 50% sporulation

Fig. III-7. Sporulation defect of Δ*phx1* / Δ*phx1* mutant diploid cells.

(A) Visualization of mating efficiency by iodine staining. Iodine vapors stain starch present in the *S. pombe* spores with dark blue. ED665, ED668, ESX5, and ESX8 haploid strains were used as negative controls.

(B) Quantification of the mating efficiency. Mating cells grown on ME plate for 3 days at room temperature were examined under the microscope (Axiovert 200M, Carl Zeiss) to count the number of zygotes and zygotic asci. The percentage of zygotes and zygotic asci formation among a total of more than 500 counted cells was presented as mating efficiency. Cells grown from three independent cultures were examined to obtain average values.

(C) The wild-type and mutant diploid cells were grown to the stationary phase (OD_{600} of 8-9; ~70 h culture) in EMM at 30°C and examined under the microscope. Representative DIC and DAPI images were presented.

(D) Quantification of the sporulation efficiency. Diploid cells grown for different lengths of time at 30°C in EMM were examined under the microscope to count the number of spore-containing asci. The percentage of asci formation among a total of more than 500 counted cells was presented as sporulation efficiency. Cells grown from three independent cultures were examined to obtain average values.

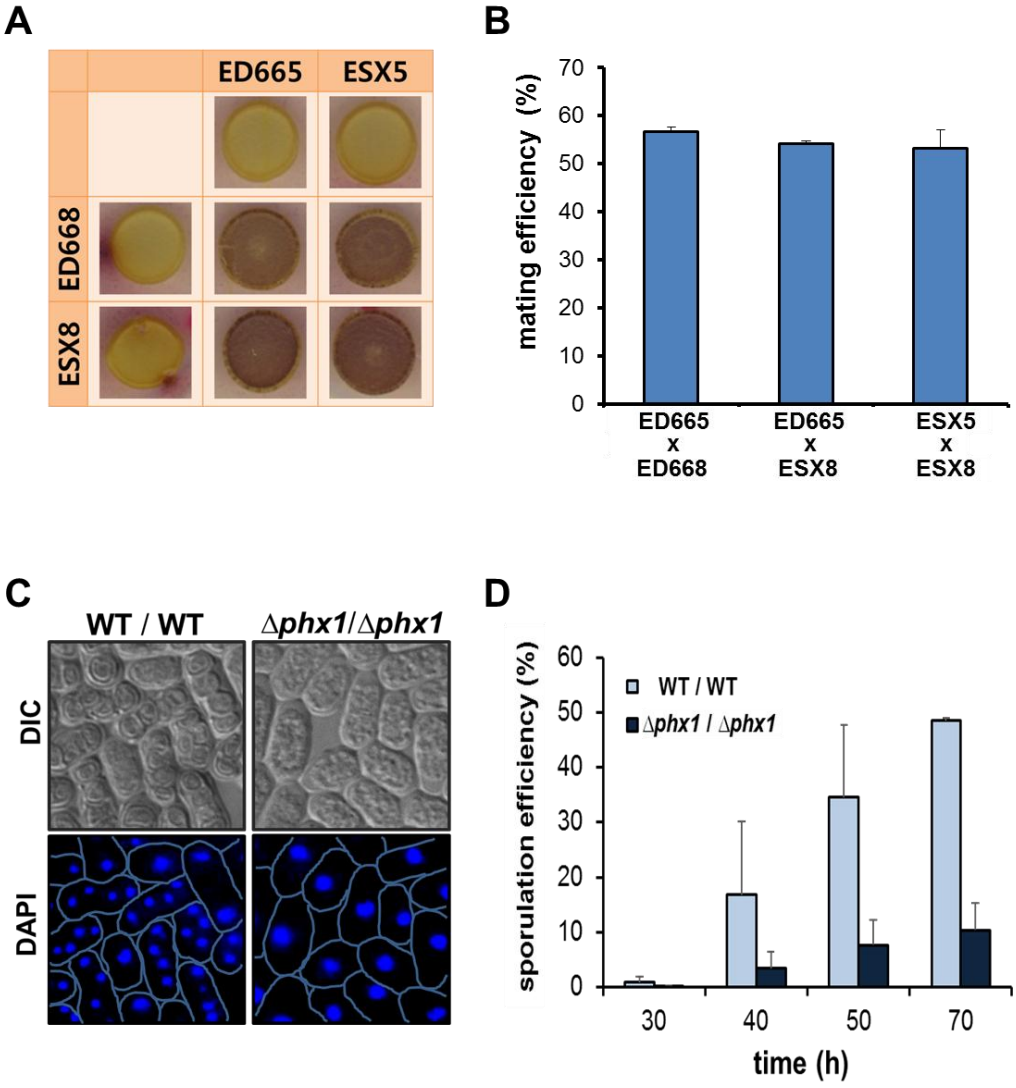
A
ED665
ESX5
ED668
ESX8
B
mating efficiency (%)
70
60
50
40
30
20
10
0
ED665 x ED668
ED665 x ESX8
ESX5 x ESX8
C
WT / WT
Δphx1/Δphx1
DIC
DAPI
D
sporulation efficiency (%)
60
50
40
30
20
10
0
WT / WT
Δphx1 / Δphx1
30
40
50
70
time (h)

efficiency, the mutant diploids exhibited only about 10% efficiency (Fig. III-7D).

III.4. Genome-Wide Transcriptional Profiling Analysis of Δ*phx1* Mutant

In order to understand the role of Phx1 in further detail, we performed microarray analysis of RNA samples obtained from the wild-type and Δ*phx1* mutant cells grown in EMM. Since Phx1 had functions during stationary phase and the viability of Δ*phx1* mutant rapidly decreased after 90 h of culture (2 days after onset of stationary phase), we prepared RNA samples from the harvested cells at 80 h of growth time. RNA samples from four independent cultures of the wild type and Δ*phx1* mutant were extracted and used as for cDNA synthesis and hybridization (by Luis López-Maury from Jürg Bähler's lab in UCL). The global analysis revealed that transcripts from 97 genes were increased by more than 2-fold in the Δ*phx1* mutant compared to the wild-type strain. In contrast, transcripts from 99 genes were decreased by less than 0.6-fold in the same condition mentioned above. The values of folds were obtained from the average of the four samples. We examined 40 transcripts among induced or repressed genes by quantitative real-time PCR, and confirmed that the microarray results were quite reliable. Table III-1 is a list of genes that showed elevated expressions in the Δ*phx1* mutant. This suggested negatively regulation by Phx1. Table III-2 represents genes that reduced expressions in the Δ*phx1* mutants. This suggested positively regulated by Phx1. By generic GO-term finder (http://go.princeton.edu/cgi-bin/GOTermFinder), we grouped these genes according to their cellular processes. The genes negatively regulated by Phx1 were involved in transport, carbohydrate/energy metabolism (especially in mitochondria-related,

Table III-1. List of the induced genes in *Δphx1* mutant cells

systematic name	gene name	Description	Induction fold Mean	(±SD)	meiotic expression	overlapped function
cellular carbohydrate & energy metabolism						
oligosaccharide catabolic process						
SPAPB24D3.10c	agl1	alpha-glucosidase Agl1,	18.84	5.0	late	
SPCC191.11	inv1	beta-fructofuranosidase,	11.32	5.2		
SPAC1039.11c		alpha-glucosidase, SPAC922.02c	2.30	0.3	middle	
tricarboxylic acid metabolic process & mitochondria related						
SPCC191.07	cyc1	cytochrome c, cyc1	2.60	0.6		
SPAC6C3.04	cit1	citrate synthase	2.37	0.5		
SPAC24C9.06c	aco1	aconitate hydratase	2.32	0.2		
NADH oxidation						
SPAC3A11.07		NADH dehydrogenase	2.21	1.3		
pentose-phosphate shunt, oxidative branch/NADPH regeneration						
SPAC26H5.09c		gfo/idh/mocA family oxidoreductase (predicted)	3.34	0.0		
SPAC3C7.13c		glucose-6-phosphate 1-dehydrogenase,	2.16	0.8	continuous	cellular response to stimulus
SPAC3A12.18	zwf1	glucose-6-phosphate 1-dehydrogenase, SPAC9.01	2.05	0.9		cellular response to stimulus
SPAC4G9.12		gluconokinase	3.02	0.6	middle	
monocarboxylic acid metabolic process						
SPACUNK4.10		2-hydroxyacid dehydrogenase,glyoxylate reductase (predicted)	3.90	2.9		
alcohol metabolic process						
SPCC1223.03c	gut2	glycerol-3-phosphate dehydrogenase Gut2,	2.55	1.1	delayed	cellular response to stimulus
SPAC9E9.09c		aldehyde dehydrogenase (predicted)	2.44	1.1		cellular response to stimulus
SPAC25B8.03	psd2	phosphatidylserine decarboxylase	2.14	1.1		
SPBC1773.05c	tms1	hexitol dehydrogenase	2.08	0.5	late	cellular response to stimulus
SPAC630.08c	erg25	C-4 methylsterol oxidase	2.07	1.5		
nucleoside metabolic process						
SPCC191.05c		nucleoside 2-deoxyribosyltransferase	2.54	1.2	transient	
SPBC800.11		inosine-uridine preferring nucleoside hydrolase	2.11	0.5	transient	
conjugation / meiosis						
SPAC23E2.03c	ste7	meiotic suppressor protein Ste7	4.82	4.7	continuous	
SPAPB8E5.05	mfm1	M-factor precursor	4.57	2.9	delayed	
SPAC22F3.12c	rgs1	regulator of G-protein signaling Rgs1	4.18	2.5	delayed	cellular response to stimulus
SPBC29B5.02c	isp4	OPT oligopeptide transporter family	4.12	2.3	continuous	cellular response to stimulus
SPAC27D7.03c	mei2	RNA-binding protein involved in meiosis Mei2	3.76	2.0	delayed	
SPAC513.03	mfm2	M-factor precursor	3.55	2.0	delayed	
SPBPJ4664.03	mfm3	M-factor precursor	3.14	1.0	delayed	
SPCC1795.06	map2	P-factor	3.10	0.0	delayed	
SPAC25B8.13c	isp7	2 OG-Fe(II) oxygenase superfamily	2.47	0.1	transient	cellular response to stimulus
SPBC32C12.02	ste11, aff1, stex	transcription factor Ste11	2.23	1.1	delayed	
SPAC22A12.07c	ogm1, oma1	protein O-mannosyltransferase Ogm1	2.05	1.2		cellular response to stimulus
SPBC2D10.06	rep1, rec16	MBF transcription factor complex subunit Rep1	2.03	0.0	early	
SPBC25B2.02c	mam1	M-factor transporter Mam1	2.85	2.2	delayed	mating
cellular response to stimulus						
SPAC343.12	rds1	conserved fungal protein, rds1	7.39	5.3	late	
SPAP14E8.02	tos4	FHA domain protein Tos4 (predicted)	4.15	0.0		response to DNA damage stress
SPBC660.05		hypothetical protein	3.12	1.7	continuous	
SPBC1271.08c		sequence orphan	3.07	1.3		
SPCC1739.08c		short chain dehydrogenase	3.02	2.2	continuous	
SPAC20G4.03c	hri1	eIF2 alpha kinase Hri1, hri1	2.19	1.2		response to osmotic stress
SPACUNK4.15		2',3'-cyclic-nucleotide 3'-phosphodiesterase,	2.08	1.1	middle	
SPAC27D7.11c		But2 family protein	2.02	0.6		
cellular response to oxidative stress						
SPAC821.10c	sod1	superoxide dismutase Sod1	2.25	1.2		
SPBC106.02c	srx1	sulphiredoxin	2.20	0.6		
SPAC11D3.16c		sequence orphan	2.09	1.5	transient	
SPAPB1A10.12c	alo1	D-arabinono-1,4-lactone oxidase	2.04	0.3		

systematic name	gene name	Description	Induction fold		meiotic expression	overlapped function
			Mean	(±SD)		
transport						
hexose transport						
SPAC1F8.01	ght3	hexose transporter	4.04	2.6	early	cellular response to stimulus
SPBC1683.08	ght4	hexose transporter	2.98	2.1	early	cellular response to stimulus
SPCC1235.14	ght5	hexose transporter	2.35	1.5	middle	
SPCC548.06c	ght8	hexose transporter	2.13	1.4	middle	
iron assimilation						
SPAC1F7.07c	fip1	iron permease	4.35	1.5		
SPAC1F7.08	fio1	iron transport multicopper oxidase	2.75	1.4		
SPBC947.05c		ferric-chelate reductase	2.58	1.6		
peptide transport						
SPBC13A2.04c	ptr2	PTR family peptide transporter	2.17	0.2		
other transport						
SPBC16A3.02c		mitochondrial peptidase	2.11	0.8	continuous	cellular response to stimulus
SPCC794.03		amino acid permease family	4.13	2.5		
SPCC569.05c		spermidine family transporter	3.73	1.6		cellular response to stimulus
SPBC1348.05		MFS family membrane transporter	3.47	1.5		
SPAC750.02c		MFS family membrane transporter	3.08	1.2	late	
SPBPB2B2.16c		MFS family membrane transporter	2.88	0.7		
SPAC323.07c		MatE family transporter	2.70	3.4	transient	
SPAC1B3.16c	vht1	vitamin H transporter Vth1	2.48	0.5		
SPCC18B5.01c	bfr1, hba2	brefeldin A efflux transporter, SPCPJ732.04c	2.36	1.0		cellular response to stimulus
SPBC530.10c	anc1	mitochondrial adenine nucleotide carrier Anc1	2.36	1.4		
SPAC1610.03c	crp79, meu5	poly(A) binding protein Crp79, mRNA export from nucleus	2.31	0.0	middle	
SPBC530.02		MFS family membrane transporter,	2.11	1.1		
SPBC359.05	abc3	iron-regulated vaculoar ABC type transporter	2.09	1.1		
SPAC222.12c	atp2	F1-ATPase beta subunit,	2.04	0.8		
non-coding RNA						
SPNCRNA.03	prl3	non-coding RNA, poly(A)-bearing RNA (predicted)	4.83	2.0		
SPNCRNA.93		non-coding RNA (predicted)	2.82	0.0		
SPNCRNA.133		non-coding RNA (predicted)	2.75	1.0		
SPNCRNA.134		non-coding RNA (predicted)	2.55	0.8		
SPNCRNA.07	meu3, prl7	non-coding RNA Meu3	2.25	0.1		
SPNCRNA.63			2.04	0.3		
others						
SPAC186.05c		hypothetical protein,	18.17	2.8		
SPAC977.07c		cell surface glycoprotein (predicted)	7.59	0.0		
SPAC186.04c		pseudogene, similar to N-terminal of transmembrane channel	5.74	1.7	continuous	
SPAC1A6.03c		phospholipase,	4.66	2.9		glycerophospholipid catabolic process
SPBC660.14	mik1	mitotic inhibitor kinase Mik1,	4.41	0.0	middle	phosphate metabolic process
SPAC212.03		hypothetical protein,	4.18	0.0		
SPAPB18E9.05c		dubious	3.74	0.7		
SPAC977.04		pseudogene	3.63	1.5		
SPAC977.05c		conserved fungal protein,	3.31	1.4		
SPAC977.02		S. pombe specific 5Tm protein family	3.07	0.6		
SPCC584.16c		sequence orphan,	2.99	1.0		
SPAC513.04		sequence orphan	2.74	0.6		
SPBC359.06		adducin N-terminal domain protein,	2.70	1.5	early	
SPAPB15E9.01c		glycoprotein, , SPAPB18E9.06c	2.67	0.2		
SPBC1348.04		methyltransferase	2.65	0.5		
SPAC977.03		methyltransferase	2.60	0.6		
SPBC9B6.03		zinc finger protein,	2.53	1.3	transient	
SPCC553.10		glycoprotein,	2.46	0.7		cell adhesion
SPCC1450.07c		D-amino acid oxidase,FAD dependent oxidoreductase	2.30	0.8	transient	
SPBPB2B2.19c		S. pombe specific 5Tm protein family	2.29	0.1	late	
SPBC1348.03		S. pombe specific 5Tm protein family	2.28	1.2		
SPBC1773.14	arg7	argininosuccinate lyase,	2.26	0.1		glutamine family amino acid biosynthetic process
SPAC977.01		S. pombe specific 5Tm protein family	2.22	0.2	late	
SPAC27E2.04c		dubious	2.14	0.0		
SPAC24C9.08		vacuolar carboxypeptidase (predicted)	2.11	0.8		vacuolar protein catabolic process

total	40
transient	7
continuous	7
delayed	9
early	4
middle	7
late	6

Table III-2. List of the repressed genes in *Δphx1* mutants

systematic name	gene name	Description	Induction fold mean	Induction fold (±SD)	meiotic expression	overapped fuction
thiamin and derivative biosynthetic process						
SPCC1223.02	nmt1,thi3	no message in thiamine, nmt1, thi3	0.07	0.11		
SPBC26H8.01	nmt2, thi2	thiazole biosynthetic enzyme, thi2, nmt2	0.46	0.33		
SPBC530.07c		TENA/THI domain	0.47	0.07		
carbohydrate metabolic process						
SPBC1105.05	exg1	glucan 1,3-beta-glucosidase I/II precursor, exg1	0.56	0.11		cell wall metabolic process
glycolysis						
SPBPB21E7.01c	eno1	enolase, eno102, SPAP8B6.07c, SPBPB8B6.07c, SPAPB21E7.01c, eno1	0.11	0.07		
SPBC354.12	gpd3	glyceraldehyde 3-phosphate dehydrogenase Gpd3, gpd3	0.45	0.09		
SPBC32F12.11	gpd1	glyceraldehyde-3-phosphate dehydrogenase Tdh1, tdh1, gpd1	0.56	0		response to stress
disaccharide metabolic process						
SPAC869.07c	mel1	alpha-galactosidase, melibiase	0.54	0.09		
SPAC22F8.05		alpha,alpha-trehalose-phosphate synthase (predicted)	0.59	0.21	middle	response to stress
alcohol catabolic process/glycerol catabolic process						
SPAC977.16c	dak2	dihydroxyacetone kinase Dak2 (PMID 9804990)	0.19	0.03	delayed	
alcohol catabolic process/pyruvate metabolic process						
SPAC13A11.06		pyruvate decarboxylase	0.08	0.06	late	
SPAC3G9.11c		pyruvate decarboxylase (predicted)	0.53	0.2	continuous	
transmembrane transport						
SPBC839.06	cta3	P-type ATPase, calcium transporting Cta3	0.36	0.23		di-, tri-valent inorganic cation homeostasis
SPAC977.17		MIP water channel	0.46	0.12		
SPAC17A2.01	bsu1	high-affinity import carrier for pyridoxine, pyridoxal, and pyridoxamine Bsu1	0.55	0.39		
SPCC757.13		dipeptide transmemembrane transporter (predicted)	0.56	0		
polyamine transport						
SPAC17C9.16c	mfs1	MFS family transmembrane transporter Mfs1	0.28	0.21	transient	
SPBC36.01c		spermidine family transporter	0.51	0.18		
neutral amino acid transport						
SPAP7G5.06	per1	plasma membrane amino acid permease Per1	0.59	0.21	transient	proline transport
SPCPB1C11.03		cysteine transporter (predicted)	0.60	0.42		
inorganic anion transport						
SPBC1683.01		inorganic phosphate transporter,	0.54	0.11		
SPAC869.05c		sulfate transporter (predicted)	0.55	0.06		
SPAC23D3.12		inorganic phosphate transporter (predicted)	0.56	0.41		
response to stress						
SPAC869.09		conserved fungal protein	0.14	0.07	late	
SPAC22H10.13	zym1	metallothionein Zym1	0.29	0.07	early	di-, tri-valent inorganic cation homeostasis
SPAC22G7.11c		conserved fungal protein	0.39	0.07	late	
SPBC8E4.05c		fumarate lyase superfamily	0.45	0.02		
SPBPB2B2.02	mug180	esterase/lipase,	0.52	0.01	middle	Meiotically up-regulated gene
SPAC11D3.01c		conserved fungal protein	0.53	0.15	late	
SPAPYUG7.06	mug67	PPPDE peptidase family (predicted)	0.58	0.17		Meiotically up-regulated gene
response to starvation						
SPAC7D4.04	taf1	Taz1 interacting factor 1	0.33	0.06		autophagy/conjugation/telomere maintenance
SPBC3E7.02c	hsp16	heat shock protein, hsp16	0.40	0.12	middle	response to heat /under conditions of DNA damage
base-excision repair						
SPBC23G7.11	mag2	DNA-3-methyladenine glycosidase Mag2,	0.52	0.12		response to stress
SPAC26A3.02	myh1	adenine DNA glycosylase (PMID 9737967)	0.57	0.08		response to stress

systematic name	gene name	Description	Induction fold mean	Induction fold (±SD)	meiotic expression	overapped fuction
peptidyl-lysine methylation						
SPCC297.04c	set7	histone lysine methyltransferase Set7, set7	0.56	0.19		
SPAC688.14	set13	ribosome L32 lysine methyltransferase Set13	0.58	0		response to stress
RNA metabolic process						
chromatin silencing						
SPBPB21E7.07	aes1	enhancer of RNA-mediated gene silencing, aes1, SPAPB21E7.07	0.36	0.26		chromatin silencing by small RNA
SPBC1105.11c	hht3, h3.3	histone H3, hht3, h3.3	0.60	0.24		response to DNA damage
gene-specific transcription from RNA polymerase II promoter						
SPBC530.08		membrane-tethered transcription factor (predicted)	0.43	0		
SPAC2E12.02	hsf1	transcription factor Hsf1	0.55	0.15		response to stress
rRNA processing /ribosome biogenesis						
SPAC140.02	gar2	nucleolar protein required for rRNA processing	0.58	0.2		
non-coding RNA						
SPNCRNA.26	prl26	non-coding RNA (predicted),poly(A)-bearing RNA	0.26	0		
SPNCRNA.74		antisense RNA (predicted)	0.30	0.06		
SPNCRNA.101		non-coding RNA (predicted)	0.31	0.06		
SPNCRNA.73		antisense RNA (predicted)	0.34	0.04		
SPNCRNA.01	prl01	non-coding RNA (predicte),possibly part of the UTR of eta2	0.37	0.05		
SPNCRNA.79		non-coding RNA (predicted)	0.43	0.13		
SPNCRNA.12	prl12	non-coding RNA (predicted),poly(A)-bearing RNA	0.47	0		
SPNCRNA.132	tos3	antisense RNA (predicted)	0.58	0.34		
SPNCRNA.104		non-coding RNA (predicted)	0.59	0		
SPNCRNA.10	prl10	non-coding RNA (predicted)	0.59	0		
SPSNORNA.32	sno12	12 small nucleolar RNA/small nucleolar RNA snR99	0.60	0.07		
vesicle-mediated transport						
vesicle organization						
SPAC824.02		GPI inositol deacylase	0.32	0.08		quality control and ER-associated degradation of GPI-anchored proteins
SPAC22E12.17c	glo3	ARF GTPase activating protein	0.37	0.03		regulation of signaling pathway
endocytosis						
SPAC3C7.02c		protein kinase inhibitor (predicted)	0.39	0.23	late	response to heat stress
SPCC4F11.04c	imt2	mannosyltransferase complex subunit	0.49	0.14	middle	
protein phosphorylation						
SPBC725.06c	ppk31, mug25	serine/threonine protein kinase, ppk31 (*S.c.* rim15 homologue)	0.09	0.01		Has a role in meiosis.
SPBC19F8.07	crk1	cyclin-dependent kinase activating kinase Crk1, crk1, mop1, mcs6	0.38	0.02	middle	cytokinesis
SPCC70.05c		serine/threonine protein kinase	0.56	0.15		
cytoskeleton organization						
SPBC1289.14		adducin N-terminal domain protein, SPBC8E4.10c	0.40	0.18		response to stress
SPAC4A8.05c	myo3,myp2	myosin II heavy chain Myo3	0.55	0.03		
SPCC417.02	dad5,hsk3, hos3	DASH complex subunit Dad5	0.56	0.08	transient	response to osmotic stress
SPCC338.17c	rad21	mitotic cohesin complex, non-SMC subunit Rad21 (kleisin)	0.57	0.04		response to stress/ DNA repair
oxidation-reduction						
SPBC1198.01		glutathione-dependent formaldehyde dehydrogenase	0.25	0.07	late	
SPAC27D7.12c	but1	neddylation pathway protein But1	0.34	0	middle	Has a role in meiosis, cell elongation
SPAC5H10.04		NADPH dehydrogenase (predicted)	0.5083	0.14		
SPBC1289.16c	cao2	copper amine oxidase-like protein Cao2	0.54	0.12	continuous	amine metabolic process
SPBC115.03	-	gfo/idh/mocA family oxidoreductase (predicted)	0.55	0.08		

systematic name	gene name	Description	Induction fold mean	Induction fold (±SD)	meiotic expression	overapped fuction
others						
SPCC569.08c	ade5	glycinamide ribonucleotide transformylase, ade5, ade8	0.60	0.14		purine metabolism
SPAC11D3.15		5-oxoprolinase (ATP-hydrolizing) (predicted)	0.52	0.01		glutathione metabolic process
SPAC869.06c		HHE domain cation binding protein (predicted)	0.04	0.05	late	mitochondria
SPAPB18E9.04c		glycoprotein	0.07	0.07		cell surface
SPBPB21E7.02c		phosphoglycerate mutase family	0.07	0.03		
SPBPB21E7.04c		human COMT ortholog 2 ,catechol O-methyltransferase activity	0.11	0.04		
SPAC1F7.06		ThiJ domain protein	0.16	0.03	late	
SPAPB18E9.03c		dubious	0.17	0		
SPBC19C7.04c		conserved yeast protein	0.24	0.26	early	
SPAC4F10.17		conserved fungal protein	0.29	0.06	late	
SPAC1093.01		PPR repeat protein (Pentatricopeptide repeat)	0.33	0.1		
SPAC11D3.02c		ELLA family acetyltransferase (predicted)	0.37	0		
SPAC15F9.01c		sequence orphan,central kinetochore associated family protein	0.42	0.01	late	
SPAC9E9.01		dubious	0.45	0.09		
SPAC30D11.02c		sequence orphan	0.46	0		
SPCPB16A4.06c		dubious	0.48	0.02		
SPACUNK4.12c	mug138	metallopeptidase	0.48	0.02	middle	congugation
SPCC417.12		carboxylesterase-lipase family	0.49	0	middle	
SPBC354.11c		dubious	0.51	0.13		
SPAC1142.01		conserved eukaryotic protein, SPAC17G6.18	0.51	0.14		
SPBC2G2.17c	Psu2	beta-glucosidase Psu2 (predicted)	0.53	0.1	late	cell wall localization
SPAC11D3.04c		SnoaL	0.54	0.11		
SPBC651.07	csa1, mug166	COP9/signalosome associated, csa1	0.54	0	middle	Has a role in meiosis.
SPAC1039.02		phosphoprotein phosphatase (predicted)	0.55	0	transient	
SPBC359.04c		cell surface glycoprotein (predicted), DIPSY family	0.55	0.01		cell adhesion
SPBPB2B2.15		conserved fungal protein	0.57	0		
SPAP27G11.16		sequence orphan	0.58	0.13		
SPBPB21E7.08		pseudogene	0.58	0.2		
SPAC652.01		conserved eukaryotic protein	0.59	0.05		
SPMIT.02		mitochondrial DNA binding endonuclease (predicted)	0.59	0.13		This protein is coded in gr oup-I intron 1 of cox1.
SPAC31G5.10	eta2	Myb family transcriptional regulator Eta2	0.60	0.03		expressed during meiosis

total	29
transient	4
continuous	2
delayed	1
early	2
middle	9
late	11

pentose phosphate pathway), conjugation /meiosis, stress response, non-coding RNA, and some other functions (Table III-3). Fig. III-8 showed the relative importance of functions of negatively regulated genes by Phx1 in microarray compared to that of total genome. The genes positively regulated by Phx1 were involved in more various processes, including response to stress, transmembrane transport, carbohydrate metabolism (especially in glycolysis), protein phosphorylation, thiamine biosynthesis, and so on (Table III-4). Fig. III-9 indicated the relative importance of functions of positively regulated genes by Phx1 in comparison with total genome functions. From this global gene expression profiles, Phx1 may have dual functions as a positive or negative regulator according to the different cellular metabolisms. Among the processes which Phx1 is involved in, we focused on thiamine synthesis, carbohydrate metabolism, sexual development, and stress response.

III.4.1. The genes that are involved in thiamine biosynthetic and metabolic processes

Remarkably, the expressions of several genes involved in thiamine biosynthesis or regulation were repressed in *phx1*-deleted mutants (Table III-2). *thi2*$^+$, *thi3*$^+$ encoding biosynthetic enzymes of thiazole and pyrimidine moiety, and *bsu1*$^+$ (*car1*$^+$) encoding pyridoxine, pyridoxal, and pyridoxamine transporter were repressed in Phx1-lacking cells. In addition, there were SPAC13A11.06 and SPAC3G9.11c, which may be predicted to encode pyruvate decarboxylase requiring thiamine pyrophosphate (TPP) and $Mg2^+$ as cofactors for activity. Besides, some genes participated in thiamine biosynthetic pathway (SPBP8B7.18c, SPAC29B12.04, SPBP8B7.17c), transporter (SPBC1604.04), and other predicted pyruvate decarboxylase genes (SPAC1F8.07c) also showed repressed expression tendency, although these genes belonged not to above 2-fold list. These results suggest that Phx1 may

Table III-3. Functional categories of the genes negatively regulated by Phx1 (total 97 genes)

Function	Number of genes	Gene name
transmembrane transport	22	*ght3, ght4, ght5, fip1, fio1, vht1* etc.
cellular carbohydrate & energy metabolism	19	*cyc1, cit1, aco1, zwf1, agl1, inv3* etc.
conjugation / meiosis	13	*mfm1, mfm2, ste7, ste11, mei2, rep1* etc.
cellular response to stress	12	*sod1, srx1, alo1, rds1, tos4, alo1* etc.
Non-coding RNA	6	*prl3, meu3*, SPNCRNA.133 etc.
others	25	*mik1, arg7* etc.

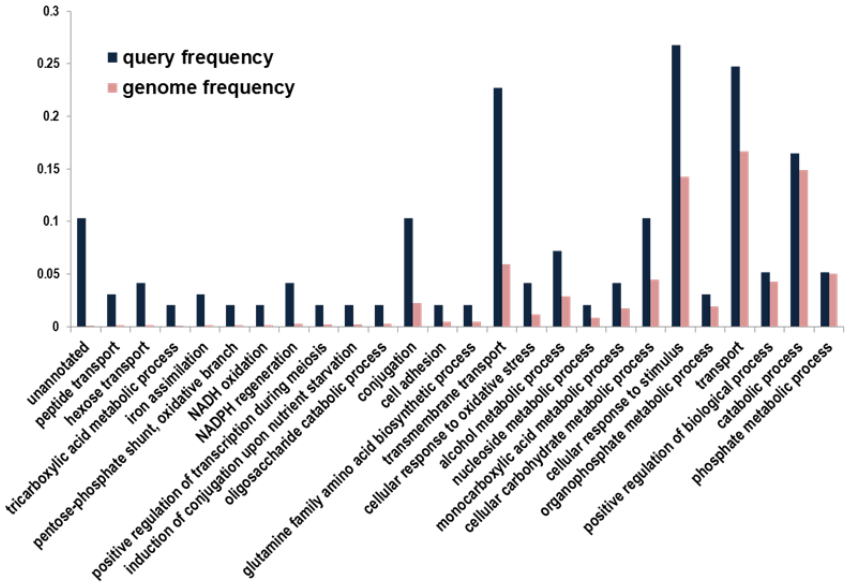

Fig. III-8. GO-term analysis of the genes negatively regulated by Phx1.

Query frequency means the ratio of the number of microarray genes in each function to total number of microarray query genes (97 genes). Genome frequency means the ratio of the number of genes in each function to total number of genes in whole genome (5000 genes). When query frequency is higher than genome frequency, the bigger the difference is the more significant the corresponding function is.

Table III-4. Functional categories of the genes positively regulated by Phx1 (total 99 genes)

Function	Number of genes	Gene name
response to stress	11	*taf1, hsp16, zym1* etc.
transmembrane transport	11	*cta3, bsu1, mfs1, per1* etc.
Non-coding RNA	11	*prl01, prl26, prl12, tos3,* SPNCRNA.73 etc.
carbohydrate metabolic process	9	*gpd3, gpd1, eno1,* SPAC13A11.06 etc.
RNA metabolic process	5	*aes1, hht3, gar2 , hsf1* etc.
oxidation-reduction	5	*but1, cao2* etc.
vesicle-mediated transport	4	*glo3, imt2* etc.
cytoskeleton organization	4	*myo3, dad5, rad21* etc.
protein phosphorylation	3	*ppk31, crk1* etc.
thiamin and derivative biosynthetic process	2	*nmt1, nmt2*
Peptidyl-lysine methylation	2	*set7, set13*
others	32	*ade5, mug138, psu2, csa1, eta2* etc.

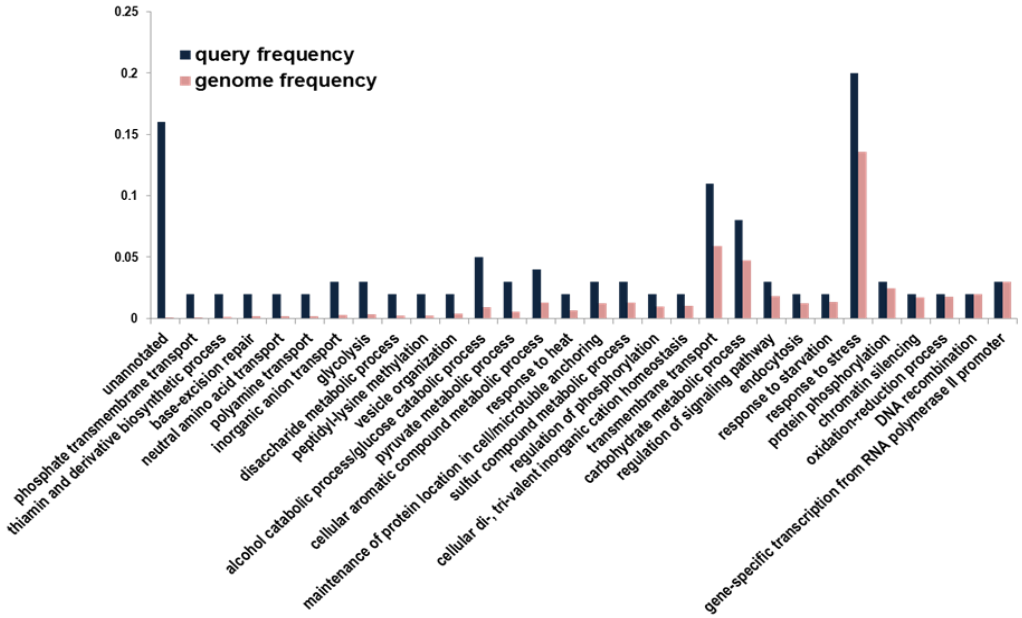

Fig. III-9. GO-term analysis of the genes positively regulated by Phx1.

The description about above graph is same with that of Fig. III-8.

be involved in thiamine biosynthesis.

III.4.2. The genes which are related with carbohydrate metabolism & mitochondrial function

Some induced genes in *phx1*-deletion mutants were involved in oligosaccharide catabolic process (*agl1*$^+$, *inv1*$^+$, SPAC1039.11c), mitochondrial function (*cyc1*$^+$, *cit1*$^+$, *aco1*$^+$, *gut2*$^+$, SPAC3A11.07), and pentose phosphate pathway (PPP) (SPAC26H5.09c, SPAC3C7.13c, *zwf1*$^+$, SPAC4G9.12). Also, there were some genes which encode hexose transporters (*ght3*$^+$, *ght4*$^+$, *ght5*$^+$, *ght8*$^+$). On the other hand, several glycolysis /gluconeogenesis-related genes (*gpd1*$^+$, *gpd3*$^+$, *eno1*$^+$), the gene involved in glycerol metabolic process (*dak2*$^+$) and some genes encoding putative pyruvate decarboxylase (SPAC13A11.06, SPAC3G9.11c) were repressed in Δ*phx1* mutants. Pyruvate decarboxylase is the enzyme that converts pyruvate to acetaldehyde in the process of ethanol fermentation. Although it could not be involved in 2-fold *cutoff* list, many gene-expression patterns in mitochondrial function, PPP, hexose transport, and glycolysis/gluconeogenesis in Δ*phx1* mutant strain confirmed these trends (data not shown). According to this result, it seems that Phx1 makes glucose flux reroute from TCA cycle to ethanol fermentation at the point of pyruvate synthesis. TCA cycle operated in the mitochondria is closely connected to cellular respiration. Furthermore, reactive oxygen species (ROS) generate as byproducts of respiration. Therefore, up-regulations of genes encoding mitochondrial-related proteins, antioxidant enzymes (Sod1, Srx1, Alo1), and PPP implied an increase of mitochondrial activity, followed by ROS productions in Δ*phx1* mutant. This phenomenon is closely consistent with the rerouting of the carbohydrate flux under oxidative stress (Ralser *et al.* 2007). Respiration brings about oxidative stress and PPP provides reducing power for antioxidant enzyme. Stress sensitivity test (Fig. III-4) and the

determination of ROS levels in Δ*phx1* mutants (Fig. III-5) supports this assumption.

In *S. cerevisiae*, glyceraldehyde-3-phosphate dehydrogenase and enolase are proteins that exist even in the stationary phase with other heat-shock proteins, whereas almost exponential-specific proteins disappeared (95%) (Boucherie 1985). Furthermore, some oxidative damaged proteins in replicatively and chronologically aged cells were the enzymes such as pyruvate decarboxylase (PDC), enolase, fructose-1,6-bisphosphate aldolase, alcohol dehydrogenases, and glyceraldehyde-3-phosphate dehydrogenase which are participated in the glycolytic and the energy metabolic pathways (Reverter-Branchat *et al.* 2004).

In Δ*phx1* mutant cells, the down-regulated genes in glycolytic and carbohydrate metabolic pathway (*gpd*$^+$, *gpd3*$^+$, *eno1*$^+$, *dak2*$^+$, PDC-encoding genes) are quite overlapped with above enzymes in *S. cerevisiae*.

In summary, Phx1 maybe recognize glucose condition in the cells and make cells endure stressful circumstance through changing of energy metabolism during stationary phase.

III.4.3. The genes that are involved in sexual development

Homozygous Δ*phx1* / Δ*phx1* diploid mutant showed low sporulation efficiency (Fig. III-7C, D), so we considered that Phx1 might have some positive roles in sexual differentiation, especially in meiotic division and spore formation. But, unexpectedly, many sexual reproduction genes were induced in Δ*phx1* strain (Table III-1). Even though this microarray had been done using heterothallic Δ*phx1* strain, it was an opposite direction to sporulation deficiency phenotype of Δ*phx1* mutant. However, according to the meiotic transcriptional program, most of genes in conjugation/meiosis category in Table III-1 were induced at initial stage of sexual development,

which means response to nutritional starvation, pheromone signaling, and conjugation (transient, continuous and delayed) (Mata *et al.* 2002). Furthermore, many genes which showed meiotic expressions were also induced in initial meiotic processes, although they belonged to other functional categories (27 of total 40 meiotic expressed genes in Table III-1 were included in the stage from transient to early). On the other hand, many reduced genes in Δ*phx1* mutant cells were middle (meiotic division) and late genes (spore formation) (20 of total 29 meiotic expressed genes in Table III-2). And the *phx1*$^{+}$ had been reported to express mRNA highly during spore formation (Mata *et al.* 2002). In Mata *et al.*'s report, each meiotic stage showed successive waves of gene expressions through sexual differentiation. And major regulators which control each meiotic stage induce their target gene expressions and switch off the previous expression wave (Mata *et al.* 2007). Therefore, it can be explained that Phx1 may also be a regulator that activates later meiotic gene expressions (meiotic division I, II, and spore formation) and represses the genes in previous meiotic stage (starvation, pheromone sensing, conjugation, S phase and DNA recombination).

The known regulators of late meiotic stage is Rsv1, Rsv2, Atf21 and Atf31. Interestingly, many target genes of Phx1 are overlapped with those of Rsv1 and Rsv2. It suggests Phx1 may cooperate with Rsv1 and Rsv2 to regulate late meiotic genes. Anyway, it is evident that Phx1 may be a regulator that involved in meiotic division and spore formation.

III.4.4. The genes which are associated with stress response and metabolite transport

In Δ*phx1* mutant cells, many stress-responsive genes were repressed (Table III-2, 4 and Fig. III-9). They are known to respond to heat, starvation, chemical stimuli, and so on. Among these genes, some of them were also involved in

meiosis. These results correlated with the functions of Phx1, which had been known so far. On the other hand, several induced genes in Δ*phx1* mutant were also involved in response to stimulus, especially oxidative stress (Table III-1, 3 and Fig. III-8). As demonstrated in Fig. III-5, Δ*phx1* mutant seemed to undergo oxidative stress by increased ROS. Therefore, we supposed these inductions of stress-responsive genes were due to high ROS accumulation in Δ*phx1* mutants at stationary phase.

In addition, from comparison analysis of microarray genes (total 196 genes) of Δ*phx1* mutant with Atf1- and Pcr1-depenent genes in response to H_2O_2 (total 180 genes) (Eshaghi *et al.* 2010), we found out Phx1 shared 20% of target genes with Atf1-Pcr1. This result provides the possibility that Phx1 may interact with Atf1-Pcr1 as co-regulators. And also 7% of Phx1-target genes were H_2O_2-responsive and Atf1/Pcr1-independent, suggesting Phx1 may regulate these genes independently of Atf1-Pcr1.

Many metabolic transport genes were regulated by Phx1. The genes encoding hexose, iron, peptide, and vitamin transporters were induced in Δ*phx1* mutant. The genes for hexose transport are known to be induced in stressful condition. Therefore, this result also reflects that Δ*phx1* mutant may experience some kinds of stresses. Iron is not only essential metal for redox, but is toxic to cells owing to production of hydroxyl radical through Fenton reaction. In *S. cerevisiae*, chronological-aged cells accumulate oxidatively damaged proteins, lipofuscin and increase iron concentration, lipid peroxidation (Reverter-Branchat *et al.* 2004). Therefore, high expressions of iron transporters may give rise to iron accumulation and are linked to ROS generation and aging.

With considering Phx1 as a putative regulator for stationary-phase maintenance, these results suggest that Phx1 may act as a protector against stress and/or aging.

III.5. Roles of Phx1 in Thiamine Biosynthesis

III.5.1. Phx1 regulates transcription of the genes involved in thiamine biosynthesis

The microarray analysis showed that the expressions of the genes, *nmt1*$^+$, *nmt2*$^+$, which are involved in thiamine biosynthesis were particularly reduced in Δ*phx1* mutant strains. In addition, the expression of the *bsu1*$^+$ (SPAC17A2.01) gene encoding pyridoxine transporter, which can also transport thiamine and be repressed by thiamine, was decreased in Δ*phx1* mutant. Therefore, the transcription levels of *nmt1*$^+$, *nmt2*$^+$, *bsu1*$^+$, and other genes involved in thiamine metabolism were confirmed by qRT-PCR in wild-type and Δ*phx1* mutant cells with or without thiamine treatment at exponential and stationary phases (Fig. III-10A). The *nmt1*$^+$, *nmt2*$^+$, and *bsu1*$^+$ genes were repressed by thiamine at both exponential and stationary phases expectedly. Interestingly, these genes were also down-regulated in *phx1*-deleted strains without thiamine only at stationary phase. To ascertain whether the repressions of these genes at stationary phase were actually due to the lack of Phx1 protein or the increased thiamine level in Δ*phx1* mutant, the expression levels of other thiamine-repressible genes (*thi4*$^+$, *pho4*$^+$, *thi9*$^+$) and non-thiamine-repressible gene, *tnr3*$^+$, were also checked by qRT-PCR (Fig. III-10A). The expressions of *thi4*$^+$, *pho4*$^+$, and *thi9*$^+$ genes were repressed and *tnr3*$^+$ gene was not repressed by thiamine as they were known. Furthermore, the expressions of *thi4*$^+$ and *pho4*$^+$ genes were decreased at stationary phase, while *thi9*$^+$ gene increased its expression at stationary phase. But, all of these genes were independent on Phx1 regulation at exponential and stationary phases (Fig. III-10A, B). Therefore, it looks like that Δ*phx1* mutant cells do not have more thiamine than wild-type cells, and the *nmt1*$^+$, *nmt2*$^+$, and *bsu1*$^+$ genes are directly regulated by Phx1 at stationary phase. In other words, the

Fig. III-10. Transcription levels of the genes involved in thiamine synthesis in wild-type and Δ*phx1* mutant cells.

(A) Expression levels of the genes involved in thiamine biosynthesis in wild-type and Δ*phx1* mutant cells with or without thiamine treatment. RNA samples from wild-type (JH43) and Δ*phx1* mutant (ESX5) cells grown in EMM liquid media with or without 100 μM thiamine treatment at exponential and stationary phase were prepared. The mRNA levels of the genes were measured by qRT-PCR, along with that of *act1*$^+$ mRNA as an internal control. The genes in box are known for thiamine-repressible genes. The *tnr3*$^+$ is non-thiamine-repressible gene. Average induction folds from three independent experiments were presented with standard deviations.

(B) Relative expression levels of the genes in (A) at stationary phase were presented. The induction fold of each gene in the thiamine non-treated wild-type cells at stationary phase sets '1' as a reference point.

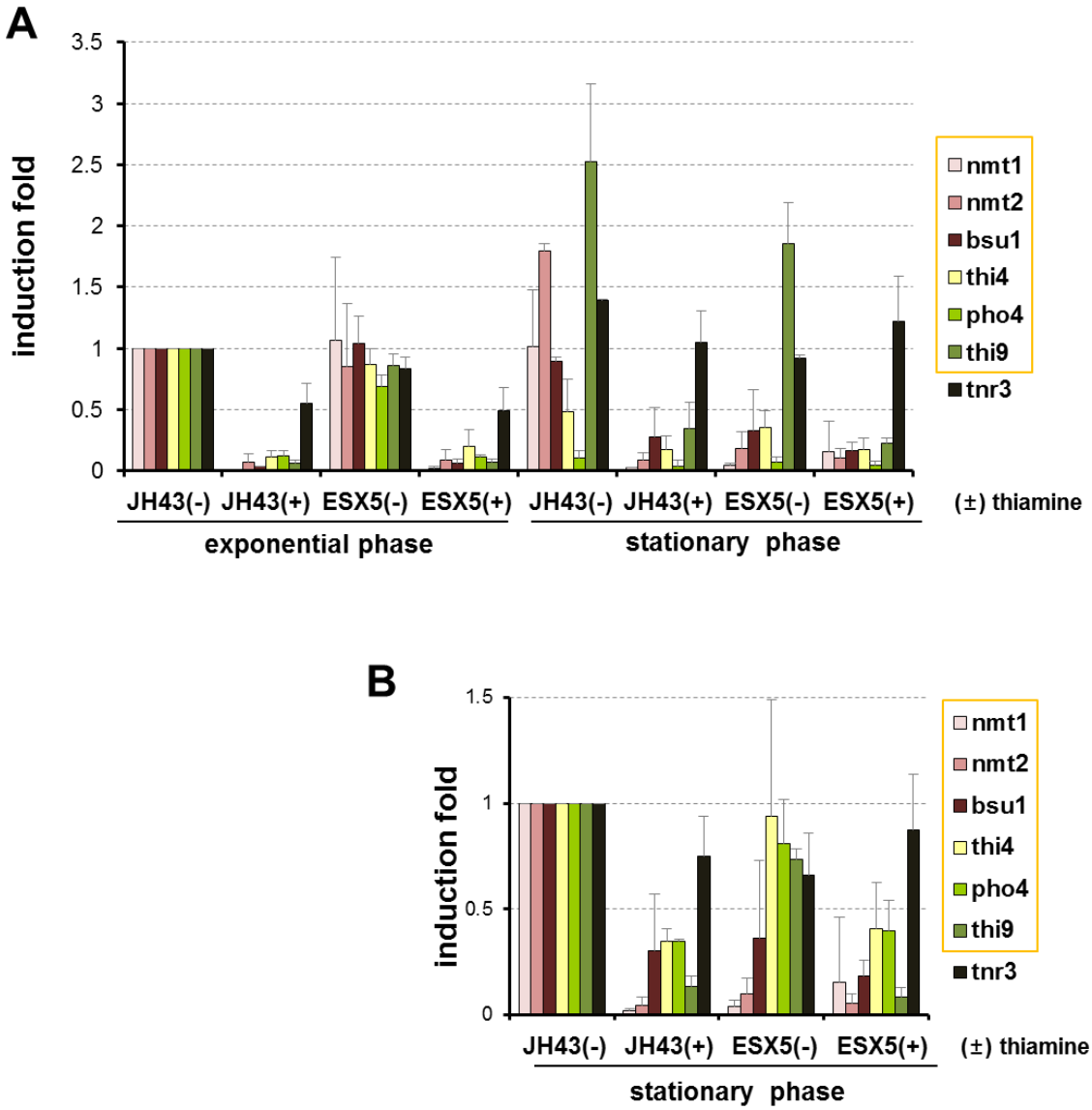
A
induction fold
3.5
3
2.5
2
1.5
1
0.5
0
JH43(-) JH43(+) ESX5(-) ESX5(+) JH43(-) JH43(+) ESX5(-) ESX5(+)
(±) thiamine
exponential phase
stationary phase
nmt1
nmt2
bsu1
thi4
pho4
thi9
tnr3
B
induction fold
1.5
1
0.5
0
JH43(-) JH43(+) ESX5(-) ESX5(+)
(±) thiamine
stationary phase
nmt1
nmt2
bsu1
thi4
pho4
thi9
tnr3

expressions of *nmt1*$^+$, *nmt2*$^+$, and *bsu1*$^+$ at exponential phase are regulated by other factors, maybe Thi1 or Thi5, and Phx1 may be a regulator required for the expressions of *nmt1*$^+$, *nmt2*$^+$, and *bsu1*$^+$ at stationary phase.

The *thi1*$^+$, *thi5*$^+$ genes encode transcriptional regulators for the *nmt1*$^+$ and *nmt2*$^+$ genes. Therefore, genetic interactions of *thi1*$^+$, *thi5*$^+$, and *phx1*$^+$ were verified by qRT-PCR. The *thi1*$^+$ is non-thiamine-repressible gene and has no genetic interaction with *thi5*$^+$ or *phx1*$^+$ at both exponential and stationary phases (Fig. III-11A, B). The *thi5*$^+$ gene was a little influenced by thiamine repression and induced more at stationary phase, but did not show any genetic interaction with *phx1*$^+$ (Fig. III-11A). The *phx1*$^+$ gene also had no genetic interaction with *thi5*$^+$ (Fig. III-11B). That is, *thi1*$^+$, *thi*$^+$*5*, and *phx1*$^+$ are not affected their expressions with each other.

In *S. cerevisiae*, *THI2*, *THI3*, and *PDC2*, whose products are regulators of thiamine biosynthesis, form a ternary complex and bind to upstream regulatory sequences of *THI* genes in the absence of TPP. It suggests that *thi1*$^+$, *thi5*$^+$, and *phx1*$^+$ in *S. pombe* may also have physical interactions, even though they have no influence on transcription levels of one another. However, we could not observe any physical interaction signal in multi-copy BiFC analysis (data not shown).

III.5.2. Intracellular thiamine pools are lower in Δ*phx1* mutants than in wild-type cells

In order to investigate whether Phx1 regulates thiamine biosynthesis directly or not, the levels of intracellular thiamine pools of cells under different growth phases were measured by HPLC. As shown in Fig. III-12A, the total amount of thiamine pools composed of TPP and thiamine decreased with culture time in both wild-type and Δ*phx1* mutant cells. At early growth phase (exponential phase), wild-type and Δ*phx1* mutant cells contained

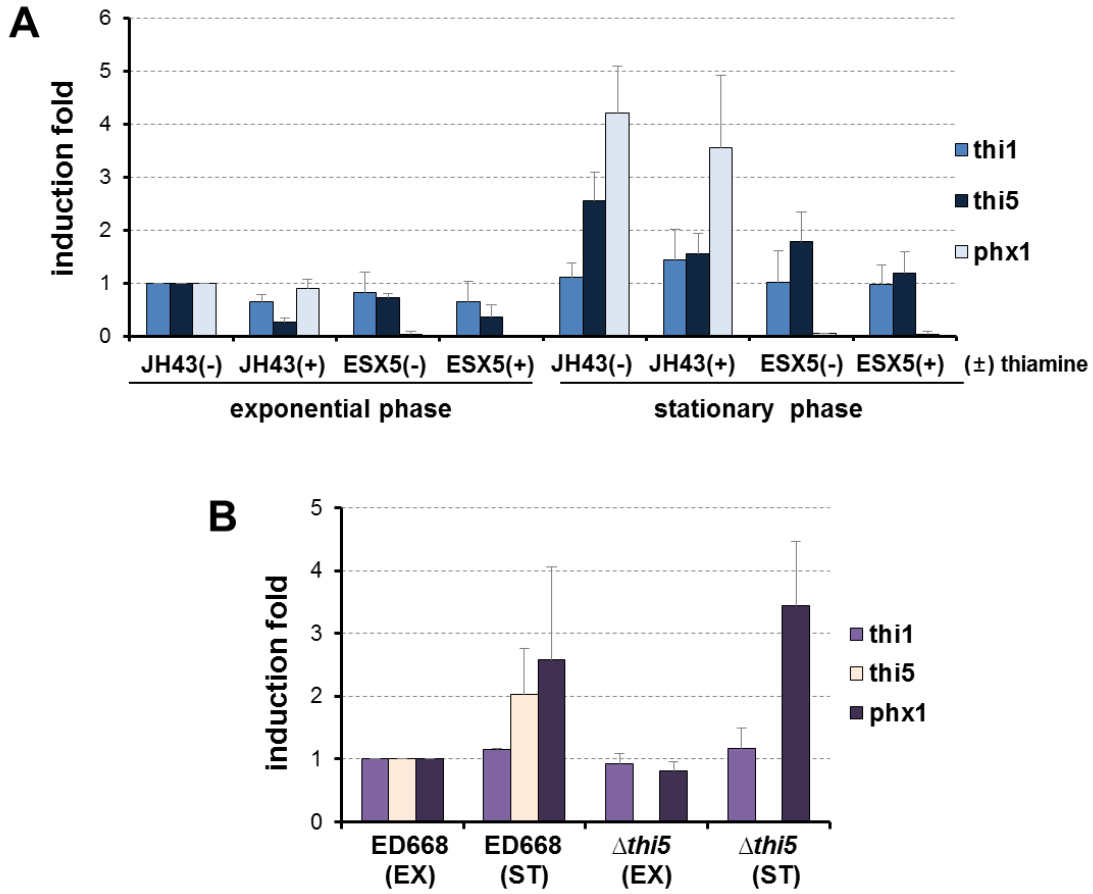

Fig. III-11. Genetic interactions of *thi1*⁺, *thi5*⁺, and *phx1*⁺.

(A) Expression levels of *thi1*⁺, *thi5*⁺, *phx1*⁺ in wild-type and Δ*phx1* mutant cells with or without thiamine treatment. RNA samples were prepared in the same conditions with Fig. III-10. The mRNA levels of the genes were measured by qRT-PCR, along with that of *act1*⁺ mRNA as an internal control. Average induction folds from three independent experiments were presented with standard deviations.

(B) Relative expression levels of *thi1*⁺, *thi5*⁺, and *phx1*⁺ at stationary phase were presented. The induction folds of each gene in the thiamine non-treated wild-type cells at stationary phase set '1' as a reference point.

Fig. III-12. Intracellular TPP, thiamine, and total pools of wild-type and Δ*phx1* mutant cells.

Wild-type (JH43) and Δ*phx1* mutant (ESX5) cells were inoculated with freshly grown cells to an initial OD_{600} of 0.02 and grown in EMM liquid media. Aliquots were removed at different time point (12 h, 36 h, 80 h) and extracted thiamine and TPP. Intracellular total thiamine pool (added thiamine levels to TPP levels) **(A)**, TPP **(B)**, and thiamine levels **(C)** were measured by HPLC analysis. The box under each graph presents the ratio of the level of Δ*phx1* mutants to that of wild-type cells. **(D)** indicates ratio of TPP to thiamine level at each condition. The average amount with standard deviations (error bars) from at least three independent experiments were presented. Astericks (*) presents p-value is below 0.05, two-tailed, student *t-test.*

A

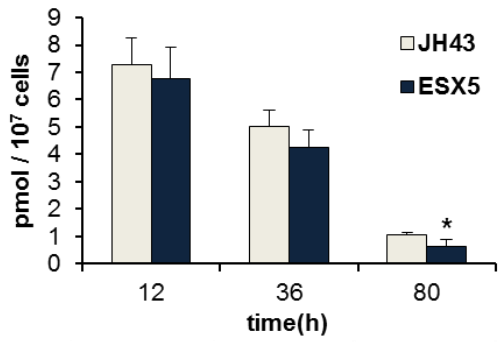

Δ / WT	0.93	0.85	0.59

B

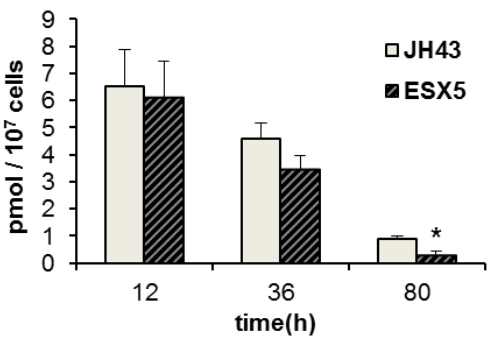

Δ / WT	0.94	0.75	0.31

C

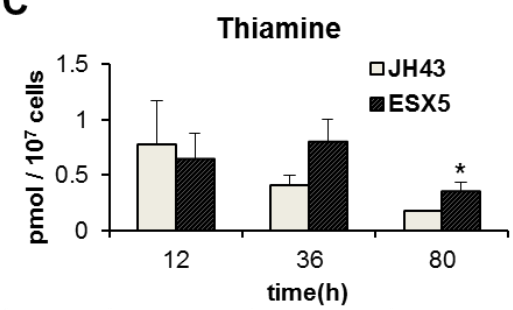

Δ / WT	0.84	1.95	1.99

D

Ratio of TPP / thiamine

time(h)	JH43	ESX5
12	8.44	9.39
36	11.13	4.29
80	5.51	0.83

similar amount of total thiamine pools (the ratio of total thiamine of Δ*phx1* mutant to wild-type cells at 12h is 0.93). But, the level in Δ*phx1* mutant cells became lower than in wild-type cells after entering stationary phase. At late stationary phase (80 h), the level of total thiamine pools of Δ*phx1* mutant is about 60% of that of wild-type cells. The intracellular level of TPP, an active form of thiamine, also decreased when cells entered stationary phase. Δ*phx1* mutant cells showed much lower TPP levels than wild-type cells (only 30% of TPP of wild-type cells at 80 h) (Fig. III-12B). The intracellular thiamine level of wild-type cells also reduced at late growth phase like as TPP level (Fig. III-12C). Interestingly, the thiamine level of Δ*phx1* mutant was about 2-fold higher than that of wild-type cells at stationary phase, but the absolute amount was very small. Fig. III-12D represents the ratio of TPP to thiamine at each time point. TMP level was not detected in both wild-type and Δ*phx1* mutant samples, maybe because of very low quantity.

Schweingruber *et al*. reported that synthesized thiamine was mainly detected as TPP, an active form of thiamine acting as a cofactor or signal molecule, in *S. pombe* (Schweingruber *et al.* 1991). Thiamine and TMP composed only about 10% of the total thiamine pool. These data coincided with the results in Fig. III-12B, C. The TPP level of Δ*phx1* mutant is considerably decreased compared to wild-type cells at stationary phase when *phx1*$^{+}$ is highly induced. Although the thiamine level of Δ*phx1* mutant was 2-fold higher than wild-type cells at stationary phase, it did not affect the level of total thiamine pool significantly. Therefore, Phx1 may activate the thiamine biosynthesis at late growth phase.

The amount of thiamine in Δ*phx1* mutant was unexpectedly larger than in wild-type cells. It looks like Δ*phx1* mutants have some defects in converting thiamine to TPP or in thiamine degradation. The only known gene encoding thiamine pyrophosphokinase which can convert thiamine to TPP is *tnr3*$^{+}$ in *S.*

pombe (Fankhauser *et al.* 1995). But the expression of *tnr3*$^{+}$ did not decrease in Δ*phx1* mutant cells (Fig. III-10A, B). Then, the defect in thiamine degradation may be a cause of thiamine increase in Δ*phx1* mutant cells. Thiamine can be degraded by thiaminase II. In *S. cerevisiae*, *THI20/21* encode HMP-P (precursor of pyrimidine moiety of thiamine) kinase, which is trifunctional protein, as they can also perform the salvage HMP phosphorylation and have a thiaminase II activity. In *S. pombe*, there is no known gene for thiaminase II, but there are three TENA/THI family genes, SPBP8B7.17c, SPBP8B7.18c, and SPBC530.07c. Interestingly, the expression of SPBC530.07c was decreased in Δ*phx1* mutant cells (Table III-2). Moreover, the SPBP8B7.17c and SPBP8B7.18c genes, the orthologous to *S. cerevisiae THI20/21*, were also slightly repressed in Δ*phx1* mutant cells, although they did not exceed the *cutoff*. Therefore, the products from these genes may have a thiaminase activity and be regulated by Phx1.

Recently, it has been reported that thiamine and its derivatives may be involved in the repair of DNA damage during UV illumination (Machado *et al.* 1997) or in stress defense under the conditions of oxidative stress and heat shock through increasing mitochondrial stability (Medina-Silva *et al.* 2006). In summary, it is suggested that Phx1 may contribute to stress-defense mechanism by regulating thiamine biosynthesis.

III.6. Roles of Phx1 in Regulating of PDC Genes

III.6.1. Phylogeny of the PDC-like enzymes

According to the results of microarray analysis of Δ*phx1* strain, the two genes, SPAC13A11.06, SPAC3G9.11c, which are predicted to encode putative pyruvate decarboxylase (PDC), were impressively reduced in Δ*phx1* mutant cells. PDC proteins, the products of *pdc* genes, are thiamine pyrophosphate

(TPP)-dependent enzymes which have a cofactor, TPP, and belong to the PDC-like group of TPP-enzyme family. To understand the function of PDC-like enzymes, phylogenetic tree was constructed for homologous to *pdc* genes. Homologous proteins that have all three domains (N-, C-terminal and central TPP binding domain) of PDC-like enzyme (Fig. I-4) were identified from Pfam database (Pfam ID; PF02776, PF00205, PF02775, respectively). To simplify phylogenetic analysis, some representative species from six kingdoms (Bacteria, Archaea, Plantae, Animalia, Fungi, and Protista) (Table III-5) were selected for further analysis. Protein sequences of selected 145 proteins were obtained from UniProt (www.uniprot.org) and aligned by using clustalW method in MEGA 5 program (Tamura *et al.* 2011). After trimming sparsely aligned regions at N- and C-terminal, remaining multiple sequence alignments are used for generating phylogenetic tree by neighbor joining (NJ) method (Saitou and Nei 1987) in MEGA 5 (Fig. III-13). The 145 proteins were clustered into three group of acetolactate synthase (ILV), 2-hydroxyacyl-CoA lyase (HACL), and pyruvate decarboxylase (PDC). The ILV group was split from the clade that contains PDC and HACL groups, and then the PDC and the HACL groups were diverged. In *S. pombe*, six proteins were searched as PDC-like enzymes, and four proteins among them were categorized in PDC group. These four proteins were named PDC1, PDC2, PDC3, and PDC4. The SPAC13A11.06 gene encoded PDC1 and the SPAC3G9.11c gene encoded PDC4. Other two proteins, PDC2 and PDC3, were encoded from the SPAC186.09 and the SPAC1F8.07c genes, respectively.

Interestingly, PDC1 and PDC4 of *S. pombe* were found in same clade with PDC1, PDC5, PDC6, THI3, and ARO10 of *S. cerevisiae.* This finding suggests that PDC1 and PDC4 are evolutionarily related and may have similar functions with those proteins of *S cerevisiae*. PDC1, PDC5, and PDC6 are known for pyruvate decarboxylases (Pronk *et al.* 1996), and THI3 is α-

Table III-5. List of species for phylogenetic analysis of PDC-like protein

Abbreviation	Species (strain)	Kingdom
BACSU	Bacillus subtilis	Bacteria
CAUCR	Caulobacter crescentus	Bacteria
CORGL	Corynebacterium glutamicum	Bacteria
DEIRA	Deinococcus radiodurans	Bacteria
DESVH	Desulfovibrio vulgaris (strain Hildenborough / ATCC 29579)	Bacteria
ECOLI	Escherichia coli (strain K12)	Bacteria
GLOVI	Gloeobacter violaceus (strain PCC 7421)	Bacteria
HAEIN	Haemophilus influenzae (strain ATCC 51907 / DSM 11121)	Bacteria
LACLA	Lactococcus lactis subsp. lactis (strain IL1403)	Bacteria
NEIG1	Neisseria gonorrhoeae (strain ATCC 700825 / FA 1090)	Bacteria
PROMA	Prochlorococcus marinus (strain SARG / CCMP1375 / SS120)	Bacteria
RHOS4	Rhodobacter sphaeroides (strain ATCC 17023 / 2.4.1 DSM 158)	Bacteria
STAA8	Staphylococcus aureus (strain NCTC 8325)	Bacteria
STRCO	Streptomyces coelicolor	Bacteria
STRR6	Streptococcus pneumoniae (strain ATCC BAA-255 / R6)	Bacteria
THET8	Thermus thermophilus (strain HB8 / ATCC 27634 / DSM 579)	Bacteria
VIBF1	Vibrio fischeri (strain ATCC 700601 / ES114)	Bacteria
METAC	Methanosarcina acetivorans (strain ATCC 35395 / DSM 2834)	Archaea
PYRFU	Pyrococcus furiosus (strain ATCC 43587 / DSM 3638)	Archaea
SULSO	Sulfolobus solfataricus (strain ATCC 35092 / DSM 1617)	Archaea
THEAC	Thermoplasma acidophilum (strain ATCC 25905 / DSM 1728)	Archaea
CHLRE	Chlamydomonas reinhardtii	Protista
DICDI	Dictyostelium discoideum	Protista
LEIMA	Leishmania major	Protista
CANAW	Candida albicans (strain WO-1)	Fungi
NEUCR	Neurospora crassa (strain ATCC 24698 / DSM 1257)	Fungi
PHYIT	Phytophthora infestans (strain T30-4)	Fungi
YARLI	Yarrowia lipolytica (strain CLIB 122 / E 150)	Fungi
YEAST	Saccharomyces cerevisiae (strain ATCC 204508 / S288c)	Fungi
SCHPO	Schizosaccharomyces pombe	Fungi
ARATH	Arabidopsis thaliana	Plantae
ANOGA	Anopheles gambiae	Animalia
CAEEL	Caenorhabditis elegans	Animalia
DANRE	Danio rerio	Animalia
DAPPU	Daphnia pulex	Animalia
DROME	Drosophila melanogaster	Animalia
XENTR	Xenopus tropicalis	Animalia
HUMAN	Homo sapiens	Animalia
MOUSE	Mus musculus	Animalia
RAT	Rattus norvegicus	Animalia

Fig. III-13. Evolutionary relationships of PDC-like enzymes.

The evolutionary history was inferred using the Neighbor-Joining method in MEGA 5 program. The analysis involved 145 amino acid sequences. All positions containing gaps and missing data were eliminated. The phylogenetic tree showed all proteins were classified into three groups of enzymes. The groups of acetolactate synthase (ILV), 2-hydroxyacyl-CoA lyase (HACL), and pyruvate decarboxylase (PDC) are indicated by curved line. The species in six kingdoms are colored differently. Black is for Bacteria, olive is for Archaea, red is for Fungi, green is for Plantae, purple is for Protista, blue is for Animalia. The enzymes of *S. pombe* were marked with black circle (●) and those of *S. cerevisiae* were marked with grey diamond (♦). The line of clade which PDC1, PDC4 of *S. pombe* belonged was depicted by thick-black line. The clade of PDC2, PDC3 of *S. pombe* belonged was depicted by dashed-blue line.

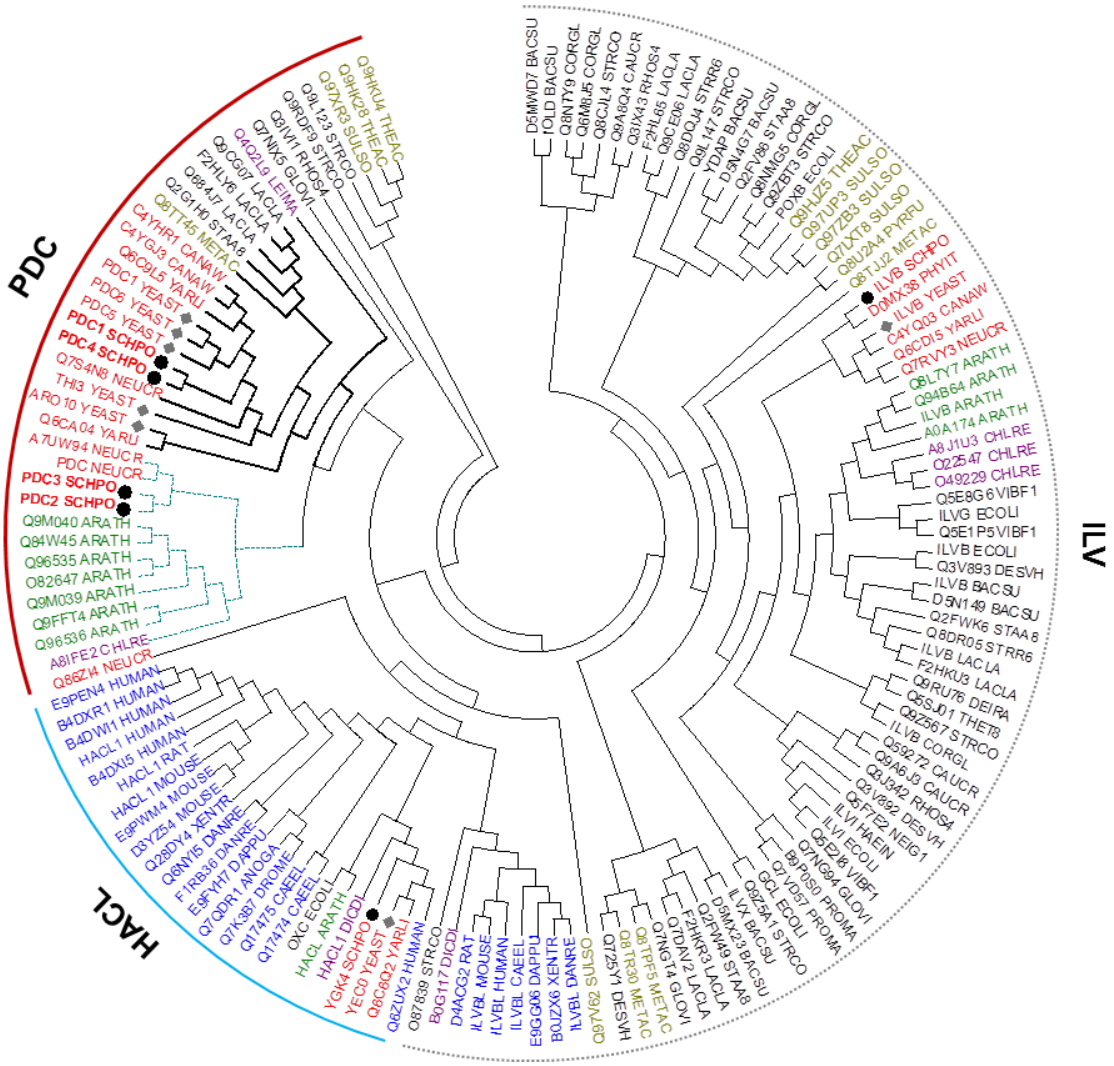

Bacteria
Archaea
Fungi
Plantae
Protista
Animalia

The enzymes of *S. pombe* (●)
The enzymes of *S. cerevisiae* (◆).

ketoisocaproate decarboxylase which is also involved in thiamine metabolism (Nishimura *et al.* 1992) and amino acid catabolism (Dickinson *et al.* 2003). ARO10 is a phenylpyruvate decarboxylase which is also involved in aromatic amino acid degradation (Vuralhan *et al.* 2003). Other PDC proteins in *S. pombe*, PDC2 (encoded from the SPAC1F8.07c gene) and PDC3 (encoded from the SPAC186.09 gene), were observed in distinctly separated clade with PDC1, 4 of *S. pombe.* These proteins are relatively close to that of *Arabidopsis thaliana*. PDC2, 3 of *S. pombe* are also suggested to have pyruvate decarboxylase activity, but more research about the functions of these proteins should be needed. The other two proteins of six PDC-like enzymes in *S. pombe* are putative oxalyl-CoA decarboxylase (YGK4; SPBC725.04) and the acetolactate synthase catalytic subunit (ILVB; ILV1) belonging to HACL and ILV group, respectively.

III.6.2. Phx1 regulates transcriptions of *pdc* genes

To investigate whether Phx1 regulates the expression of *pdc* genes or not, the mRNA level of *pdc* genes (*pdc1*; SPAC13A11.06, *pdc2*; SPAC1F8.07c, *pdc3*; SPAC186.09 and *pdc4*; SPAC3G9.11c) were measured by qRT-PCR along with the control *act1*$^+$ mRNA. Fig. III-14A demonstrated that the relative mRNA levels of *pdc1*$^+$, *pdc3*$^+$, and *pdc4*$^+$ increased at stationary phase. Especially, *pdc1*$^+$ and *pdc4*$^+$ were dramatically induced at stationary phase. On the contrary, mRNA of *pdc2*$^+$ decreased considerably at stationary phase. Furthermore, while *pdc2*$^+$ did not respond to thiamine treatment or *phx1* gene deletion, the expression of *pdc1*$^+$, *pdc3*$^+$, and *pdc4*$^+$ were repressed by thiamine and also reduced in Δ*phx1* mutant cells at exponential phase (Fig. III-14B). At stationary phase, thiamine treatment did not affect all of the *pdc* genes in wild-type strain, but the mRNA levels of *pdc1*$^+$, *pdc3*$^+$, and *pdc4*$^+$ decreased in Δ*phx1* mutant strains (Fig. III-14C). The expression levels of *pdc1*$^+$ and *pdc4*$^+$

Fig. III-14. Transcription levels of the *pdc* genes in wild-type and Δ*phx1* mutant cells.

(A) Expression levels of *pdc* genes in wild-type cells at exponential and stationary phase. RNA samples from wild-type cells (JH43) grown in EMM liquid media at exponential and stationary phase were prepared. The mRNA levels of *pdc1*$^{+}$, *pdc2*$^{+}$, *pdc3*$^{+}$, and *pdc4*$^{+}$ were measured by qRT-PCR, along with that of *act1*$^{+}$ mRNA as an internal control. Average induction folds from three independent experiments were presented with standard deviations.

(B) Relative expression levels of the *pdc* genes in wild-type and Δ*phx1* mutant cells with or without thiamine treatment (100μM) at exponential phase were presented. The induction folds of each gene in the thiamine non-treated wild-type cells at exponential phase set '1' as a reference point.

(C) Relative expression levels of the *pdc* genes in same condition with (B) at stationary phase were presented. The induction folds of each gene in the thiamine non-treated wild-type cells at stationary phase set '1' as a reference point.

A Relative expressions of *pdc* genes

Gene name	Systematic name	exponential	stationary
pdc1	SPAC13A11.06	1	74.59 ± 44.07
pdc2	SPAC1F8.07c	1	0.14 ± 0.06
pdc3	SPAC186.09	1	4.75 ± 2.98
pdc4	SPAC3G9.11c	1	2523.29 ± 238.52

B

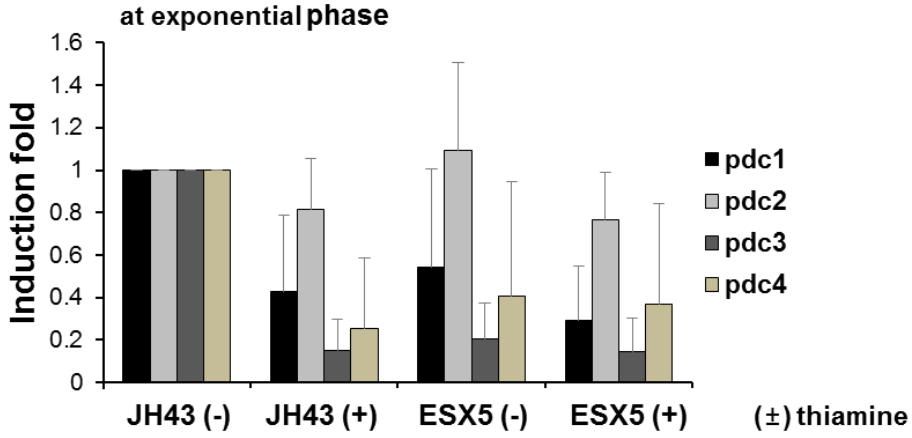

C

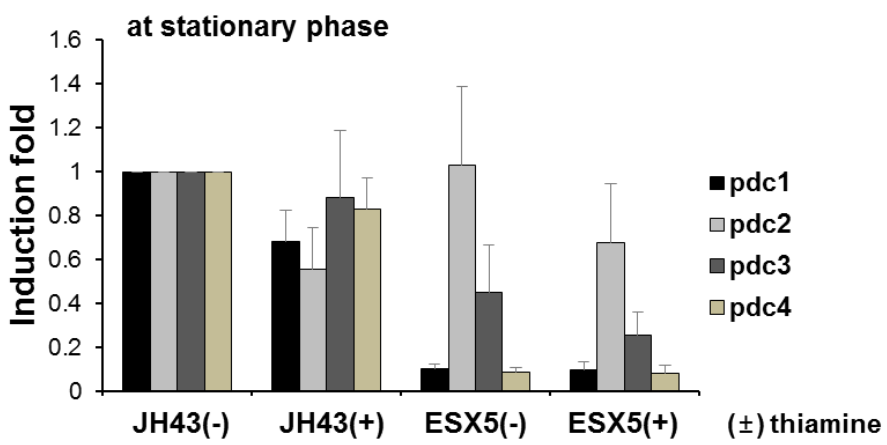

were extremely lower in Δ*phx1* mutants at stationary phase compared with wild-type cells. These results indicate that *pdc*1$^+$, *pdc3*$^+$ and *pdc4*$^+$ are induced highly at stationary phase and these inductions are due to the regulatory factor, Phx1.

Recently, Bähler's group applied direct high-throughput sequencing of complementary DNAs (RNA-Seq) and high-density tiling arrays to the transcripts of *S. pombe (*Wilhelm *et al.* 2008*)*. According to the tiling arrays using Affymetrix chips containing 25-mer probes tiled at ~20-nucleotide intervals across both strands of the *S. pombe* genome, the transcript level of *pdc1*$^+$ dramatically increased during the late meiotic process, namely spore formation (Fig. III-15A). The reverse strand contains antisense RNA (SPNCRNA.533), but this antisense RNA seems to strengthen the tendency of sense RNA profile. The transcript of *pdc2*$^+$ maintained extremely high during exponential phase and initial meiotic process, but decreased at quiescent phase, stress condition, and in late meiotic process (Fig. III-15B). The *pdc3*$^+$ gene expressed rarely in most conditions (growth phase, meiotic differentiation, and environmental stress) (Fig. III-15C). The mRNA level of *pdc4*$^+$ gene showed extremely strong induction at quiescent phase, stress condition, and meiosis. (especially the first and the third meiotic processes including conjugation and S phase) (Fig. III-15D). These reports nearly coincided with the results of quantitative real-time PCR in Fig. III-14.

III.6.3. PDC activity is decreased in Δ*phx1* mutant

In order to test whether Phx1 regulates *pdc* genes, pyruvate decarboxylase (PDC) activity assay was performed in wild-type and Δ*phx1* mutant cells. Fig. III-16A demonstrated that PDC enzyme activity of wild-type cells increased around 3-fold more at stationary phase than at exponential phase. It suggests that enzymes which have PDC activity are more required for the stationary

Fig. III-15. Tiling array profiles of *pdc* genes.

(from *S. pombe* GeneDB linked with the resources of Bähler lab, *http://old.genedb.org/genedb/pombe/*)

Tiling-chip hybridization signals (in which the strength of color reflects the signal-distribution quartile) across the genomic region are shown in the center for forward (top) and reverse (bottom) strands, with rows reflecting 8 experimental conditions. The profile of *pdc1*$^+$**(A)**, *pdc2*$^+$ **(B)**, *pdc3*$^+$ **(C)**, and *pdc4*$^+$ **(D)** are indicated.

[MM-E; exponential EMM, YE-E; exponential YE, ME0; no Nitrogen 12 h (25℃), ME1; low Nitrogen 1 h+2 h, ME2; low Nitrogen 3 h+4 h, ME3; low Nitrogen 5 h+6 h, ME4; low Nitrogen 7 h+8 h, HS: heat-shock (YE 39°C, 15 min), OX; oxidative stress (YE 0.5 mM H_2O_2, 15 min), ST; Quiescent (EMM 1% Nitrogen)]

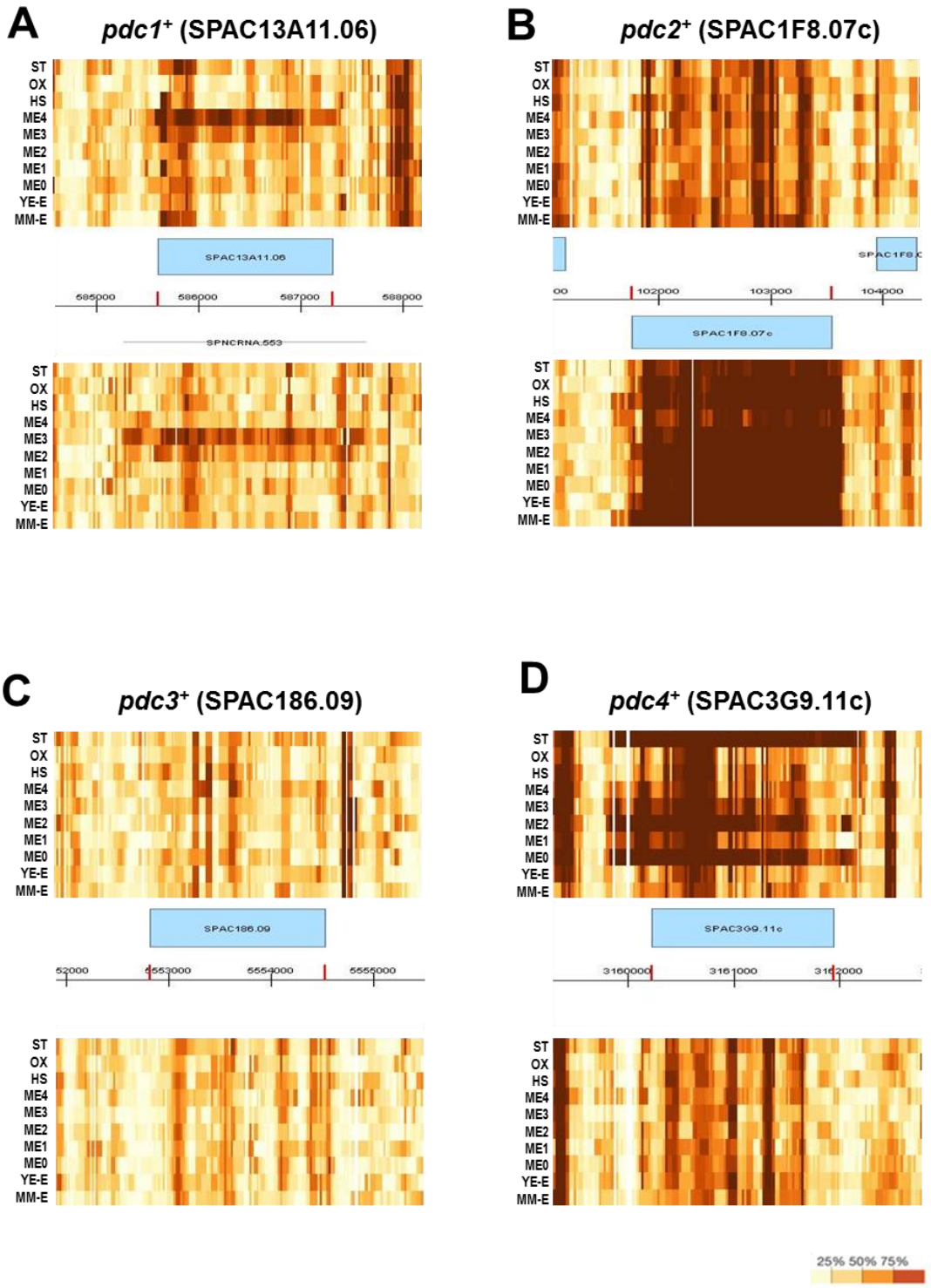
A
pdc1+ (SPAC13A11.06)
B
pdc2+ (SPAC1F8.07c)
C
pdc3+ (SPAC186.09)
D
pdc4+ (SPAC3G9.11c)
ST
OX
HS
ME4
ME3
ME2
ME1
ME0
YE-E
MM-E
SPAC13A11.06
SPAC1F8.07c
SPAC186.09
SPAC3G9.11c
SPNCRNA.553
25% 50% 75%

Fig. III-16. Pyruvate decarboxylase activity in Δ*phx1* mutant.

(A) JH43, ESX5 were inoculated to OD_{600} of 0.02 in EMM and grown to OD_{600} of 1.0 (around 20 h of culture time) and 10 (around 50 h of culture time) for the exponential (EX) and stationary (ST) phase. Then the cells were harvested at each growth points and cell extracts were prepared. The pyruvate decarboxylase activity was measured. Error bar means standard deviation from 3 independent experiments.

(B) JH43 and ESX5 were grown to stationary phase (same condition with panel A) and cell extracts were prepared. 0.1 mM TPP was added or not in each sample and PDC activity assay was performed.

(C) Model of Phx1 regulation on PDC activity.

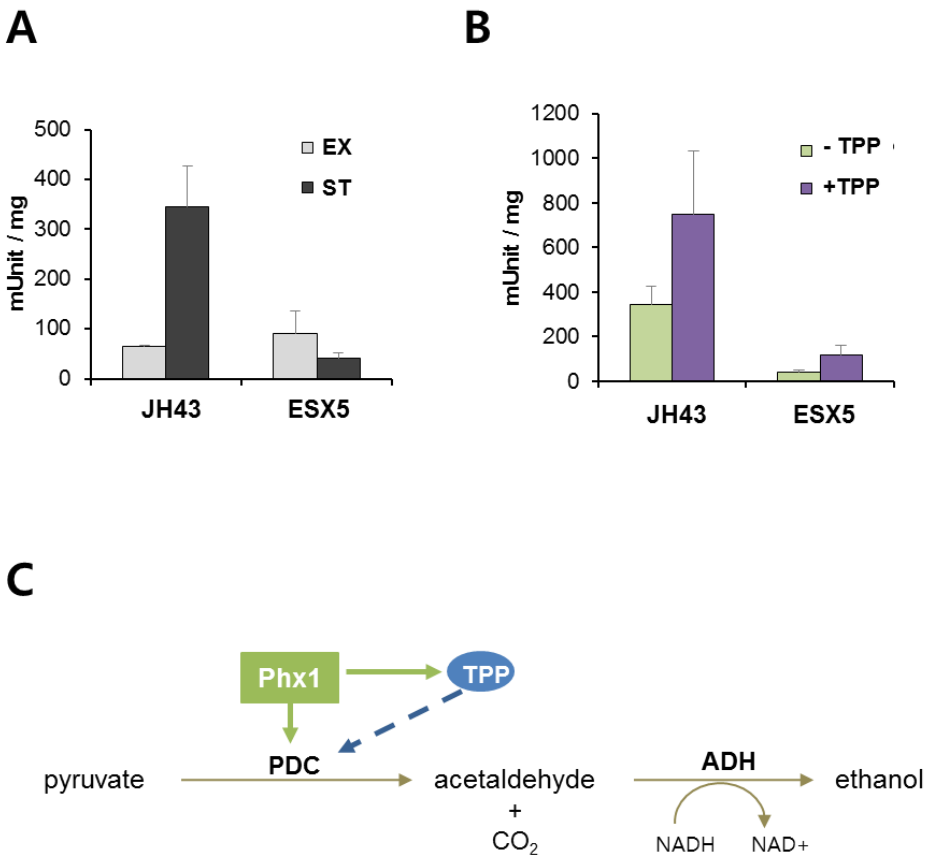
A
500
400
300
200
100
0
mUnit / mg
EX
ST
JH43
ESX5
B
1200
1000
800
600
400
200
0
mUnit / mg
- TPP
+TPP
JH43
ESX5
C
Phx1
TPP
PDC
pyruvate
acetaldehyde
+
CO2
ADH
ethanol
NADH
NAD+

phase, although PDC is known for the enzyme for fermentation. In case of Δ*phx1* mutant strain, cells showed similar PDC activity at exponential phase compared with wild-type cells. The stationary-phase Δ*phx1* mutant cells, however, did not elevate PDC activity as much as wild-type cells. PDC activity of Δ*phx1* mutant cells at stationary phase was even lower than at exponential phase. To investigate whether the decline of PDC activity in stationary-phase Δ*phx1* cells was really due to the low levels of PDC apoproteins or due to the shortage of active cofactor TPP, PDC enzyme assay was re-performed with or without thiamine treatment in wild-type and Δ*phx1* mutant cells at stationary phase. Fig. III-16B showed that the Phx1-depleted cells could not increase PDC activity despite abundant thiamine. It means that reduced PDC activity in Δ*phx1* mutant cells was caused by scarcity of PDC proteins, not by insufficiency of TPP. Phx1 may positively regulate the expressions of *pdc* genes, followed by increased synthesis of PDC proteins. Previously, we observed Phx1 led to thiamine biosynthesis (Fig. III-10, 12). Therefore, it can be suggested that synthesized TPP by Phx1 contributes to PDC activation, providing its cofactor TPP (Fig. III-16C).

III.6.4. *pdc* mutants show long-term survival defect

As *pdc1*$^+$, *pdc3*$^+$, and *pdc4*$^+$ genes were induced during stationary phase and these inductions might be caused by Phx1, their roles in long-term survival were investigated. For this purpose, Δ*pdc1*, Δ*pdc3*, and Δ*pdc4* strains (constructed by Bioneer Co.) were used. The *pdc2*$^+$ gene is essential, thus we could not obtain Δ*pdc2* strain. The Δ*pdc1*, Δ*pdc3*, and Δ *pdc4* mutants did not show any growth defect during vegetative growth phase in YES and EMM media. However, Δ*pdc1* and Δ*pdc4* mutant cells decreased viability more than wild-type cells after entering stationary phase in YES media (Fig. III-17A, B).

Fig. III-17. Viability of Δ*pdc* mutant cells in long-term culture.

(A) Long-term survival of wild-type (ED666) and Δ*pdc1* mutant (based on ED666, constructed by Bioneer Co.) cells cultured in YES liquid media

(B) Long-term survival of wild-type (ED668), Δ*pdc3* and Δ*pdc4* mutant (based on ED668, constructed by Bioneer Co.) cells cultured in YES liquid media

(C) Long-term survival of wild-type (ED665), Δ*pdc1*, Δ*pdc3*, and Δ*pdc4* mutant (based on ED665) cells cultured in YES liquid media

(D) Long-term survival of wild-type (ED665), Δ*pdc1,* Δ*pdc3*, and Δ*pdc4* mutant (based on ED665) cells cultured in EMM liquid media

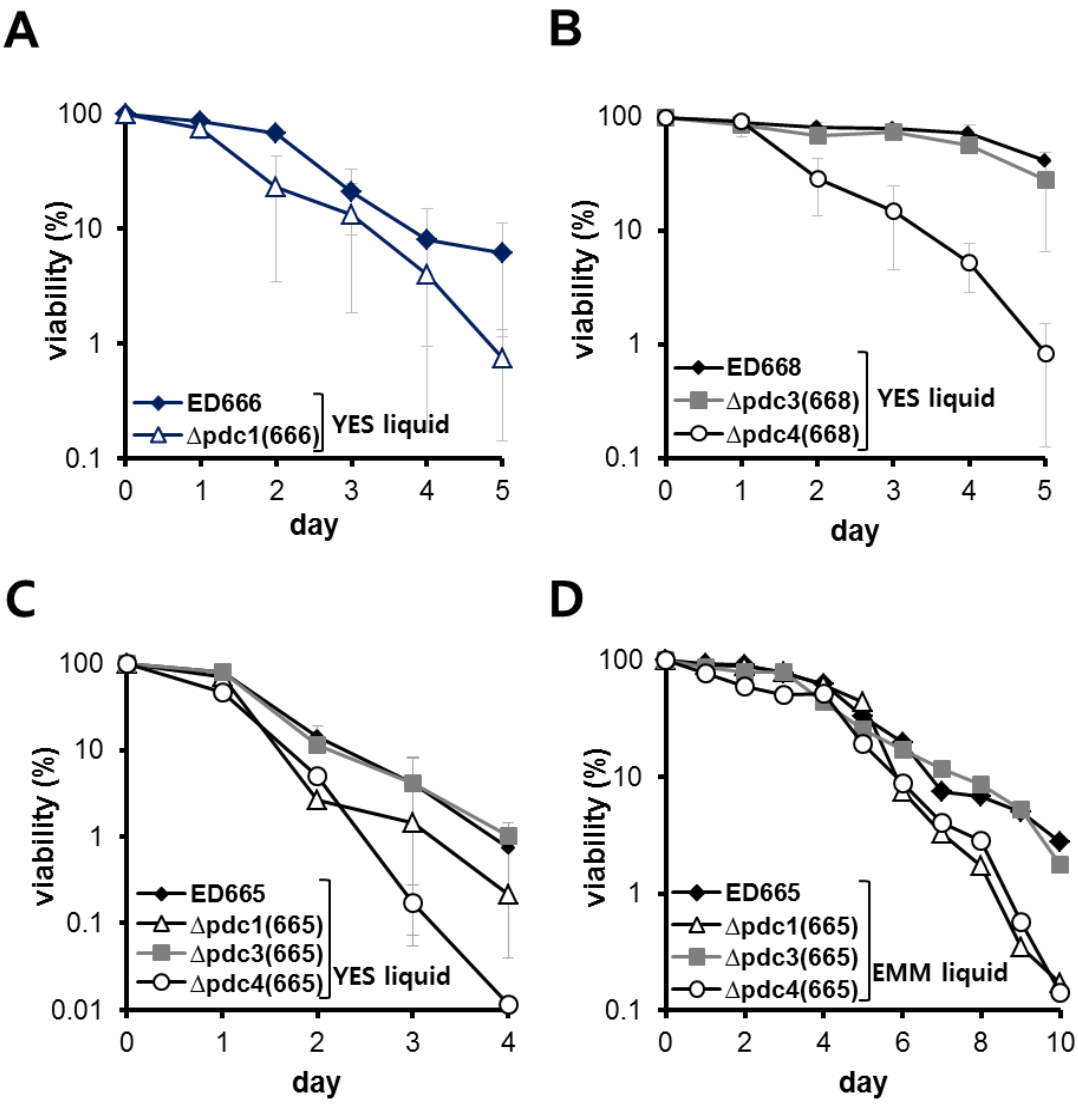
A
100
10
1
0.1
viability (%)
0
1
2
3
4
5
day
ED666
Δpdc1(666)
YES liquid
B
100
10
1
0.1
viability (%)
0
1
2
3
4
5
day
ED668
Δpdc3(668)
Δpdc4(668)
YES liquid
C
100
10
1
0.1
0.01
viability (%)
0
1
2
3
4
day
ED665
Δpdc1(665)
Δpdc3(665)
Δpdc4(665)
YES liquid
D
100
10
1
0.1
viability (%)
0
2
4
6
8
10
day
ED665
Δpdc1(665)
Δpdc3(665)
Δpdc4(665)
EMM liquid

The Δ*pdc1* mutant was constructed based on ED666 strain, and the Δ*pdc3* and Δ*pdc4* mutants were based on ED668 strain. For comparing all of these three mutants together, genotype changings of three Δ*pdc* strains to ED665-based one were made. Fig. III-17C demonstrated that Δ*pdc1* and Δ*pdc4* mutants based on ED665 genotype also showed long-term survival defects as like as in Fig. III-17A, B. The long-term survival of the Δ*pdc* mutant cells cultured in EMM were also observed (Fig. III-17D). In this condition, the ED665-based Δ*pdc1* and Δ*pdc4* cells lost their viability more rapidly than the wild type. Although these results need to be confirmed, it suggests the *pdc1*$^+$ and the *pdc4*$^+$ genes make cells maintain viability for longer period of time.

III.6.5. Overproduction of Pdc4 protein enhances long-term survival

To further investigate the function of Pdc4 protein in long-term survival, we next overexpressed *pdc4*$^+$ in wild type under the control of the *nmt1* promoter. Wild-type cells transformed with pREP42-*pdc4*$^+$ were cultured on EMM liquid medium. As shown in Fig. III-18A, overproduction of Pdc4 in the wild-type strain greatly enhanced long-term viability. It suggests that Pdc4 confers fitness to cells during stationary phase and makes cells live longer. Moreover, flocculation was observed in Pdc4-overproducing cells (Fig. III-18B). This flocculation phenotype is consistent with the flocculation of Phx1 overproducing cells (Kwon 2004). We also checked the morphology of Pdc4 overproducing cells, but could not detect any filamentous form (data not shown). Anyway, these findings give more evidences that *pdc4*$^+$ gene may be a transcriptional target of Phx1, and Phx1 overproduction may mediate invasive growth and flocculation via the transcriptional activation of *pdc4*$^+$.

The mechanisms of nonsexual flocculation of heterothallic strains in *S. pombe* were little known yet. However, recently several results have been reported that *S. pombe* exhibits nonsexual flocculation and invasive growth in

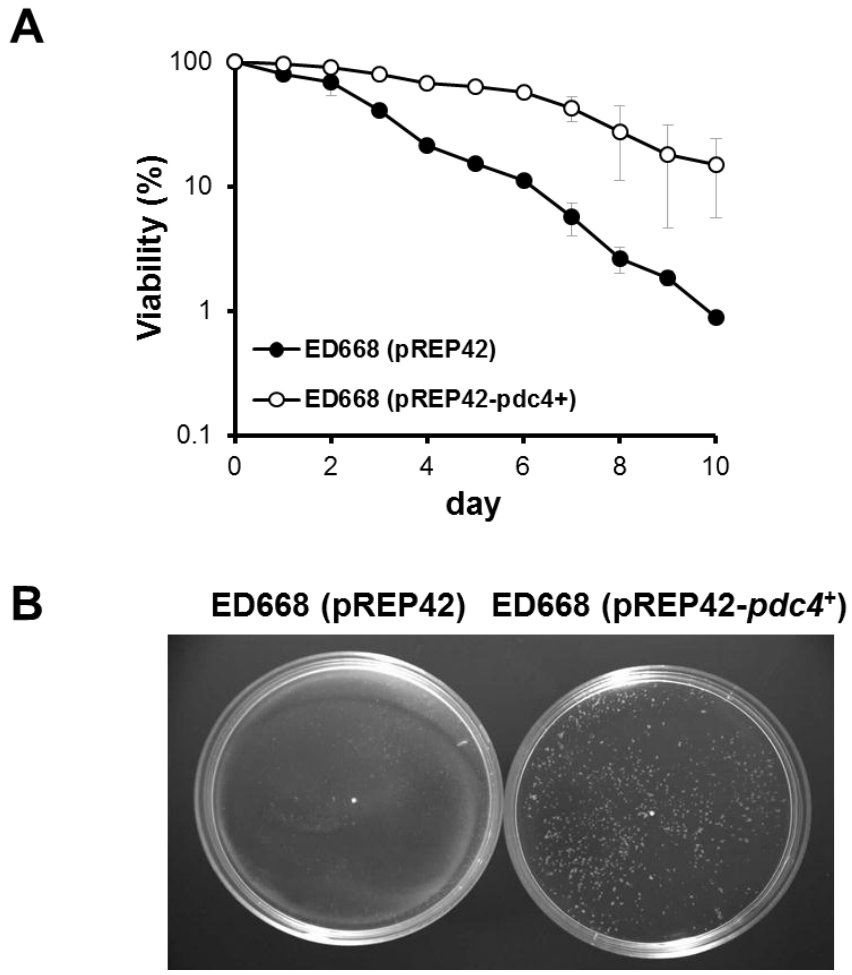

Fig. III-18. Pdc4-overproducing cells enhance the long-term survival and induce nonsexual flocculation.

(A) Long-term survival of wild-type and Pdc4-overproducing cells cultured in EMM media.

(B) Flocculation phenotypes of wild-type (ED668) and Pdc4-overproducing cells. ED668 cells transformed with pREP42 or pREP42-*pdc4*$^{+}$ were cultured in EMM liquid media for 20 h.

response to nitrogen limitation, and this is mediated via the expression of *gsf2*$^{+}$ gene by Pvg4 regulation (Matsuzawa *et al.* 2011; Matsuzawa *et al.* 2012). The flocculation phenotype of Pdc4-overproducing cells suggests that Pdc4 may be involved in nutritional starvation signaling and also have some relation with the flocculation-regulating genes (ex. *pvg4*$^{+}$, or *gsf2*$^{+}$).

III.7. Upstream Signaling Pathways for Phx1 Regulation

III.7.1. Regulation of long-term survival by the protein kinase Sck2 is mediated via Phx1

To investigate in more detail about long-term survival in *S. pombe*, we focused on the connections between Phx1 and other aging-related factors. The *sck2*$^{+}$, the homologue of the *S. cerevisiae SCH9* gene, was known to have pro-aging effect in *S. pombe* (Roux *et al.* 2006). The Δ*sck2* mutant lived longer than wild-type strain as like long-lived *SCH9* mutants in *S. cerevisiae*. To investigate whether Sck2 and Phx1 act in the same pathway, the Δ*sck2* Δ*phx1* double deletion strain was constructed. The Δ*sck2* mutants extended chronological life span as previously reported (Roux *et al.* 2006) and Δ*phx1* mutant shortened chronological life span as already shown in Fig. III-3. Interestingly, deletion of *phx1*$^{+}$ gene abolished life span extension caused by deficiency of *sck2*$^{+}$ (Fig. III-19A), suggesting that Phx1 was associated with the longevity regulatory pathway controlled by Sck2 as a downstream effector of the pathway.

To understand the interaction mechanism of Sck2 and Phx1, we examined the genetic and physical interactions between *sck2*$^{+}$ and *phx1*$^{+}$ genes and between Sck2 and Phx1 proteins by qRT-PCR and BiFC analysis, respectively. As shown in Fig. III-19B, the mRNA expression of *phx1*$^{+}$ did not be affected

Fig. III-19. Phx1 is required for chronological life span extension of Δ*sck2* mutant strain.

(A) Long-term survival of wild-type, Δ*sck2* (JY05), Δ*phx1* (ESX5) and Δ*sck2* Δ*phx1* (JY06) mutants. Deletion of the *phx1*$^+$ gene reverses life span extension associated with deficiency of *sck2*$^+$.

(B) Expression levels of *phx1*$^+$ and *sck2*$^+$ in wild-type and Δ*sck2* mutant strains. RNA samples from wild-type (ED665) and Δ*sck2* mutant (JY05) cells grown in YES liquid media for exponential (EX) and stationary (ST) phase were prepared. The mRNA level of *phx1*$^+$ and *sck2*$^+$ were measured by qRT-PCR, along with that of *act1*+ mRNA as an internal control. Average induction folds from three independent experiments were presented with standard deviations.

(C) Bimolecular fluorescence complementation (BiFC) analysis for detection the interaction between Phx1 and Sck2. ED665 cells co-transformed with pREP42-*sck2*$^+$-VN and pREP41-*phx1*$^+$-VC were examined by fluorescence microscope. The cells co-transformed with pREP42- *sck2*$^+$-VN and pREP41-VC were examined as a negative control. Fluorescence and DIC images were visualized by fluorescence microscopy (Axiovert 200M, Carl Zeiss).

(D) Identification of putative Akt and Akt/14-3-3 motifs in Phx1. The residues 576-581 are for Akt phosphorylation, and the residues 645-652 are for both Akt phosphorylation and 14-3-3 protein binding . The residues 645-650 are for Akt phosphorylation and the residues 647-652 are for 14-3-3 protein binding. The phosphorylation site is marked with asterisk (*). Akt phosphorylation motif and Akt phosphorylation/14-3-3 binding motif were presented below.

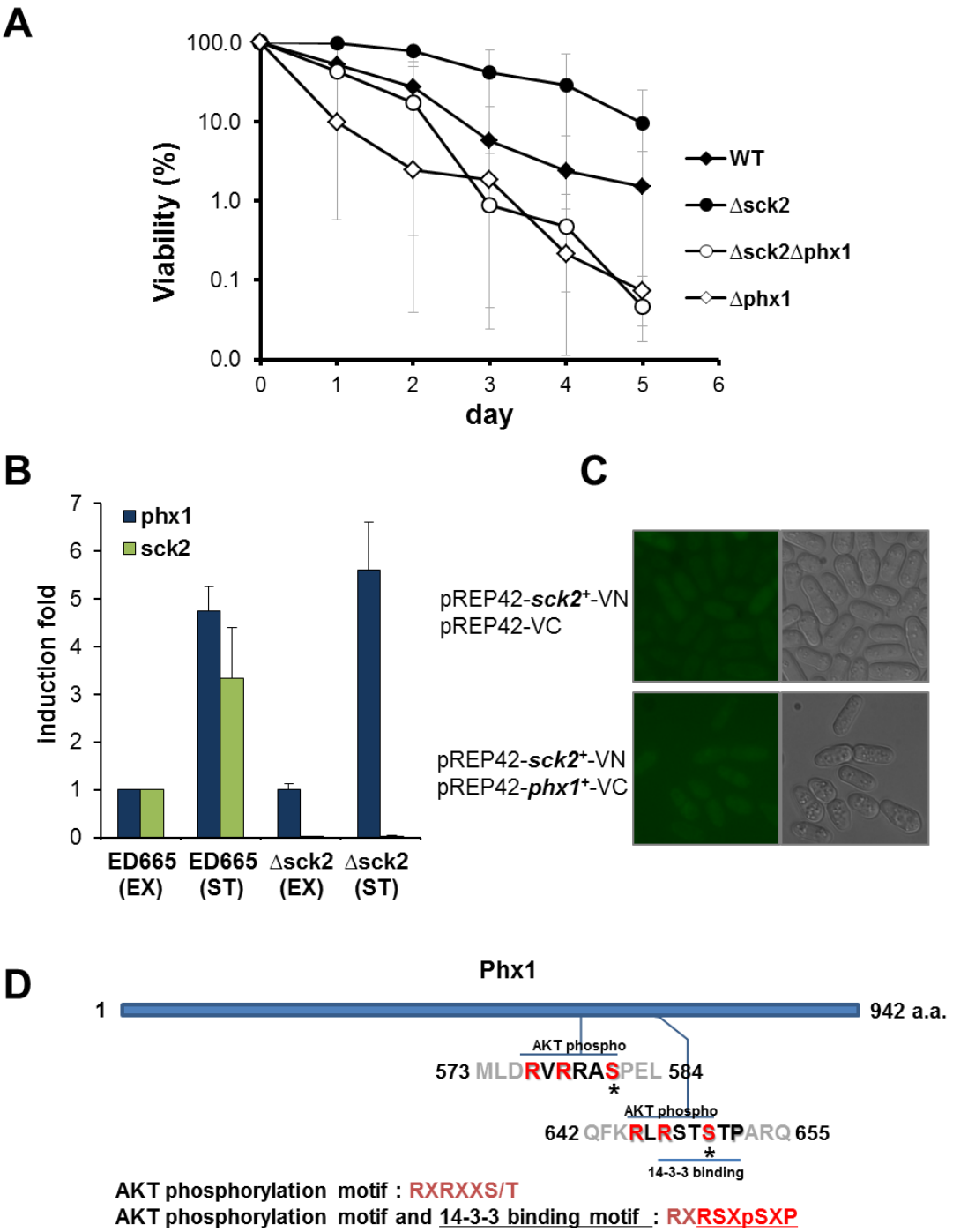
A
100.0
10.0
1.0
0.1
0.0
Viability (%)
0
1
2
3
4
5
6
day
WT
Δsck2
Δsck2Δphx1
Δphx1
B
phx1
sck2
induction fold
0
1
2
3
4
5
6
7
ED665 (EX)
ED665 (ST)
Δsck2 (EX)
Δsck2 (ST)
C
pREP42-sck2+-VN
pREP42-VC
pREP42-sck2+-VN
pREP42-phx1+-VC
D
Phx1
1
942 a.a.
AKT phospho
573 MLDRVRRASPEL 584
AKT phospho
642 QFKRLRSTSTPARQ 655
14-3-3 binding
AKT phosphorylation motif : RXRXXS/T
AKT phosphorylation motif and 14-3-3 binding motif : RXRSXpSXP

by deficiency of *sck2*$^{+}$ at exponential and stationary phases. To examine whether Sck2 physically interacts with Phx1 *in vivo* Bimolecular Fluorescence Complementation (BiFC) analysis (Sung and Huh 2007; Kim *et al.* 2010) was performed. The *sck2*$^{+}$ and *phx1*$^{+}$ genes were cloned in pREP42-VN and pREP41-VC plasmids with *nmt* promoter and co-transformed into the cells. The cells containing pREP42- *sck2*$^{+}$ -VN and pREP41-VC plasmid were used as negative controls. No Venus fluorescence signals were detected in the cells containing both Sck2-VN and Phx1-VC proteins (Fig. III-19C). According to BiFC analysis, it seemed that there was no interaction between Sck2 and Phx1. However, since these results included multi-copy effects either, physical interaction between Sck2 and Phx1 also should be confirmed by other *in vivo* and *in vitro* methods as like immunoprecipitation and so on.

Sck2 is a AKT/PKB homolog protein. AKT is a serine/threonine-specific protein kinase that plays an important role in many cellular processes such as glucose metabolism, cell-cycle regulation, cell proliferation, and apoptosis. AKT phosphorylation motif is known as RXRXXS/T, which overlaps with 14-3-3 binding motif RSXpSXP (Yaffe *et al.* 2001). Interestingly, we identified two Akt recognition sites on Phx1 protein and one of these two sites overlaps with 14-3-3 protein binding motif (Fig. III-19D). It suggests that Phx1 may be a phosphorylation target of Sck2. Therefore, it should be confirmed whether Phx1 is phosphorylated by Sck2 in the future.

III.7.2. cAMP/Pka1 pathway negatively regulates Phx1

The cAMP/Pka1 pathway was also known to control chronological aging along with Sck2 pathway in *S. pombe* (Roux *et al.* 2006). Pka1 is unique PKA catalytic subunit and is required for growth and exit from stationary phase in *S. pombe* (Fujita and Yamamoto 1998). Therefore, we investigated whether Phx1 is involved in the Pka1 pathway for long-term survival. As expectedly,

Fig. III-20. Phx1 is required for chronological life span extension of Δ*pka1* mutant.

(A) Long-term survival of wild-type (ED666), Δ*pka1* (from Bioneer Co.) and Δ*pka1* Δ*phx1* (JY07) mutants. Deletion of *phx1*$^+$ decreases chronological life span extension associated with deficiency in *pka1*$^+$.

(B) Expression levels of *phx1*$^+$, *rsv1*$^+$, and *pka1*$^+$ in wild-type and Δ*pka1* mutant strains. RNA samples from wild-type (ED666) and Δ*pka1* mutant (from Bioneer Co.) cells grown in YES liquid media for exponential (EX) and stationary (ST) phases were prepared. The mRNA levels of *phx1*$^+$ *rsv1*$^+$ and *pka1*$^+$ were measured by qRT-PCR, along with that of *act1*$^+$ mRNA as an internal control. Average induction folds from three independent experiments were presented with standard deviations.

(C) Identification of putative PKA phosphorylation motifs on Phx1 protein. The residues 578-582 are for PKA phosphorylation. This motif region is overlapped with Akt phosphorylation motif (the residues 576-581). The phosphorylation site is marked with asterisk (*). PKA phosphorylation motif was presented below.

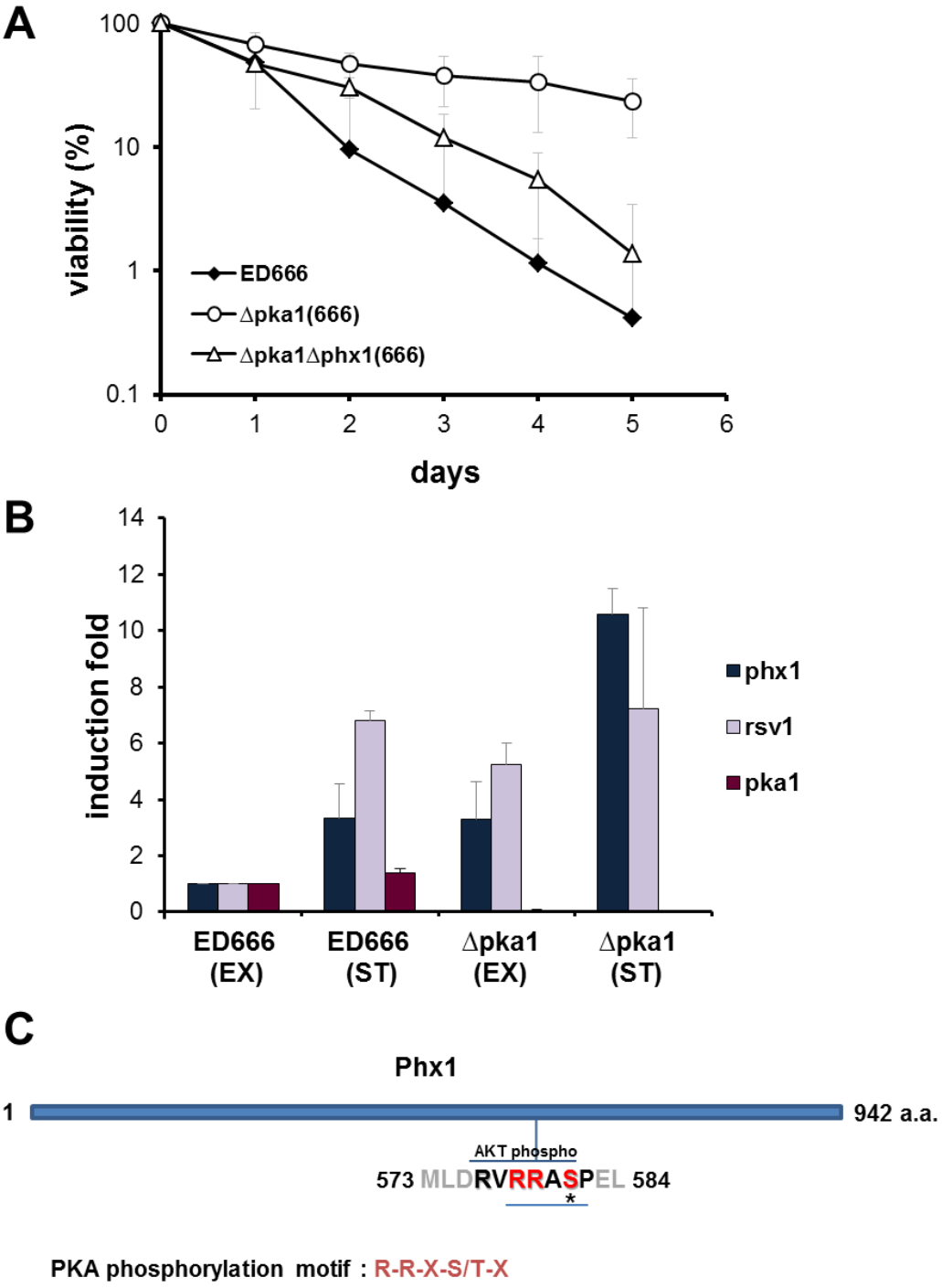
A
100
10
1
0.1
viability (%)
ED666
Δpka1(666)
Δpka1Δphx1(666)
0
1
2
3
4
5
6
days
B
14
12
10
8
6
4
2
0
induction fold
phx1
rsv1
pka1
ED666 (EX)
ED666 (ST)
Δpka1 (EX)
Δpka1 (ST)
C
Phx1
1
942 a.a.
AKT phospho
573 MLDRVRRASPEL 584
*
PKA phosphorylation motif : R-R-X-S/T-X

cells deleted for *pka1*$^+$ also extended chronological life span (Fig. III-20A). To investigate whether *phx1*$^+$ affects the long-term survival of Δ*pka1*, the Δ*pka1* Δ*phx1* double mutant strain was constructed. Interestingly, these double deletions made cells lose viability more than Δ*pka1* single mutant in stationary phase (Fig. III-19A). It implies that Pka1, as another upstream kinase, may regulate the long-term survival of Phx1.

Since Pka1 pathway is a major signaling pathway for glucose starvation and *phx1*$^+$ was highly induced in glucose-starved condition (Fig. III-1), we examined whether Pka1 pathway was involved in *phx1*$^+$ induction. Quantitative real-time PCR was performed to determine the level of *phx1*$^+$ mRNA in Δ*pka1* mutants depending on growth phases in YES media. As shown in Fig. III-20B, the mRNA expression of *phx1*$^+$ was induced more in exponentially growing Δ*pka1* mutant cells than in wild type. The expression of *rsv1*$^+$ gene whose transcription is negatively regulated by the cAMP/Pka1 pathway (Hao *et al.* 1997) was examined together as a positive control. Interestingly, *phx1*$^+$ induction increased more in Δ*pka1* mutants compared to in wild-type cells even at stationary phase. Therefore, it is supposed that cAMP/Pka1 pathway represses *phx1*$^+$ transcription in glucose-rich medium.

Since Pka1 is a protein kinase, there may be a transcription factor regulated by Pka1 for *phx1*$^+$ expression. Rst2, a transcription factor that is required for gluconeogenesis and sexual development, is known for phosphorylation target of Pka1 (Higuchi *et al.* 2002). Therefore, Rst2 can be a putative transcription activator of *phx1*$^+$. However, an in-depth study to find transcription regulators for *phx1*$^+$ induction should be needed.

Phx1 carries putative PKA target sequences (R-R-X-S/T-X) in the residues 578-582 (Fig. III-20C). This region is overlapped with AKT phosphorylation motif previously described (Fig. III-19D), not with AKT/14-3-3 motif. Anyway, it is possible that Pka1 regulates Phx1 phosphorylation as well as its

transcription.

Fructose bisphosphatase (Fbp1) is a key enzyme for gluconeogenesis. The *fbp1*$^{+}$ is a glucose-repressible gene induced during glucose starvation and stationary phase, and cAMP/Pka1 pathway represses *fbp1*$^{+}$ expression. Since *phx1*$^{+}$ was also induced in glucose-starved condition and stationary phase (Fig. III-1 and 2), we examined whether *fbp1*$^{+}$ expression is under the control of Phx1. Northern blot hybridization showed that the expression of *fpb1*$^{+}$ in Δ*phx1* mutant was a little more decreased than in wild type at stationary phase (Fig. III-21A, B). It means that *fbp1*$^{+}$ expression is partially dependent on Phx1.

The *rsv1*$^{+}$, *rsv2*$^{+}$ (required for stationary phase viability) genes were identified to be related with fission yeast long-term survival. They have zinc finger motifs and may be DNA-binding proteins. The *rsv1*$^{+}$ gene was induced by glucose starvation and negatively regulated by the cAMP/Pka1 pathway (Hao *et al.* 1997). Rsv1 protein also represses glucose-metabolism genes during meiosis (Mata *et al.* 2007). The *rsv2*$^{+}$ gene was involved in chronological life span extension and meiosis (Ohtsuka *et al.* 2012). Since the functions and phenotypes of these genes were partially overlapped with that of *phx1*$^{+}$, we investigated the interactions among those genes. At first, for the *in vivo* physical interactions between Phx1 and Rsv1, BiFC analysis was examined. The cells co-transformed with pREP41- *phx1*$^{+}$-VC and pREP42-*rsv1*$^{+}$-VN plasmids were tinged with Venus fluorescence, but no fluorescence in the cells containing pREP41- *phx1*$^{+}$-VC and pREP- *rsv2*$^{+}$-VN plasmids was detected (Fig. III-21C). These results suggest that Rsv1 may be an interacting partner of Phx1.

Previously, we suggested that Phx1 had a conserved region besides homeodomain (Fig. I-1) and this region might act as an interacting motif for binding partners. Although this suggestion should be needed to be confirmed,

Fig. III-21. Genetic and physical interactions between Phx1 and the targets of Pka1.

(A) Phx1-dependent expression of *fbp1*$^+$ gene. The *fbp1*$^+$ transcripts were detected by northern blot analysis with rRNA as a loading control in wild-type (JH43) and Δ*phx1* mutant cells (ESX5) grown in EMM liquid media to exponential (EX) and stationary (ST) phases.

(B) Expression levels of *fbp1*$^+$ in wild-type and Δ*phx1* mutant cells were measured by qRT-PCR. RNA samples from wild-type (JH43) and Δ*phx1* mutant (ESX5) cells grown in EMM liquid media for stationary phase were prepared. The mRNA levels of *fbp1*$^+$ were measured by qRT-PCR, along with that of *act1*$^+$ as an internal control. Average induction folds from three independent experiments were presented with standard deviations. ST; stationary phase.

(C) Bimolecular fluorescence complementation (BiFC) analysis to detect the interactions of Phx1 with Rsv1 and Rsv2. ED665 cells co-transformed with pREP42-*rsv1*$^+$-VN and pREP41-*phx1*$^+$-VC, or with pREP42-*rsv2*$^+$-VN and pREP41-*phx1*$^+$-VC were examined by fluorescence microscope. The cells co-transformed with pREP42-VN and pREP41-*phx1*$^+$-VC were examined as a negative control. Fluorescence and DIC images were visualized by fluorescence microscopy (Axiovert 200M, Carl Zeiss).

(D) Expression levels of *rsv1*$^+$ in wild-type (JH43) and Δ*phx1* (ESX5) mutant cells at exponential (EX) and stationary (ST) phase. The mRNA levels of *rsv1*$^+$ was measured by qRT-PCR. Average induction folds from three independent experiments were presented with standard deviations.

(E) Expression levels of *phx1*$^+$ in wild-type (ED668) and Δ*rsv1* mutant (from Bioneer Co.) cells at exponential (EX) and stationary (ST) phase. The mRNA levels of *phx1*$^+$ was measured by qRT-PCR. Average induction folds from three independent experiments were presented with standard deviations.

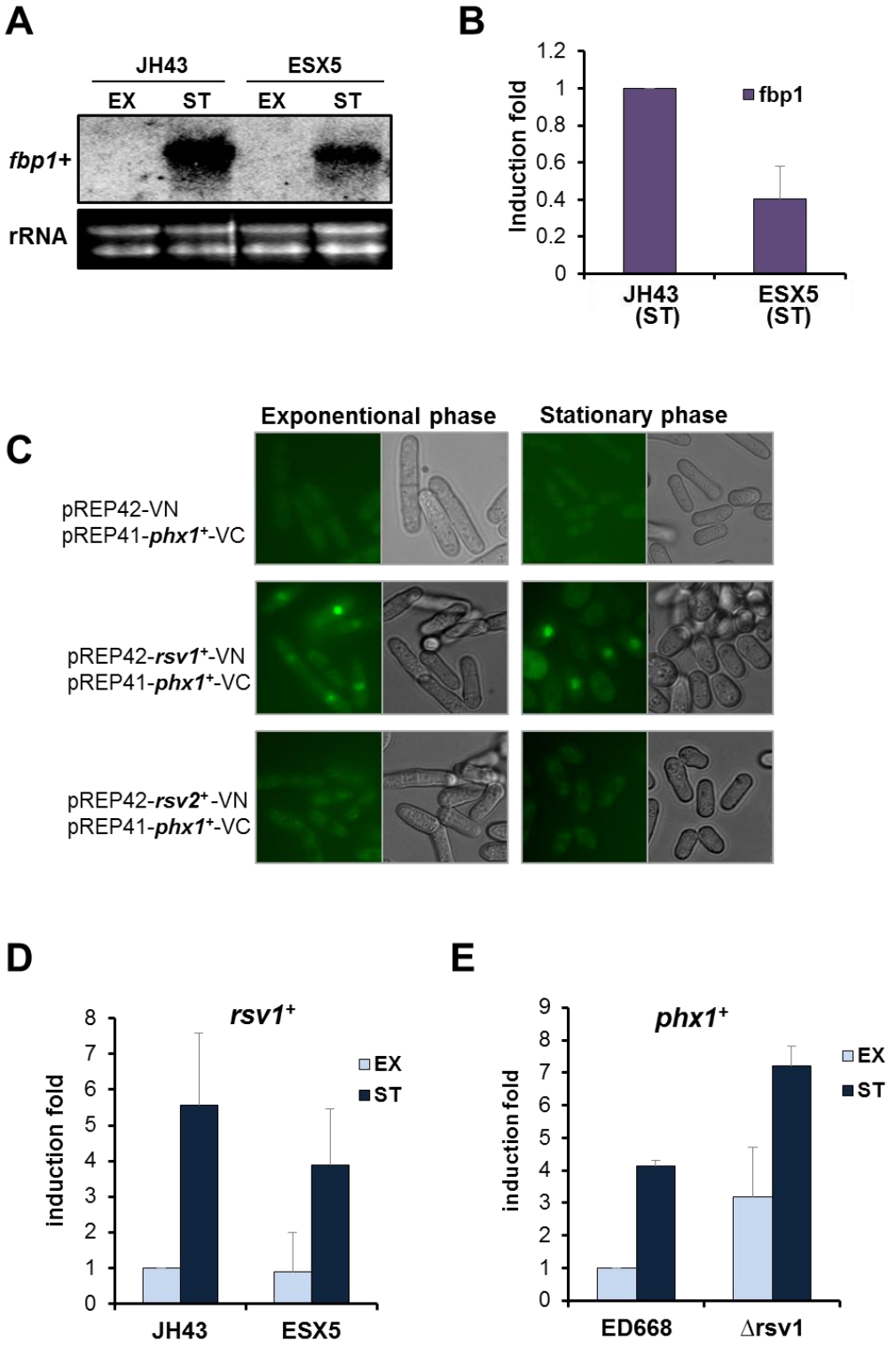
A
JH43
ESX5
EX
ST
EX
ST
fbp1+
rRNA
B
Induction fold
1.2
1
0.8
0.6
0.4
0.2
0
fbp1
JH43 (ST)
ESX5 (ST)
C
Exponentional phase
Stationary phase
pREP42-VN
pREP41-phx1+-VC
pREP42-rsv1+-VN
pREP41-phx1+-VC
pREP42-rsv2+-VN
pREP41-phx1+-VC
D
rsv1+
induction fold
8
7
6
5
4
3
2
1
0
EX
ST
JH43
ESX5
E
phx1+
induction fold
9
8
7
6
5
4
3
2
1
0
EX
ST
ED668
Δrsv1

anyway, Rsv1 could be a putative binding partner of Phx1. In addition, we measured mRNA levels of *rsv1*$^+$ and *phx1*$^+$ in each other mutant by qRT-PCR (Fig. III-21D, E). However, there was no genetic interaction with each other. Therefore, it seems that *phx1*$^+$ and *rsv1*$^+$ are not involved in regulation of each other's expression.

Rokeach's group reported that both *pka1*$^+$ and *sck2*$^+$ control longevity and they compensate for each other (Roux *et al.* 2006). As like in *S. cerevisiae*, the Pka1 and Sck2 may control their targets separately, but also be partially redundant signal transduction pathways. And they may have common target genes for redundancy of their function. From the results that *Δphx1* diminished the long-term viability of Δ*pka1* or Δ*sck2* mutants, we can suggest Phx1 may have a possibility to be a common target factor of Pka1 and Sck2.

III.7.3. Sty1 MAP kinase pathway may be the upstream regulator of Phx1

In *S. pombe*, another signaling pathway linked to life span extension is stress-responsive Sty1 MAP kinase pathway. Sty1 is activated at the onset of stationary phase in EMM media and *Δsty1* mutants decreased chronological life span (Zuin *et al.* 2010). Therefore, we also checked the relation between the *phx1*$^+$ and the *sty1*$^+$ genes. As shown in Fig. III-22A, the absence of *sty1*$^+$ decreased the *phx1*$^+$ expression at stationary phase. The *atf1*$^+$ gene encoding a major downstream target of Sty1, was also decreased as known before. However, *rsv1*$^+$ was not affect by Sty1. It suggests Sty1 regulates transcription level of *phx1*$^+$ as like as *atf1*$^+$ at stationary phase. Since Sty1 is a MAP kinase, we examined whether a transcription factor, Atf1, target of Sty1, regulates *phx1*$^+$ expression. As demonstrated in Fig. III-22B and C, Δ*atf1* and Δ*phx1* did not affect to each other's expression. Therefore, the transcription of *phx1*$^+$ may be regulated by Sty1, independently of Atf1. Atf1 regulates its own

Fig. III-22. Genetic and physical interactions of Sty1, Atf1, and Phx1.

(A) Expression levels of *phx1*$^+$, *rsv1*$^+$, *atf1*$^+$, and *sty1*$^+$ in wild-type and Δ*sty1* mutant cells. RNA samples from wild-type (ED668) and Δ*sty1* mutant (from Bioneer Co.) cells grown to exponential (EX) and stationary (ST) phases in YES liquid media were prepared. The mRNA levels of *phx1*$^+$, *rsv1*$^+$, *atf1*$^+$, and *sty1*$^+$ were measured by qRT-PCR, along with that of *act1*$^+$ as an internal control. Average induction folds from three independent experiments were presented with standard deviations.

(B) Expression levels of *atf1*$^+$ and *phx1*$^+$ in wild-type (JH43) and Δ*phx1* (ESX5) mutant cells at exponential (EX) or stationary (ST) phase. The mRNA levels of *atf1*$^+$ and *phx1*$^+$ were measured by qRT-PCR. Average induction folds from three independent experiments were presented with standard deviations.

(C) Expression levels of *phx1*$^+$ and *atf1*$^+$ in wild-type (ED668) and Δ*atf1* mutant (from Bioneer Co.) cells at exponential (EX) or stationary (ST) phase. The mRNA levels of *phx1*$^+$ was measured by qRT-PCR. Average induction folds from three independent experiments were presented with standard deviations.

(D) Bimolecular fluorescence complementation (BiFC) analysis to detect the interaction between Phx1 and Sty1. ED665 cells co-transformed with pREP42-*sty1*$^+$-VN and pREP41-*phx1*$^+$-VC were examined by fluorescence microscope. The cells co-transformed with pREP41-VC and pREP42-*sty1*$^+$-VN were examined as a negative control. Fluorescence and DIC images were visualized by fluorescence microscopy (Axiovert 200M, Carl Zeiss).

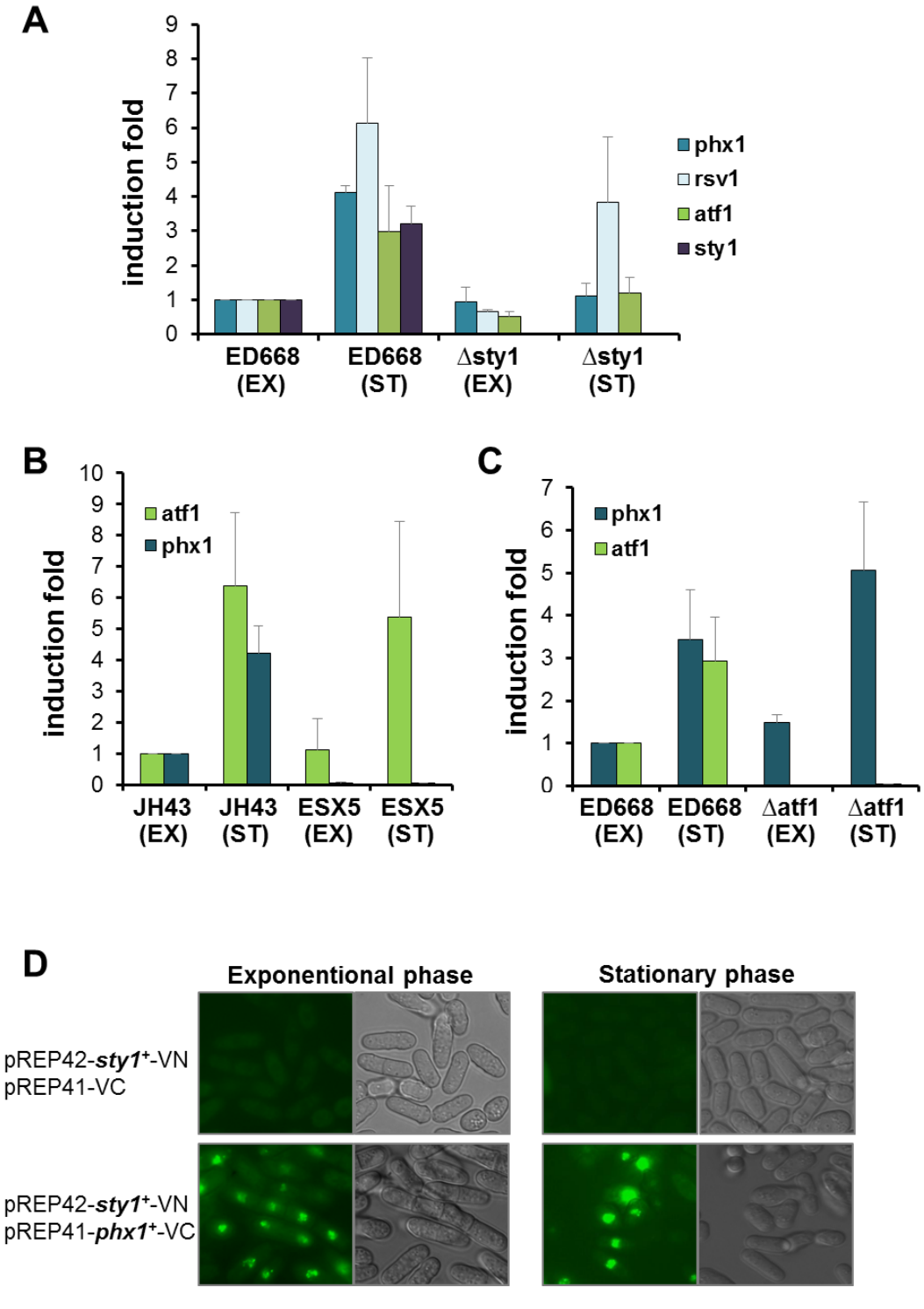
A
induction fold
phx1
rsv1
atf1
sty1
ED668 (EX)
ED668 (ST)
Δsty1 (EX)
Δsty1 (ST)
B
induction fold
atf1
phx1
JH43 (EX)
JH43 (ST)
ESX5 (EX)
ESX5 (ST)
C
induction fold
phx1
atf1
ED668 (EX)
ED668 (ST)
Δatf1 (EX)
Δatf1 (ST)
D
Exponentional phase
Stationary phase
pREP42-sty1+-VN
pREP41-VC
pREP42-sty1+-VN
pREP41-phx1+-VC

transcription by auto-regulation. Phx1 also has a possibility to regulate its transcription by itself as like Atf1. Moreover, Phx1 seemed to show physical interaction with Sty1, because bright fluorescence was detected in the nucleus of the cells containing BiFC constructs (Fig. III-22D). Therefore, it is suggested that Sty1 regulates Phx1 activation by phosphorylation. However, more experimental data should be provided for detecting direct phosphorylation of Phx1 by Sty1.

III.8. Phenotype of Phx1-Overproducing Cells

III.8.1. Elongation of cell size

Phx1-overproducing cells showed flocculation when cultured in liquid media and invasive growth when grown on agar media (Kwon 2004). In addition to these phenotypes, overproduction of Phx1 makes cells elongate their size (Fig. III-23A). The average range of *S. pombe* haploid cell size is 7~8 (newly born) to 12~15 μm (at division) at exponential phase (Mitchison and Nurse 1985). However, when Phx1 was overproduced, the cells lengthened their size into 12~15 (newly born) to 20~21 μm (at division). The width (3~4 μm) of the cells was not different between wild-type and Phx1-overproducing cells. Similarly, homozygous Δ*phx1* / Δ*phx1* diploid cells displayed small cell size (Fig. III-23B). Wild-type homozygous diploid appeared 9~14 μm (new born) to 20~25 μm (at division) range of cell size at exponential phase. On the other hand, homozygous Δ*phx1* / Δ*phx1* diploid strain only showed 4~5 (new born) to 10~11 μm (at division) at same growth phase. Although the difference of cell size between wild-type and Δ*phx1* / Δ*phx1* mutant cells disappeared at stationary phase, small cell size of exponentially growing diploid mutant implied that these mutant cells experienced some kinds of defects.

Fig. III-23. Phx1-overproducing cells and homozygous Δ*phx1* / Δ*phx1* mutant diploid cells change their cell sizes.

(A) Cell elongation phenotype by *phx1*$^{+}$ overexpression. ED665 strains transformed with pREP2 (for control cells) or pREP2- *phx1*$^{+}$ (for Phx1-overproducing cells) plasmids were grown at 30℃ in thiamine-free minimal medium. Cell images were obtained by using phase contrast microscopy. Bar= 5 μm. Cell sizes were measured by Axiovision AC program. **(B)** Homozygous Δ*phx1* / Δ*phx1* mutant diploid cells shortened their size. Wild-type diploid (obtained during mating process of ED665 and ED668 strains ; ED665 / ED668) and Δ*phx1* / Δ*phx1* mutant diploid (obtained during mating process of ESX5 and ESX8 strains; ESX5 / ESX8) were grown at 30℃ in EMM medium. Cell images were obtained by using phase contrast microscopy. Bar= 5 μm. Cell sizes were measured by Axiovision AC program.

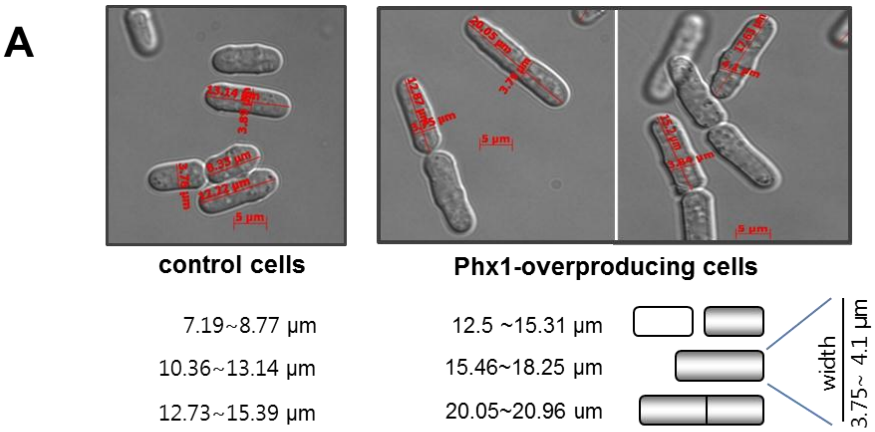
A
control cells
Phx1-overproducing cells
7.19~8.77 µm
10.36~13.14 µm
12.73~15.39 µm
12.5 ~15.31 µm
15.46~18.25 µm
20.05~20.96 um
width
3.75~ 4.1 µm

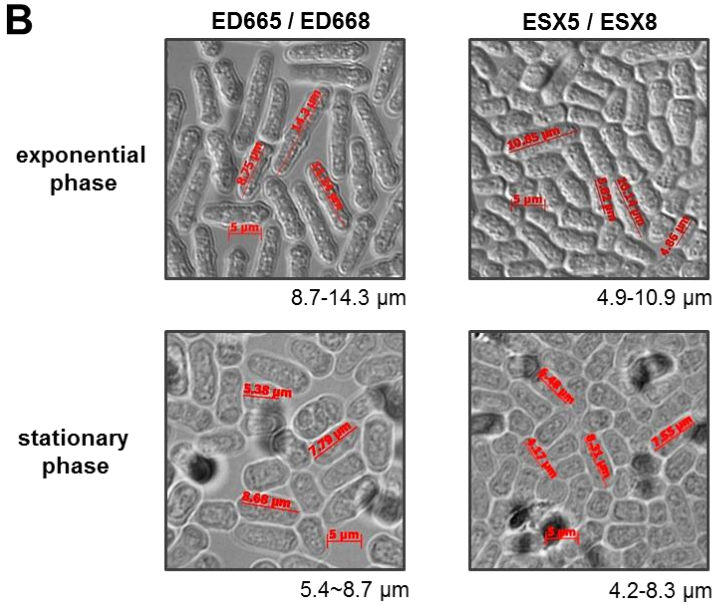
B
ED665 / ED668
ESX5 / ESX8
exponential phase
8.7-14.3 µm
4.9-10.9 µm
stationary phase
5.4~8.7 µm
4.2-8.3 µm

Among the repressed genes in Δ*phx1* mutant strain, the *but1*$^+$ (for proteins that bind to Uba three, SPAC27D7.12c) gene was reported to be involved in cell elongation (Yashiroda and Tanaka 2003). Δ*but1* mutant did not show any growth defect. However, when this gene was overexpressed, cells became elongated compared with the control cells. In Hideki's report, overexpression of *but1*$^+$ seemed to inhibit the NEDD8 pathway which is similar with ubiquitin/proteasome pathway. Therefore, Phx1 may also be involved in this pathway through *but1*$^+$ regulation.

S. pombe cells can show long and branched form as invasive phenotype under conditions of low nitrogen and high glucose (Amoah-Buahin *et al.* 2005). It suggests Phx1 overproducing cells may response to the nutrient changing conditions.

III.9. Conclusion

Phx1 is a homeobox-containing protein whose synthesis is elevated during the stationary phase. It resides primarily in the nucleus and contains the transcriptional activating ability when bound to DNA, supporting its role as a transcriptional regulator. Its synthesis is induced by nutrient starvation, various oxidative stresses, and by heat shock. Furthermore, it prevents the ROS accumulation during stationary phase. These coincide with the roles of Phx1 in long-term survival and stress resistance. Phx1 is also critically required for the meiotic spore formation from diploid cells. Taken all these observations together, it is quite clear that Phx1 is a novel regulator that confers cells with fitness to survive during the nutrient-lacking stationary phase. And it enhances viability and ability to form spores for the future, most likely through reprogramming gene expression pattern (Fig. III-24).

Phx1 increases the gene expressions involved in thiamine biosynthesis, followed by maintaining intracellular thiamine levels. Phx1 also contributes

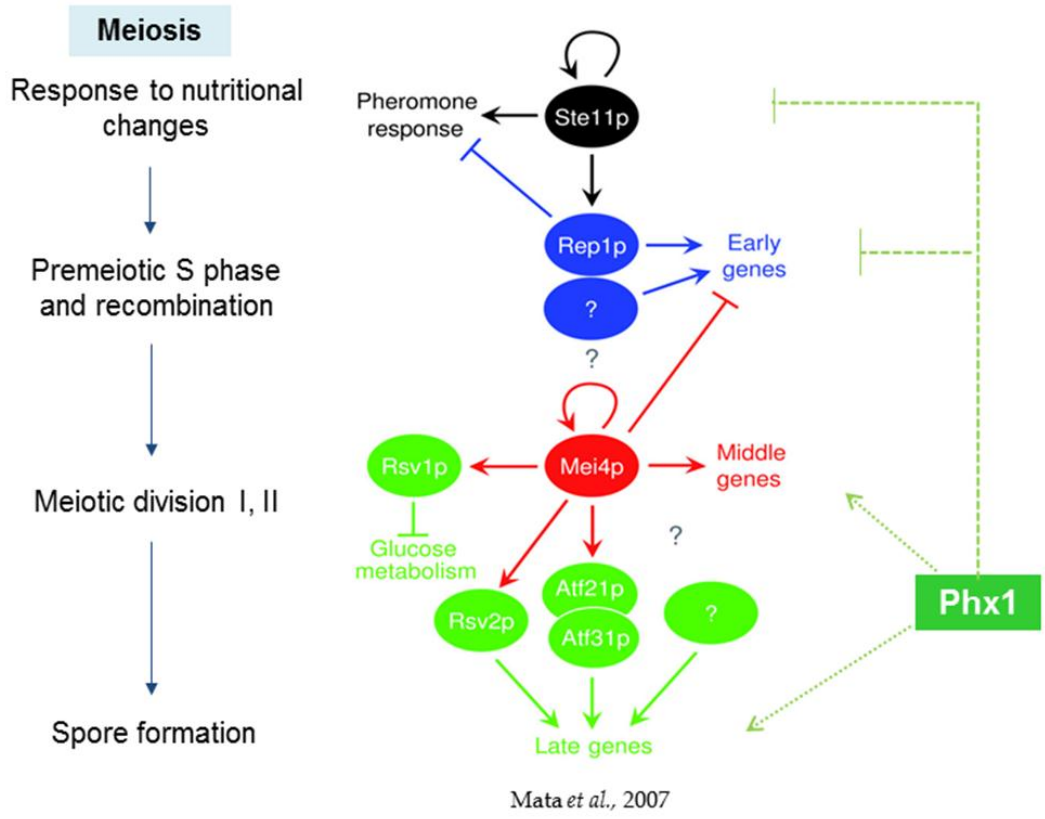

Fig. III-24. Model for Phx1 regulatory pathway controlling meiosis.

Arrows indicate activation and cross bars indicate repression. Dash lines present the putative regulation of Phx1. Each step of meiosis (left) corresponds to the step which each master regulator (Ste11, Rep1, Mei4, Atf21/31, Rsv2) controls (right).

to the increased pyruvate decarboxylase (PDC) activity by inducing the *pdc1*$^+$ and *pdc4*$^+$ expressions. Interestingly, thiamine pyrophosphate (TPP) is a cofactor of PDC enzymes. Phx1 may not only increase PDC apoproteins but also provide TPP to these apoproteins for their activity.

During stationary phase, Phx1 induces the gene expression in glycolysis/gluconeogenesis, (*gpd1*$^+$, *gpd3*$^+$, *eno1*$^+$, *fbp1*$^+$), glycerol synthesis (*gpd1*$^+$, *gpd3*$^+$, *dak2*$^+$), and fermentation (*pdc1*$^+$, *pdc3*$^+$, *pdc4*$^+$), but decreases the gene expression in cellular respiration related with TCA cycle and electron transport chain (*aco1*$^+$, *cit1*$^+$, *cyc1*$^+$, *etc.*) and in pentose phosphate pathway (*zwf1*$^+$, SPAC26H5.09c, SPAC3C7.13c, SPAC4G9.12). Fermentation and respiration share the initial pathway of glycolysis, but diverge from pyruvate. It seems that Phx1 make reroute pyruvate from TCA cycle to fermentation. Respiration is one of the efficient ways a cell gains useful energy to fuel cellular activity. However, it also generates ROS as byproduct. ROS is known for a main causative agent to chronological aging. Therefore, it is needed tight regulatory mechanism about redox balance for fitness of cell survival. Phx1 may be a tuning factor for this mechanism.

The *pdc1*$^+$ and *pdc4*$^+$ genes, the transcriptional targets of Phx1, are also required for long-term survival. It suggests the longevity regulation of Phx1 is mediated by these genes. Pyruvate decarboxylase (PDC) enzymes convert pyruvate to acetaldehyde, leading to ethanol fermentation. Acetaldehyde, then, is converted to ethanol by alcohol dehydrogenase (ADH) enzymes. The overexpression of *adh1*$^+$ gene was also capable of increasing the chronological life span in fission yeast *S. pombe* (Roux *et al.* 2010). Therefore, ADH enzymes can also be downstream targets to recognize the signal of longevity regulation from Phx1. In addition, NAD^+ produced by ADH enzymatic process can activate Sir2, NAD^+-dependent histone deacetylase, which is known for anti-aging factor in mammals (Fig. III-25).

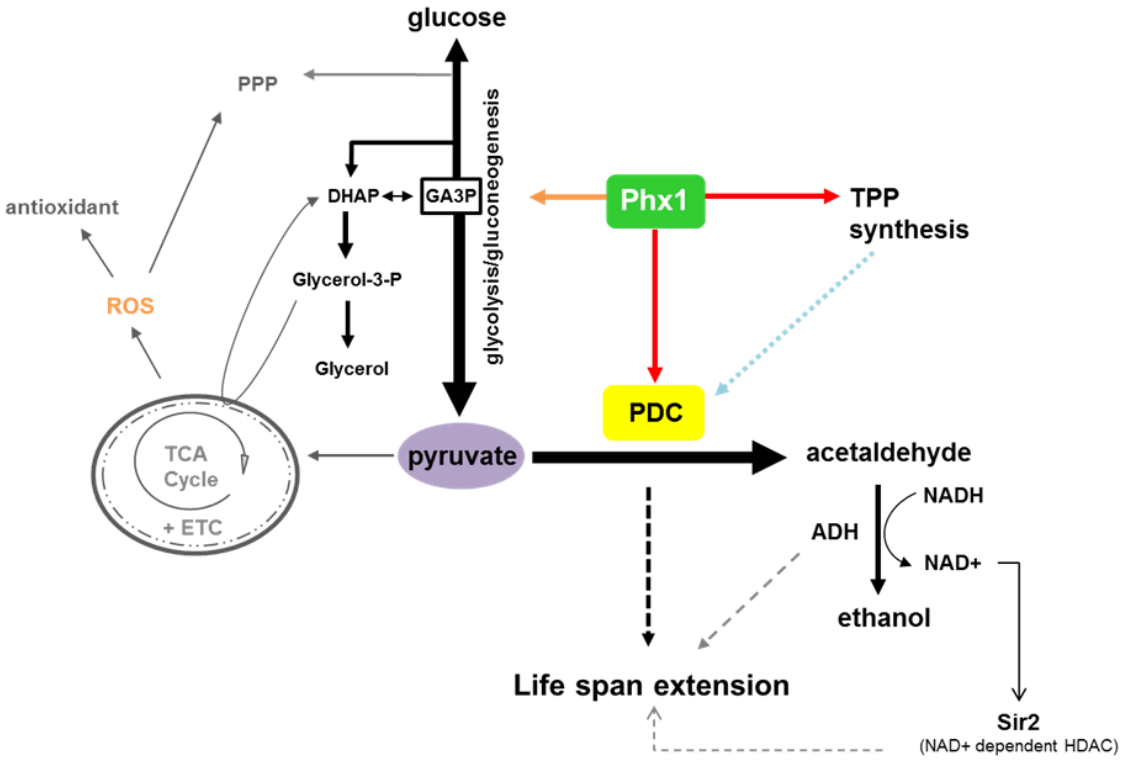

Fig. III-25. Model for Phx1 regulatory pathway controlling long-term survival.

Arrows indicate activation and cross bars indicate repression. In the metabolic pathway, thick or dark lines indicate preferring directions, and thin and pale lines indicate avoiding directions by Phx1. Dashed lines present indirect or putative mechanisms.

Sck2 and Pka1 pathway are the nutrient-sensing pathways which also have pro-aging effects. These pathways seem to regulate Phx1 antagonistically. Otherwise, Sty1, stress-activated MAP kinase, seems to regulate Phx1 positively. Although how they regulate Phx1 has not been known in detail, Phx1 certainly get some kinds of signals such as starvation or stress from these kinases (Fig. III-26).

In summary, Phx1 maybe recognize nutrient condition in the cells and make cells endure stressful circumstance through changing of energy metabolism during stationary phase and through spore formation during meiosis (Fig. III-27). Elucidation of the detail mechanisms of signaling pathway as well as its other target genes will be of interest to understand the mechanism of long-term survival and sporulation specificity in fungi as well as common across other organisms.

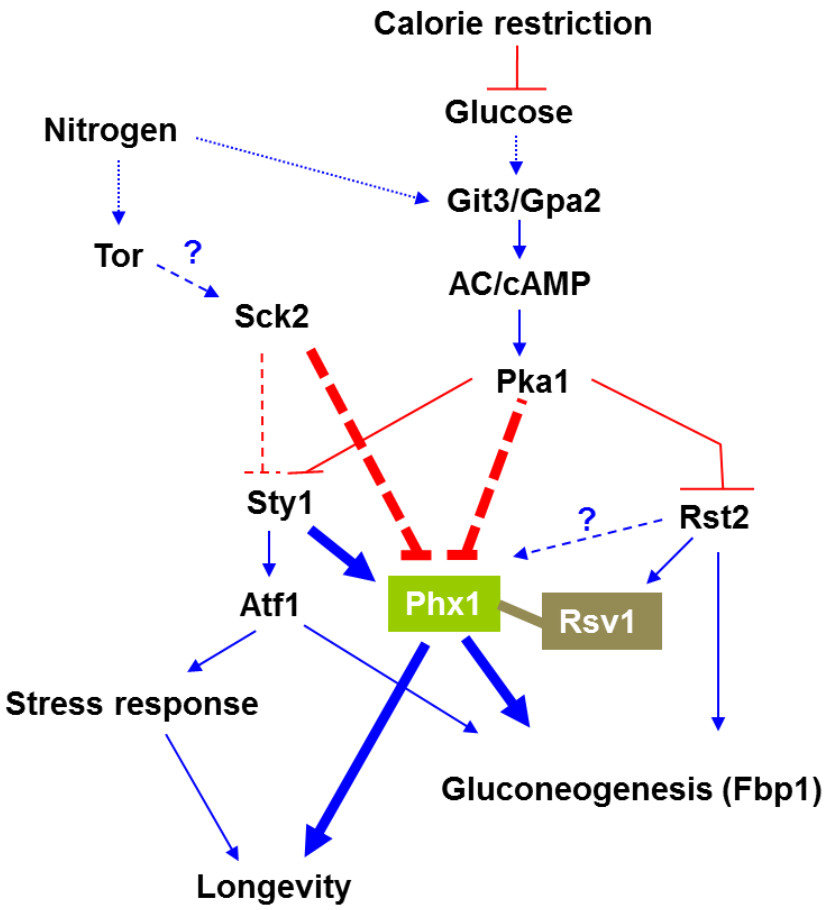

Fig. III-26. Model for upstream signaling pathways for Phx1 regulation.

Arrows indicate activation and cross bars indicate repression. Dashed lines present indirect mechanisms, and dashed lines with question mark present putative mechanisms. Phx1 may physically interact with Rsv1.

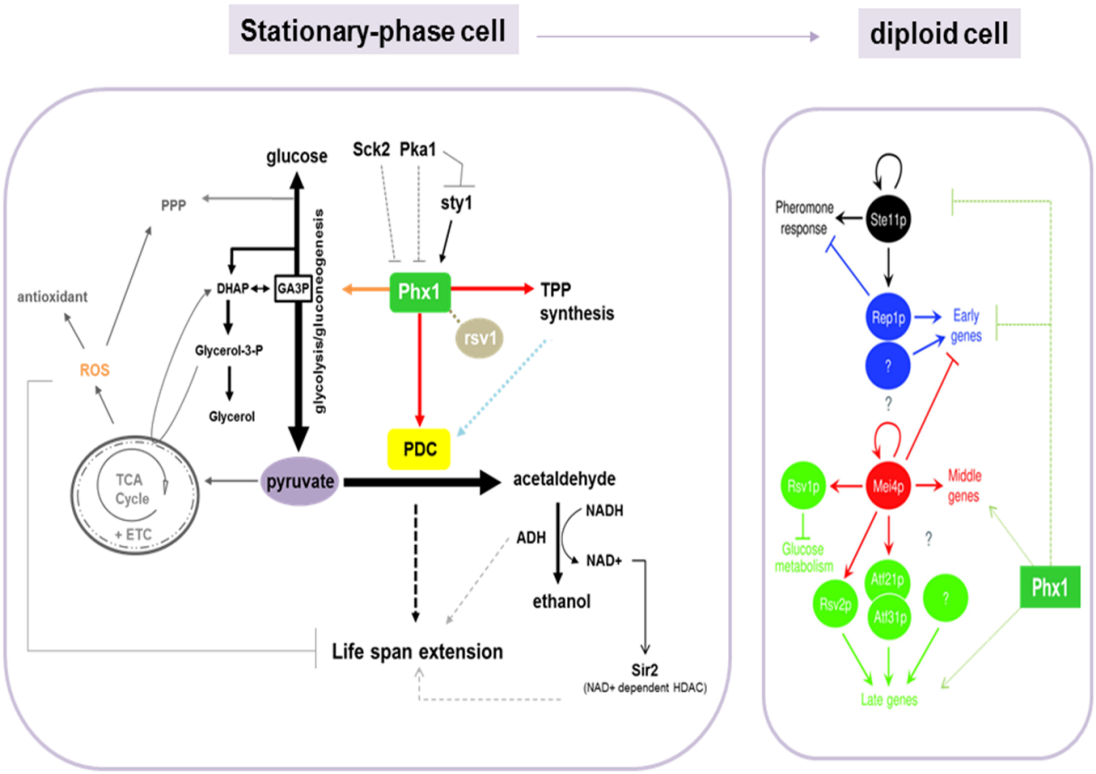

Fig. III-27. Proposed model for Phx1 regulatory pathway during stationary phase in haploid cells and meiosis in diploid cells.

Overall regulatory model of Phx1 in haploid and diploid cells. Arrows indicate activation and cross bars indicate repression. In the metabolic pathway, thick or dark lines indicate preferring directions, and thin and pale lines indicate avoiding directions by Phx1. Dashed lines present indirect or putative mechanisms.

CHAPTER IV.

REFERENCES

Alfa C, Cold Spring Harbor Laboratory. 1993. *Experiments with fission yeast : a laboratory course manual*. Cold Spring Harbor Laboratory Press, Plainview, N.Y.

Aligianni S, Lackner DH, Klier S, Rustici G, Wilhelm BT, Marguerat S, Codlin S, Brazma A, de Bruin RA, Bahler J. 2009. The fission yeast homeodomain protein Yox1p binds to MBF and confines MBF-dependent cell-cycle transcription to G1-S via negative feedback. PLoS Genet 5: **E1000626.**

Amoah-Buahin E, Bone N, Armstrong J. 2005. Hyphal Growth in the Fission Yeast Schizosaccharomyces pombe. *Eukaryot Cell* 4: 1287-1297.

Arnaise S, Zickler D, Poisier C, Debuchy R. 2001. pah1: a homeobox gene involved in hyphal morphology and microconidiogenesis in the filamentous ascomycete Podospora anserina. *Mol Microbiol* 39: 54-64.

Arndt GM, Atkins D. 1996. pH sensitivity of Schizosaccharomyces pombe: effect on the cellular phenotype associated with lacZ gene expression. *Curr Genet* 29: 457-461.

Banerjee-Basu S, Baxevanis AD. 2001. Molecular evolution of the homeodomain family of transcription factors. *Nucleic Acids Res* 29: 3258-3269.

Barker MG, Walmsley RM. 1999. Replicative ageing in the fission yeast Schizosaccharomyces pombe. *Yeast* 15: 1511-1518.

Bettendorff L, Wins P. 2009. Thiamin diphosphate in biological chemistry: new aspects of thiamin metabolism, especially triphosphate derivatives acting other than as cofactors. *FEBS J* 276: 2917-2925.

Bhoite LT, Allen JM, Garcia E, Thomas LR, Gregory ID, Voth WP, Whelihan K, Rolfes RJ, Stillman DJ. 2002. Mutations in the pho2 (bas2) transcription factor that differentially affect activation with its partner proteins bas1, pho4, and swi5. *J Biol Chem* 277: 37612-37618.

Boucherie H. 1985. Protein synthesis during transition and stationary phases under glucose limitation in Saccharomyces cerevisiae. *J Bacteriol* 161: 385-392.

Bradford MM. 1976. A rapid and sensitive method for the quantitation of microgram quantities of protein utilizing the principle of protein-dye binding. *Anal Biochem* 72: 248-254.

Burglin TR. 1988. The yeast regulatory gene PHO2 encodes a homeo box.

Cell 53: 339-340.

Costelloe SJ, Ward JM, Dalby PA. 2008. Evolutionary analysis of the TPP-dependent enzyme family. *J Mol Evol* 66: 36-49.

Dickinson JR, Salgado LE, Hewlins MJ. 2003. The catabolism of amino acids to long chain and complex alcohols in Saccharomyces cerevisiae. *J Biol Chem* 278: 8028-8034.

Eshaghi M, Lee JH, Zhu L, Poon SY, Li J, Cho KH, Chu Z, Karuturi RK, Liu J. 2010. Genomic binding profiling of the fission yeast stress-activated MAPK Sty1 and the bZIP transcriptional activator Atf1 in response to H2O2. *PLoS One* 5: e11620.

Fabrizio P, Gattazzo C, Battistella L, Wei M, Cheng C, McGrew K, Longo VD. 2005. Sir2 blocks extreme life-span extension. *Cell* 123: 655-667.

Fabrizio P, Longo VD. 2003. The chronological life span of Saccharomyces cerevisiae. *Aging Cell* 2: 73-81.

Fankhauser H, Zurlinden A, Schweingruber AM, Edenharter E, Schweingruber ME. 1995. Schizosaccharomyces pombe thiamine pyrophosphokinase is encoded by gene tnr3 and is a regulator of thiamine metabolism, phosphate metabolism, mating, and growth. *J Biol Chem* 270: 28457-28462.

Fujita M, Yamamoto M. 1998. S. pombe sck2+, a second homologue of S. cerevisiae SCH9 in fission yeast, encodes a putative protein kinase closely related to PKA in function. *Curr Genet* 33: 248-254.

Gehring WJ. 1987. Homeo boxes in the study of development. *Science* 236: 1245-1252.

Ha CW, Huh WK. 2011. The implication of Sir2 in replicative aging and senescence in Saccharomyces cerevisiae. *Aging (Albany NY)* 3: 319-324.

Hannum C, Kulaeva OI, Sun H, Urbanowski JL, Wendus A, Stillman DJ, Rolfes RJ. 2002. Functional mapping of Bas2. Identification of activation and Bas1-interaction domains. *J Biol Chem* 277: 34003-34009.

Hao Z, Furunobu A, Nagata A, Okayama H. 1997. A zinc finger protein required for stationary phase viability in fission yeast. *J Cell Sci* 110 (Pt 20): 2557-2566.

Herman PK. 2002. Stationary phase in yeast. *Curr Opin Microbiol* 5: 602-607.

Higuchi T, Watanabe Y, Yamamoto M. 2002. Protein kinase A regulates

sexual development and gluconeogenesis through phosphorylation of the Zn finger transcriptional activator Rst2p in fission yeast. *Mol Cell Biol* 22: 1-11.

Jakubowski W, Bilinski T, Bartosz G. 2000. Oxidative stress during aging of stationary cultures of the yeast Saccharomyces cerevisiae. *Free Radic Biol Med* 28: 659-664.

Kaeberlein M, Burtner CR, Kennedy BK. 2007. Recent developments in yeast aging. *PLoS Genet* 3: e84.

Kaeberlein M, Powers RW, 3rd, Steffen KK, Westman EA, Hu D, Dang N, Kerr EO, Kirkland KT, Fields S, Kennedy BK. 2005. Regulation of yeast replicative life span by TOR and Sch9 in response to nutrients. *Science* 310: 1193-1196.

Kelly M, Burke J, Smith M, Klar A, Beach D. 1988. Four mating-type genes control sexual differentiation in the fission yeast. *EMBO J* 7: 1537-1547.

Kim KD, Chung WH, Kim HJ, Lee KC, Roe JH. 2010. Monothiol glutaredoxin Grx5 interacts with Fe-S scaffold proteins Isa1 and Isa2 and supports Fe-S assembly and DNA integrity in mitochondria of fission yeast. *Biochem Biophys Res Commun* 392: 467-472.

Konig S. 1998. Subunit structure, function and organisation of pyruvate decarboxylases from various organisms. *Biochim Biophys Acta* 1385: 271-286.

Kowalska E, Kozik A. 2008. The genes and enzymes involved in the biosynthesis of thiamin and thiamin diphosphate in yeasts. *Cell Mol Biol Lett* 13: 271-282.

Kronstad JW, Staben C. 1997. Mating type in filamentous fungi. *Annu Rev Genet* 31: 245-276.

Kwon E-S. 2004. Multi-copy suppressors of growth defects caused by depletion of Cu, Zn-containing superoxide dismutase in schizosaccharomyces pombe. p. 186. Seoul National University, Seoul.

Kwon ES, Jeong JH, Roe JH. 2006. Inactivation of homocitrate synthase causes lysine auxotrophy in copper/zinc-containing superoxide dismutase-deficient yeast *Schizosaccharomyces pombe*. *J Biol Chem* 281: 1345-1351.

Lamming DW, Latorre-Esteves M, Medvedik O, Wong SN, Tsang FA, Wang C, Lin SJ, Sinclair DA. 2005. HST2 mediates SIR2-independent life-span extension by calorie restriction. *Science* 309: 1861-1864.

Longo VD, Fabrizio P. 2002. Regulation of longevity and stress resistance: a molecular strategy conserved from yeast to humans? *Cell Mol Life Sci* 59: 903-908.

Lyne R, Burns G, Mata J, Penkett CJ, Rustici G, Chen D, Langford C, Vetrie D, Bahler J. 2003. Whole-genome microarrays of fission yeast: characteristics, accuracy, reproducibility, and processing of array data. *BMC Genomics* 4: 27.

Machado CR, Praekelt UM, de Oliveira RC, Barbosa AC, Byrne KL, Meacock PA, Menck CF. 1997. Dual role for the yeast THI4 gene in thiamine biosynthesis and DNA damage tolerance. *J Mol Biol* 273: 114-121.

Mata J, Lyne R, Burns G, Bahler J. 2002. The transcriptional program of meiosis and sporulation in fission yeast. *Nat Genet* 32: 143-147.

Mata J, Wilbrey A, Bahler J. 2007. Transcriptional regulatory network for sexual differentiation in fission yeast. *Genome Biol* 8: R217.

Matsuyama A, Arai R, Yashiroda Y, Shirai A, Kamata A, Sekido S, Kobayashi Y, Hashimoto A, Hamamoto M, Hiraoka Y et al. 2006. ORFeome cloning and global analysis of protein localization in the fission yeast Schizosaccharomyces pombe. *Nat Biotechnol* 24: 841-847.

Matsuzawa T, Morita T, Tanaka N, Tohda H, Takegawa K. 2011. Identification of a galactose-specific flocculin essential for non-sexual flocculation and filamentous growth in Schizosaccharomyces pombe. *Mol Microbiol* 82: 1531-1544.

Matsuzawa T, Yoritsune K, Takegawa K. 2012. MADS box transcription factor Mbx2/Pvg4 regulates invasive growth and flocculation by inducing gsf2+ expression in fission yeast. *Eukaryot Cell* 11: 151-158.

McQuire TA, Young PG. 2006. Joint regulation of the nmt1 promoter and sporulation by Thi1 and Thi5 in Schizosaccharomyces pombe. *Curr Genet* 50: 269-279.

Medina-Silva R, Barros MP, Galhardo RS, Netto LE, Colepicolo P, Menck CF. 2006. Heat stress promotes mitochondrial instability and oxidative responses in yeast deficient in thiazole biosynthesis. *Research in microbiology* 157: 275-281.

Miotto B, Graba Y. 2010. Control of DNA replication: a new facet of Hox proteins? *Bioessays* 32: 800-807.

Mitchison JM, Nurse P. 1985. Growth in cell length in the fission yeast Schizosaccharomyces pombe. *J Cell Sci* 75: 357-376.

Mojzita D, Hohmann S. 2006. Pdc2 coordinates expression of the THI regulon in the yeast Saccharomyces cerevisiae. *Mol Genet Genomics* 276: 147-161.

Moreno S, Klar A, Nurse P. 1991. Molecular genetic analysis of fission yeast Schizosaccharomyces pombe. *Methods Enzymol* 194: 795-823.

Mukai Y, Ohno-Yamashita Y, Oshima Y, Harashima S. 1997. The role of cysteine residues in the homeodomain protein Mat alpha 2 in mating-type control of Saccharomyces cerevisiae. *Mol Gen Genet* 255: 166-171.

Muller FL, Lustgarten MS, Jang Y, Richardson A, Van Remmen H. 2007. Trends in oxidative aging theories. Free Radic Biol Med 43: 477-503.

Nagai T, Ibata K, Park ES, Kubota M, Mikoshiba K, Miyawaki A. 2002. A variant of yellow fluorescent protein with fast and efficient maturation for cell-biological applications. Nat Biotechnol 20: 87-90.

Neely LA, Hoffman CS. 2000. Protein kinase A and mitogen-activated protein kinase pathways antagonistically regulate fission yeast fbp1 transcription by employing different modes of action at two upstream activation sites. Mol Cell Biol 20: 6426-6434.

Nishimura H, Kawasaki Y, Kaneko Y, Nosaka K, Iwashima A. 1992. A positive regulatory gene, THI3, is required for thiamine metabolism in Saccharomyces cerevisiae. *J Bacteriol* 174: 4701-4706.

Nosaka K. 2006. Recent progress in understanding thiamin biosynthesis and its genetic regulation in Saccharomyces cerevisiae. *Appl Microbiol Biotechnol* 72: 30-40.

Ohtsuka H, Azuma K, Kubota S, Murakami H, Giga-Hama Y, Tohda H, Aiba H. 2012. Chronological lifespan extension by Ecl1 family proteins depends on Prr1 response regulator in fission yeast. *Genes Cells* 17: 39-52.

Pan Y, Schroeder EA, Ocampo A, Barrientos A, Shadel GS. 2011. Regulation of yeast chronological life span by TORC1 via adaptive mitochondrial ROS signaling. *Cell metabolism* 13: 668-678.

Pronk JT, Yde Steensma H, Van Dijken JP. 1996. Pyruvate metabolism in

Saccharomyces cerevisiae. *Yeast* 12: 1607-1633.

Ralser M, Wamelink MM, Kowald A, Gerisch B, Heeren G, Struys EA, Klipp E, Jakobs C, Breitenbach M, Lehrach H et al. 2007. Dynamic rerouting of the carbohydrate flux is key to counteracting oxidative stress. *J Biol* 6: 10.

Reverter-Branchat G, Cabiscol E, Tamarit J, Ros J. 2004. Oxidative damage to specific proteins in replicative and chronological-aged Saccharomyces cerevisiae: common targets and prevention by calorie restriction. *J Biol Chem* 279: 31983-31989.

Roux AE, Arseneault G, Chartrand P, Ferbeyre G, Rokeach LA. 2010. A screen for genes involved in respiration control and longevity in Schizosaccharomyces pombe. *Ann N Y Acad Sci* 1197: 19-27.

Roux AE, Leroux A, Alaamery MA, Hoffman CS, Chartrand P, Ferbeyre G, Rokeach LA. 2009. Pro-aging effects of glucose signaling through a G protein-coupled glucose receptor in fission yeast. *PLoS Genet* 5: e1000408.

Roux AE, Quissac A, Chartrand P, Ferbeyre G, Rokeach LA. 2006. Regulation of chronological aging in Schizosaccharomyces pombe by the protein kinases Pka1 and Sck2. *Aging Cell* 5: 345-357.

Saitou N, Nei M. 1987. The neighbor-joining method: a new method for reconstructing phylogenetic trees. *Mol Biol Evol* 4: 406-425.

Schweingruber AM, Dlugonski J, Edenharter E, Schweingruber ME. 1991. Thiamine in Schizosaccharomyces pombe: dephosphorylation, intracellular pool, biosynthesis and transport. *Curr Genet* 19: 249-254.

Shah N, Sukumar S. 2010. The Hox genes and their roles in oncogenesis. *Nature reviews Cancer* 10: 361-371.

Sung MK, Huh WK. 2007. Bimolecular fluorescence complementation analysis system for in vivo detection of protein-protein interaction in Saccharomyces cerevisiae. *Yeast* 24: 767-775.

Tamura K, Peterson D, Peterson N, Stecher G, Nei M, Kumar S. 2011. MEGA5: molecular evolutionary genetics analysis using maximum likelihood, evolutionary distance, and maximum parsimony methods. *Mol Biol Evol* 28: 2731-2739.

Torres-Guzman JC, Dominguez A. 1997. HOY1, a homeo gene required for hyphal formation in Yarrowia lipolytica. *Mol Cell Biol* 17: 6283-6293.

Tylicki A, Ziolkowska G, Bolkun A, Siemieniuk M, Czerniecki J, Nowakiewicz A. 2008. Comparative study of the activity and kinetic properties of malate dehydrogenase and pyruvate decarboxylase from Candida albicans, Malassezia pachydermatis, and Saccharomyces cerevisiae. *Can J Microbiol* 54: 734-741.

Vivancos AP, Jara M, Zuin A, Sanso M, Hidalgo E. 2006. Oxidative stress in Schizosaccharomyces pombe: different H2O2 levels, different response pathways. *Mol Genet Genomics* 276: 495-502.

Vuralhan Z, Morais MA, Tai SL, Piper MD, Pronk JT. 2003. Identification and characterization of phenylpyruvate decarboxylase genes in Saccharomyces cerevisiae. *Appl Environ Microbiol* 69: 4534-4541.

Wang L, Griffiths K, Jr., Zhang YH, Ivey FD, Hoffman CS. 2005. Schizosaccharomyces pombe adenylate cyclase suppressor mutations suggest a role for cAMP phosphodiesterase regulation in feedback control of glucose/cAMP signaling. *Genetics* 171: 1523-1533.

Wei M, Fabrizio P, Hu J, Ge H, Cheng C, Li L, Longo VD. 2008. Life span extension by calorie restriction depends on Rim15 and transcription factors downstream of Ras/PKA, Tor, and Sch9. *PLoS Genet* 4: e13.

Wilhelm BT, Marguerat S, Watt S, Schubert F, Wood V, Goodhead I, Penkett CJ, Rogers J, Bahler J. 2008. Dynamic repertoire of a eukaryotic transcriptome surveyed at single-nucleotide resolution. *Nature* 453: 1239-1243.

Wilkinson MG, Samuels M, Takeda T, Toone WM, Shieh JC, Toda T, Millar JB, Jones N. 1996. The Atf1 transcription factor is a target for the Sty1 stress-activated MAP kinase pathway in fission yeast. *Genes Dev* 10: 2289-2301.

Wood V Gwilliam R Rajandream MA Lyne M Lyne R Stewart A Sgouros J Peat N Hayles J Baker S et al. 2002. The genome sequence of Schizosaccharomyces pombe. *Nature* 415: 871-880.

Yaffe MB, Leparc GG, Lai J, Obata T, Volinia S, Cantley LC. 2001. A motif-based profile scanning approach for genome-wide prediction of signaling pathways. Nat Biotechnol 19: 348-353.

Yashiroda H, Tanaka K. 2003. But1 and But2 proteins bind to Uba3, a catalytic subunit of E1 for neddylation, in fission yeast. *Biochem Biophys Res Commun* 311: 691-695.

Zakany J, Duboule D. 2007. The role of Hox genes during vertebrate limb development. *Curr Opin Genet Dev* 17: 359-366.

Zhao Y, Lieberman HB. 1995. Schizosaccharomyces pombe: a model for molecular studies of eukaryotic genes. *DNA Cell Biol* 14: 359-371.

Zuin A, Carmona M, Morales-Ivorra I, Gabrielli N, Vivancos AP, Ayte J, Hidalgo E. 2010. Lifespan extension by calorie restriction relies on the Sty1 MAP kinase stress pathway. *EMBO J* 29: 981-991.

Zuin A, Gabrielli N, Calvo IA, Garcia-Santamarina S, Hoe KL, Kim DU, Park HO, Hayles J, Ayte J, Hidalgo E. 2008. Mitochondrial dysfunction increases oxidative stress and decreases chronological life span in fission yeast. PLoS One 3: e2842.

국문초록

분열성 효모에서 *phx1*$^{+}$ 유전자는 세포 내에 과량으로 존재할 때 Cu / Zn-containing superoxide dismutase (CuZn-SOD) 결핍에 의해 유발되는 lysine 영양결핍증을 극복하는 인자로 처음에 분리되었다. Phx1 단백질을 과량 생산하면, lysine 생합성 과정의 첫 번째 단계에 작용하는 효소이며 동시에 산화 스트레스에 취약한 homocitrate synthase 의 합성이 증가한다. Phx1 단백질은 아미노산 말단 근방에 DNA 에 결합할 수 있는 잘 보존된 homeodomain 을 가지고 있어서 전사조절 인자로 여겨진다. 그러나 Phx1 단백질의 기능은 현재까지 잘 알려지지 않았다.

Phx1 단백질의 기능을 연구하기 위해, Phx1 단백질의 발현 패턴과 그것의 결손균주 표현형을 살펴보았다. *phx1*$^{+}$ 유전자의 전사량은 세포가 정체 생장기에 들어갈 때 상당히 증가하고, 정체 생장기 내내 높게 유지되었다. 질소와 탄소를 제공하는 영양소의 공급을 낮추면 *phx1*$^{+}$ 유전자의 발현량은 지수 생장기에도 증가하는데, 이는 세포가 영양 고갈 환경 시에 Phx1 단백질의 기능을 필요로 함을 의미한다. Phx1 에 형광 단백질인 GFP 를 결합시켜 형광을 관찰한 결과, Phx1 단백질은 핵 안에 존재하고, 정체 생장기와 영양고갈 시기에 그 발현이 더욱 명확해지는 것을 확인하였다. *phx1*$^{+}$ 유전자가 결손된 돌연변이는 장기간의 배양 시에 야생형 균주에 비해 생존률이 감소한다. 반면에 Phx1 단백질을 과량 발현해주면 야생형 균주보다 장기간 생존률이 증가한다. 또한 *phx1*$^{+}$ 유전자 결손 돌연변이는 여러 종류의 산화 물질, 열 충격, 알코올 처리 등에 민감하였고, 정체 생장기에 야생형 균주보다 활성 산소량이 더 많이

축적되었다. *phx1*$^{+}$ 유전자 결손 이배체의 자낭포자 생성률을 측정한 결과, 야생형 균주보다 상당량 감소되었음을 확인하였다.

전사조절 인자인 Phx1 의 조절을 받는 유전자들을 알아내기 위해 microarray 분석을 하였다. 정체 생장기까지 키운 야생형과 *phx1*$^{+}$ 유전자 결손 균주의 범유전체적인 전사량 분석을 통해, *phx1* 결손 균주에서 97 개 유전자의 발현량이 증가하고 99 개 유전자의 발현량이 감소함을 알아내었다. 이 유전자들은 탄수화물 대사, 생식 세포 분화, thiamine 합성, 스트레스 반응, 물질 수송 등 다양한 과정에 참여하였다. Phx1 은 특히 pyruvate decarboxylase (PDC)를 위한 유전자인 *pdc1*$^{+}$, *pdc4*$^{+}$ 와 thiamine 합성을 위한 유전자인 *nmt1*$^{+}$, *nmt2*$^{+}$, *bsu1*$^{+}$ 의 발현을 증가시켰다. 이러한 전사조절 결과와 같은 방향으로, *phx1* 결손 균주에서 pyruvate decarboxylase 의 효소 활성도와 합성된 thiamine 의 양이 야생형 균주에 비해 적음을 확인하였다. 게다가, *pdc1* 과 *pdc4* 결손 균주는 장기간 생존률이 떨어지는 경향을 보였다. 이것은 pyruvate decarboxylase 효소가 Phx1 의 조절을 받아 장기간 생존을 유지하는 데 필요한 인자임을 의미한다.

Phx1 단백질을 활성화시키는 신호를 찾기 위해, 분열성 효모 내에서 노화를 가속화 시키는 Sck2 와 cAMP/Pka1 신호 전달 경로와 Phx1 의 관계를 탐구하였다. Phx1 단백질은 Sck2 나 Pka1 에 의해 인산화될 수 있는 모티프를 가지고 있다. *sck2*$^{+}$ 와 *phx1*$^{+}$ 유전자가 동시에 결손된 균주와 *pka1*$^{+}$ 과 *phx1*$^{+}$ 유전자가 동시에 결손된 균주를 제작하여 장기간 생존률을 측정한 결과, *phx1*$^{+}$ 결손이 *sck2*$^{+}$ 나 *pka1*$^{+}$ 유전자가 단독 결손되었을 때 나타나는 수명 연장 효과를 단축시킴을 알 수 있었다. 이는 Sck2 와 Pka1 이 상위단계에서 Phx1 을 부정적으로 조절하는 인자임을 의미한다. 분열성 효모에서 스트레스 반응을 관장하는 Sty1 MAP kinase 신호절달

경로의 수명 조절 효과 및 Phx1 단백질과의 관계 또한 탐구하였다. 흥미롭게도 정체생장기에서 Sty1 이 결핍되면, *phx1*$^{+}$ 유전자의 발현량이 Sty1 의 주요한 타겟 단백질인 Atf1 전사조절 인자와 상관없이 감소하였다. 또한, Bimolecular fluorescence complementation (BiFC) 분석을 통해 Sty1 과 Phx1 단백질이 물리적으로 결합함을 확인할 수 있었다. 이 결과들은 Phx1 이 Sty1 의 인산화 타겟이 될 수 있음을 시사한다.

위의 내용들을 종합하자면, Phx1 은 정체 생장기와 영양 고갈 시에 발현이 증가하는 전사 조절 인자이다. Phx1 은 세포가 장기간 생존하고, 산화, 열, 알코올 등의 스트레스에 저항할 수 있게한다. 또한 감수분열 시에 포자 형성 과정에 중요한 역할을 한다. 더 나아가 이러한 Phx1 의 활동은 Pka1, Sck2, Sty1 이라는 상위 조절자에 의해 조율을 받는다. 그리고 장기간 생존을 위해 Phx1 은 세포 내에서 최소한 두 개의 pyruvate decarboxylase 효소의 발현 및 활성을 증가시킨다. Pyruvate decarboxylase 효소가 어떻게 장기간 생존에 기여하는 지는 앞으로 밝혀야할 과제이다.

주요 단어들

: 분열성 효모, Phx1, 전사 조절 인자, 정체 생장기, 영양 고갈, 장기간 생존, 스트레스 저항성, 산화 스트레스, 열 충격, 활성 산소 축적, 감수 분열, DNA microarray, pyruvate decarboxylases, thiamine 생합성, Sck2 신호 전달 경로, cAMP/Pka1 신호 전달 경로, Sty1 MAPK 신호 전달 경로, Bimolecular Fluorescence Complementation

감사의 글

대학원에 입학한 지 7년 반이라는 시간이 흘렀습니다. 결코 짧지 않은 시간입니다. 처음 대학원 진학을 결정했을 때는, 학부 때 미처 채우지 못한 학문적 갈증을 해소할 수 있지 않을까 하는 막연한 기대감만 지녔던 것 같습니다. 만만치 않은 대장정일거라는 생각은 하지 못한 채로요. 그래서 많이 부딪히고, 깨지고, 의심하고, 고민했습니다. 그래도 어떻게 여기까지 오게 되었네요. 돌이켜보면, 그 과정 중에 어느 하나 결코 버릴 것 없는 값진 시간이었다는 생각이 듭니다. 조그만 실수마저, 나에 대해 더 알게하고, 성장하게 하는 소중한 경험이었습니다. 하지만 그 과정을 잘 겪어나갈 수 있게 도와주신 분들이 곁에 없었다면 이 자리까지 오지 못했을 것입니다.

먼저, 인생의 선배님으로서, 과학자로서, 저의 롤모델이 되어주신 노정혜 선생님, 꾸준한 학문적 열정을 보여주시는 선생님을 보며 흔들릴 때마다 마음을 다잡을 수 있었습니다. 감사드리고 존경합니다. 바쁘신 와중에도 부족한 논문을 심사해 주시고, 많은 조언을 해 주신 석영재 선생님, 정우현 선생님, 한지숙 선생님, 허원기 선생님께 감사의 말씀을 드립니다. 앞으로 더 열심히 부족한 부분을 채워나가겠습니다.

그리고 여러 실험실 선배님들, 저에게 실험과 인생의 지침을 가르쳐 주신 은수오빠, 정말 많이 배웠습니다. 감사해요. 똑똑하시고 못하는 게 없으신 듯한 준석오빠, 열심히 실험하시는 모습이 귀감이 되었던 원식오빠, 엄마같이 대해주신 이름이 예쁜 지윤언니, 저의 실없는 행동들을 재밌어하고 좋아해 주셨던 보은언니, 맛있는 것도 많이 만들어 주시고 사소한 부분까지 챙겨주셨던 소영언니, 쓰지만 정신을 바짝 차리게 되는 냉철한 조언을 해 주셨던 민식오빠, 신중함과 깔끔함을 배울 수 있었던 이야기가 잘 통하는 주홍오빠, 도움도 많이 받고 실례도 많이 범해서 고맙고 죄송한 용준오

빠, 이해와 배려심이 깊은 친오빠 같은 강록오빠, 차도남인 듯 했는데 알고보면 친근한 시영오빠, 한 우물만 판다는 것이 무엇인가를 보여준 정호오빠,다가가기 어려워 보였지만 알고보면 따뜻한 그리고 미안한 게 많은 효섭, 많이 챙겨주시고 도와주셔서 큰 의지가 되었던 충전제 같은 경동오빠, 실험 뿐만 아니라 생활의 많은 부분을 같이 공유하고 머리 맞대 고민해 주었던 은경언니, 실험실에서 가장 많은 활동을 함께 하며 미운정고운정 듬뿍 든 경창오빠, 무심한 듯 하지만 뻗은 손을 뿌리치지 않고 잡아주는 유복오빠. 선배님들이 있기에 든든했고, 길을 잃지 않을 수 있었습니다. 감사합니다.

공부가 즐거운 일이 될 수 있다는 걸 보여 준 입학동기 아름이, 놀라운 암기력을 보여줬던 석현오빠, 옆자리에 앉게 되서 은근히 친해지게 된 기백오빠, 선후배 이상의 정을 나누었으리라 믿는 혜미, 주어야 할 도움과 배려를 오히려 많이 받은듯 한 인도신사 아툴, 등만 맞대고 있어도 든든했던 밤 실험 동기 효진이, 집중력과 안정감을 배우고 싶은 수진이, 명석함과 쿨함이 부러운 지선이, 멋있는데 성격도 좋은 쿨가이 해민이, 허술함 속에 예리함을 지니고 있는 임기응변의 귀재 승환이, 후배로 받게 되어 오히려 고맙고 감사한 은정이, 그리고 앞으로 즐겁고 열정적으로 실험실 생활을 해나가길 바라는 민지, 지은이. 후배들에게 해 준 것보다 받은 게 더 많은 것 같습니다. 감사합니다.

학부 졸업 이후에도 서로 격려와 응원을 아끼지 않은 검도부 여부원들, 선화, 주영, 미령아. 고맙고, 앞으로도 계속 우정 이어나가자. 대학원 생활 동안 밖에서 힘이 되어주고, 즐거운 추억을 공유하고, 나의 길을 지지해 준 소중한 친구 혜린, 화평, 진희야, 고등학교, 대학교 친구들아, 모두 고맙다. 그리고 곁에서 힘이 되어 주었던 정호에게도 감사한 마음을 전합니다.

사랑하는 나의 가족들. 눈에 넣어도 아프지 않을 것 같은 너무 예쁜 조카 도영아, 태영아. 너희들은 존재 자체만으로도 감사하단다. 늘 힘이 되는 이야기만 해 주고, 굳이 말하지 않아도 든든한 지원군임을 느끼게 해 주는

문주언니, 수완오빠. 감사합니다. 늘 격려와 응원을 전해주셨던 친척 분들. 받은 사랑보다 더 베풀며 살겠습니다. 그리고 마지막으로 저를 이 세상에 있게 해 주시고, 보살펴 주시고, 무한 애정을 보여주신 부모님. 제가 가는 길을 존중해 주시고, 지원해 주셔서 감사합니다. 앞으로 잘할게요. 건강하게 오래오래 사세요. 사랑합니다.